western australian marine science institution

Pathways to Production: Biogeochemical Processes in Kimberley Coastal Waters

Matthew R. Hipsey[1,4], Jim Greenwood[2,4], Miles J. Furnas[3,4], Allison S. McInnes[1], A. David McKinnon[3], M. James McLaughlin[2], Nicole Patten[1], Louise C. Bruce[1], Thomas Ngyuen[1], Kenji Shimizu[2], Nicole Jones[1,4], Anya M. Waite[1,4]

1 The University of Western Australia, Perth, Western Australia

2 CSIRO Oceans and Atmosphere, Perth, Western Australia

3 Australian Institute of Marine Science (AIMS), Townsville, Queensland, Australia

4 Western Australia Marine Science Institute (WAMSI), Perth, Western Australia

WAMSI Kimberley Marine Research Program

Final Report

Project 2.2.2

Jul 2017

western australian marine science institution

CSIRO

THE UNIVERSITY OF WESTERN AUSTRALIA

Australian Government | Australian Institute of Marine Science

WAMSI Kimberley Marine Research Program

Initiated with the support of the State Government as part of the Kimberley Science and Conservation Strategy, the Kimberley Marine Research Program is co-invested by the WAMSI partners to provide regional understanding and baseline knowledge about the Kimberley marine environment. The program has been created in response to the extraordinary, unspoilt wilderness value of the Kimberley and increasing pressure for development in this region. The purpose is to provide science based information to support decision making in relation to the Kimberley marine park network, other conservation activities and future development proposals.

Front cover images (L-R)

Image 1: Satellite image of the Kimberley coastline (Image: Landgate)

Image 2: Deployment of the rosette sampler from the *R.V. Solander* to collect water samples (Image: N. Patten)

Image 3: Humpback whale breaching (Image: Pam Osborn)

Image 4: Model simulation of coastal productivity in Collier Bay (Image: M. Hipsey)

Year of publication: Mar 2017

Metadata: http://catalogue.aodn.org.au/geonetwork/srv/eng/metadata.show?id=477988

Citation: Hipsey MR, Greenwood J, Furnas M, McKinnon D, McInnes AS, Mclaughlin J, Patten N, Bruce LC, Ngyuen T, Shimuzu K, Jones N, Waite A (2017) Pathways to Production: Biogeochemical Processes in Kimberley Coastal Waters. Report of Project 2.2.2 prepared for the Kimberley Marine Research Program, Western Australian Marine Science Institution, Perth, Western Australia, 101 pp.

Author Contributions: The project was originally conceived by AW, MF, ADM and JG. NP / ADM / MF collected field data during the two cruises and undertook laboratory analysis of the samples. TN undertook laboratory analysis of samples and analysis of cruise data. Model development work was undertaken by JG, KS, JM, NJ, LCB and MRH. MRH and JG wrote the report with contributions from MF, ADM and DM.

Corresponding author and Institution: Matthew Hipsey, The University of Western Australia

Funding Sources: This project was funded by the Western Australian Marine Science Institution (WAMSI) as part of the Kimberley Marine Research Program (KMRP), a $30M program with seed funding of $12M provided by the State Government as part of the Kimberley Science and Conservation Strategy. The Program has been made possible through co-investment from the WAMSI Joint Venture partners and further enabled by data and information provided by Woodside Energy Ltd.

Competing Interests: The commercial investors and data providers had no role in the data analysis, data interpretation, the decision to publish or in the preparation of manuscripts. The authors have declared that no competing interests exists.

Acknowledgements: We wish to thank the masters and crew of the AIMS vessel RV *Solander* for their assistance in field sampling in often difficult conditions.

Collection permits/ethics approval: No collection permits were required for the production of this report.

Contents

Executive Summary

One of the few remaining pristine coastal environments in the world, the Kimberley is highly valued for its biodiversity, cultural values, tourism and fisheries. The biodiversity of the Kimberley coast is fuelled by oceanic and terrestrially derived nutrient resources, yet there has been limited prior research about how nutrients vary or how they are used and recycled across the region. Building this understanding is essential to inform future management of the Kimberley coast and marine parks.

This project has therefore been undertaken to address both of the major research priorities emphasised in the Kimberley Marine Research Program Science Plan: (a) providing the bio-physical characterisation required for marine resource management and (b) improving understanding of ecosystem function and how this might change in response to future trends in human use. In particular, this project has aimed to elucidate the processes controlling carbon and nutrient flows through pelagic ecosystems in the Kimberley region. Specifically, we have sought to link physical processes and riverine inputs to food web structure and function, improving process understanding of pathways and material flows that connect habitats, populations and bioregions in the Kimberley. We have identified sources of nutrients and how they translate to productivity for consumers, and through this work have supported the development of an improved understanding of how such processes may be modified by a changing climate.

Through a series of field cruises, laboratory experiments and modelling, the aims of this project were to:

1. **Define variation in nutrients, light and microbial communities of the Kimberley coast.**

   The bulk of the data used in this study was collected over two research voyages:

   - KIM5887, occurred in October 2013 and represents typical dry season environmental conditions.
   - KIM5938, occurred in March 2014 and represents typical wet season environmental conditions.

   In addition, data collected during separate Kimberley research cruises were also further analysed to support the aims of the work. Data collection during the cruises included: profiling for physical attributes, nutrient concentrations, light, chlorophyll-a, and samples collected for subsequent detailed analysis of the pelagic planktonic community.

   The data provide detailed insights into how nutrients vary in this complex coastline, both spatially and temporally, and the unique planktonic assemblage within this region.

2. **Understand the limiting factors on productivity and trophic pathways.**

   The strong change in light climate with distance off-shore led us to investigate how phytoplankton have adapted to photosynthesise along this sharp gradient.

   Samples were processed in the laboratory to assess cellular response to light intensity and highlighted the adaptation of the nearshore phytoplankton community to the turbid conditions by tolerating low light levels. These response curves and in situ measures of photosynthesis have provided an ability to estimate how primary productivity varies over the region.

   In addition, secondary productivity was computed using novel enzyme based methods and used to quantify rates of grazing, respiration and biomass accumulation of the zooplankton community. Three zooplankton size classes were compared to highlight the trophic transfer of carbon and nitrogen through the food web, and this was further supported through stable isotope assessment.

3. **Quantify the nutrient pathways to production**

   The extensive information has provided key insights into how carbon and nutrients vary within the Kimberley coast and are transferred from primary to secondary producers. To complement the data collection, a shelf-scale hydrodynamic-biogeochemical model was developed to investigate the

influence of oceanic and terrestrial nutrients.

Model simulations highlighted the importance of tidally-driven upwelling and vertical mixing to regional productivity across the Kimberley shelf.

The combined biological dataset and information from the regional model was used to develop an improved basis for a high-resolution hydrodynamic-biogeochemical model able to simulate drivers of productivity in Collier Bay, as an example of the broader Kimberley region.

Key findings and implications for management

Ensuring sustainable local management plans and regional policies are developed in the Kimberley must be founded on evidence about the biophysical character of the systems, and robust predictions of how future changes will alter the system. Understanding the biogeochemical drivers of primary and secondary productivity is critically important to ensure effective management of the coast given projected changes in climate and human uses. This project has provided key information on the oceanographic and biological responses associated with nutrient supply that determines the off-shore and near-shore productivity of the Kimberley region, and then has linked these with higher trophic levels, providing information required to establish the scientific basis for natural resource management in the Kimberley marine estate.

Key findings from the research include:

- This dataset has identified key rates of primary and secondary production for the region, allowing us to put the Kimberley ecosystem and its dynamics in context of other coastal systems within Australia, and elsewhere in the globe. Some unique differences between other coastal systems were identified, but we also noted that levels of nutrients and primary productivity are in fact similar to other systems in northern Australia.
- In particular, our findings show that there is a uniquely adapted pelagic microbial community in the coastal embayments that can exist in the highly variable environment, that is associated with strong spatial gradients in light and the seasonal variation in the delivery of nutrients. Along the coastal margin the euphotic depth is so low that one would expect limited productivity, but in contrast the rapid rates of vertical mixing promote a highly efficient community of planktonic primary producers, that have different sensitivities to light than their counterparts on the shelf region.
- Results from the numerical modelling suggest that a transition from light to nitrogen limitation controls primary productivity with distance off-shore, and this differs between wet and dry conditions, and between different phytoplankton groups.
- Scenario modelling has given indicative estimates of nitrogen input into coastal areas from ocean upwelling to be upto 20%, but this translates to only 5% increase in primary productivity in the nearshore zone, with implications for the sensitivity of the marine parks to changes in terrestrial nutrient supply.

The light data, in particular, may also be used to assist guiding conservation decisions and areas that are set for protection, since in areas where the amount of light reaching the benthos is <1% of the surface light there is limited potential for benthic vegetation and more diverse communities. Furthermore, the detailed understanding of ecosystem processes developed here have provided critical input into a coupled hydrodynamic-biogeochemical model, which can also be used going forward to assess scenarios that can inform an adaptive management processes designed to minimize negative impacts from climate change, tourism, recreational and commercial fisheries, pearling and aquaculture.

Changes in productivity may occur due to changes in ocean conditions brought about by climate change, and also due to changes in land-use and subsequent river inputs of nutrients and sediment. The foundational biophysical datasets on pelagic primary productivity, community metabolism, community and food web structure can provide baseline support for the development, design and delivery of a program to monitor the long-term health of this ecosystem.

Future research and monitoring recommendations

Given the high turbidity levels that are already experienced in the near-shore zone, it could be argued that strong light limitation would override further anthropogenic increases in nutrients, however, we have demonstrated the phytoplankton productivity in this region is already highly tuned to the turbid conditions and can rapidly photosynthesise in the top several metres of the water column despite the rapid rates of vertical mixing and high light attenuation. It is therefore possible that productivity could be impacted by increased nutrient inputs, despite the high rates of tidal flushing, however, it remains unclear what magnitude of extra nutrients would be required to create problematic conditions such as algal blooms or low oxygen. This research has not investigated the extent to which land management practices and current development proposals in the Kimberley would increase nutrient export to the coast, however, prior data collection has indicated that hotspots of nutrient input can be significant (Gunaratne et al. 2017), and further research on this at a larger scale across the Kimberley is therefore recommended.

It also remains unclear how increasing tourism activities, including increased boating and coastal developments, will contribute to nutrient loads in the coastal areas. Issues associated with *Lyngbya* spp. have been reported in Roebuck Bay, despite high rates of tidal flushing, suggesting that significant point sources can contribute to decline in environmental quality in the region. Monitoring of nutrient levels and phytoplankton (e.g. cholorphyll-a) is therefore recommended in areas experiencing increased human activity. In addition, the large impact of the riverine inputs on coastal productivity was apparent, yet data on nutrient levels in the rivers entering the Kimberley coast is either very sparse or non-existent. Given emerging land-use development pressures in Kimberley catchments, it is recommended that the State Government and traditional owners develop a strategy for monitoring river nutrient and sediment levels, particularly where rivers are entering near culturally sensitive coastal areas. Monitoring in important areas such as whale calving grounds is also recommended to assist in improving our understanding of the link between nutrient cycling on the coastal margins, nutrient upwelling, and water column production. Opportunities for routine monitoring of nutrients and chlorophyll-a should also be considered for off-shore industrial facilities to assist in providing information that can be used to further develop our understanding of Kimberley marine biogeochemistry.

In addition, the light and chlorophyll-a data collected should also be further utilised to help calibrate algorithms for interpretation of satellite imagery that is available to be used for tracking water colour; this opportunity was not undertaken in this project, but is recommended to be undertaken in the future to allow cost-effective monitoring of the seasonal and long-term water quality changes in the region.

Products and tools

The main products from this research include i) foundational biophysical datasets, ii) conceptual models of the system, and iii) validated high-resolution numerical models.

The data products will be essential for managers, consultants and other scientists who require knowledge of baseline conditions, and which can be used to assess the relative significance of any future changes. The conceptual models developed shed new insights into the region, at both the shelf and coastal embayment scale, and provide a level of understanding that was not clear prior to this project. This conceptual model will be useful in planning and management exercises and shaping thought processes about emerging pressures and the potential for impacts.

Both the data and conceptual model have been used as the scientific basis to develop two major numerical modelling platforms. These include:

- *ROMS-BGC*: a shelf-scale simulation model able to explore how upwelling of nutrients onto the shelf and into the coastal zone compares to riverine inputs from the Kimberley rivers and catchments. This model predicts basic nutrient cycles and productivity dynamics, and is suitable for assessing how climate change will impact productivity across the Kimberley region.
- *TUFLOW-FV – AED2* : a flexible mesh approach with hybrid vertical co-ordinates good for resolving

complex coastline/islands and inlets. The model has a custom biogeochemical/ecological configuration based on the data collected, where possible, including locally relevant model parameterisations for light, sediment, nutrients, carbon and plankton. It has future potential for further integration with benthic mapping data. Most suited for undertaking scenarios of river nutrient, sediment and carbon inputs, and assessing changes in productivity due to changes in river inputs. Can be used for marine park nutrient budgeting, and also Environmental Impact Assessment of aquaculture developments, or other developments.

These two models, and the validated approaches and parameters which they are based upon, are now established and able to support the development, design and delivery of a program to monitor the long-term health of this ecosystem, and to assess specific scenarios related to climate change, tourism, recreational and commercial fisheries, pearling and aquaculture, or other coastal developments associated with port and mining infrastructure.

1 Introduction

The Kimberley Marine Research Program (KMRP) Science Plan recently outlined the WA State and Commonwealth initiative to develop the scientific basis for the management of the Kimberley marine estate. This plan includes undertaking research to understand human uses, indigenous coastal knowledge, physical and biological oceanography, benthic primary productivity, ecological connectivity, and catchment - ocean interactions, which together can be used to support knowledge integration and prediction. This report documents outputs from the WAMSI KMRP Project 2.2.2, which was broadly focused on describing biogeochemical processes in Kimberley coastal waters.

The biodiversity of the Kimberley coast is fuelled by oceanic and terrestrially derived nutrient resources, yet there has been limited prior research about how nutrients vary spatially and temporally, or how they are used and recycled across the region. The transfer of carbon from primary production to upper trophic levels (i.e. fish) via mesozooplankton involves many microbial linkages at the lower end of the food web, the strength of which is poorly established in Australian waters. Building this understanding is essential to inform future management of the Kimberley coast and marine parks, by supporting the development of conceptual models of the drivers of productivity in marine parks, and providing baseline information by which future impacts can be assessed. This research project on "Biogeochemical Processes" has therefore sought to provide key information on the oceanographic and biological forces associated with nutrient supply that determine the nearshore productivity of the Kimberley region and how this supports life higher up the food chain. Specifically, the objectives of the project were to:

1. Define the **nutrient status**, **light climate** and **microbial communities** of primary and secondary producers along the Kimberley coast.
2. Estimate **limiting factors controlling productivity** and the strength of **food web interaction** and how these pathways are defined by seasonal trends.
3. Integrate our knowledge through the development and use of **coupled hydrodynamic-biogeochemical modelling** tools to define nutrient pathways contributing to production, and as a tool to predict response of the Kimberley coast to future environmental change.

Addressing the above objectives provides important information needed to establish the scientific basis for natural resource management in the Kimberley marine environment, including informing coastal zone management and the development of management plans for marine parks recently established within the region.

1.1 Research Approach

Through a series of field cruises, laboratory experiments and numerical modelling, the above objectives of the project were addressed. The approach taken for each is summarised as:

Assessment of the variation in nutrient, light and microbial communities of the Kimberley coast: For this objective, the bulk of the data was collected over two research voyages:

- KIM5887, October 2013 representative of dry season environmental conditions.
- KIM5938, March 2014 representation of wet season environmental conditions.

In addition, data collected during earlier Kimberley research cruises were also compiled and further analysed to support the aims of this work. Data collection during the cruises included: profiling for physical attributes, measurement of nutrient concentrations, determination of light attenuation, chlorophyll-a, and collection of samples collected for subsequent detailed analysis of the pelagic microbial community.

Assessment of the limiting factors on productivity and trophic pathways: The strong change in light climate and nutrient availability with distance offshore led us to hypothesize that phytoplankton have adapted to photosynthesise along this sharp gradient, relative to other environments. Sampling was therefore focused to

compare primary productivity along the coast vs shelf waters. Samples taken were processed in the laboratory to assess phytoplankton cellular response to light intensity to ascertain if the nearshore phytoplankton community were adapted to the turbid conditions. In addition, secondary productivity was computed using novel enzyme based methods and used to quantify rates of grazing, respiration and biomass accumulation of the zooplankton community. Three zooplankton size classes were compared to estimate the rates of trophic transfer of carbon and nitrogen through the food web. In addition, this was further supported through assessment of stable isotope data taken from a range of planktonic size fractions and compared between near-shore and off-shore sites.

Quantification of the nutrient pathways to production: The extensive information gained from the above field and laboratory experimental work aimed to characterise the structure of the pelagic community and empirically determine the indicative rates of carbon and nutrient transfers. However, in order to answer questions about the function of the marine ecosystem, a range of hydrodynamic-biogeochemical modelling was undertaken to investigate the influence of oceanic vs terrestrial nutrients and the dominant drivers of productivity and to generalise the magnitude and importance of various nutrient pathways. Given the scope of these research questions and the range of spatio-temporal scales being assessed in the project, and consideration of data availability, three separate modelling initatives were undertaken:

- A simple 1-D (vertical) analysis of light and productivity exploring the relationship between the unique vertical mixing conditions and the light attenuation characteristics of the region (Chapter 5)
- A shelf-scale nutrient tracer assessment using a regional (large-scale) hydrodynamic model simulation (Chapter 7)
- A local (fine-scale) finite volume hydrodynamic-biogeochemical model for more detailed exploration of the link between hydrodynamics and trophich relationships within Collier Bay (Chapter 8)

The simulations have been undertaken to progressively advance our understanding of the key factors contributing to the patterns observed in field data set. The development of the models has also provided a set of decision support tools that can assess management and climate change scenarios.

1.2 Report Structure

The combination of the various data collection activities and modelling that was undertaken to satisfy the project objectives is described within Chapters 2 – 8 of this report. As the field data is central to the project and relevant to most chapters, Chapter 2 provides an overview of the research voyages and data collection approaches undertaken, in addition to a summary of other cruises that have been undertaken that were able to contribiute data to the analysis. Chapters 3 & 4 align with Objective 1 and describe the hydrodynamic, biogeochemical and ecologcical character of the region, presenting data spanning both the shelf and coastal embayment scales. Chapters 5 & 6 align with Objective 2 and describe experimental and modelling work undertaken to identify rates of productivity, environmental limitation factors, and the strength of planktonic food web interaction. Chapters 7 & 8 align with Objective 3, and present the results of two parallel investigations that developed coupled hydrodynamic-biogeochemical models for the shelf-scale and coastal embayment scale, respectively. A summary of the research, relevance to management, and reccomendations for future research is provided in Chapter 9.

2 Field Cruises and Sampling Details

The project has involved the synthesis of a wide range of physical and biogeochemical data collected for the region, including collection of a substantial new dataset undertaken as part of this project. The main data collection activities occurred during two WAMSI field cruises, in addition to analysis of data from several prior cruises (Table 2.1). Overall, the different cruises spanned a range of different focus regions within the Kimberley coastal waters and a range of sampling and experimental approaches, details of which are described in the sub-headings below. Technical details of the sampling approaches are outlined in relevant Chapters.

Table 2.1. Summary of the six research voyages (RV) which form the basis of the data analysis within this report.

RV	Year & Dates	Stations	Relevant Chapters
Southern Surveyor	**2010**: 15 Apr – 2 May	002-169	3,4,5,7
Solander	**2011**: 20–30 Jan	KIM002-KIM045	4,6
Solander	**2011**: 11–22 Oct	KIM053-KIM107	4,6
Solander	**2013**: 28 Feb – 10 Mar	KIM115-KIM194	4,6
Solander (this project)	**2013**: 23–30 Oct	KIM197-KIM272	3,4,5,6,8
Solander (this project)	**2014**: 11–22 Mar	KIM273-KIM370	3,4,5,6,8

2.1 Data Sourced from Previous Cruises

April 2010: A research trip in the Kimberley was conducted in April 2010 on board the RV Southern Surveyor. A number of stations from the coast to the shelf-edge (Figure 2.1) were occupied and sampled for water quality (nutrients, particulate organic matter, turbidity, and chlorophyll pigment), phytoplankton productivity, and zooplankton (handpicked and size fraction samples from bongo nets). In addition, terrestrial samples were carefully handpicked from the banks of the Derby River and Fitzroy River, with plankton and sediments further sampled from these inland river regions.

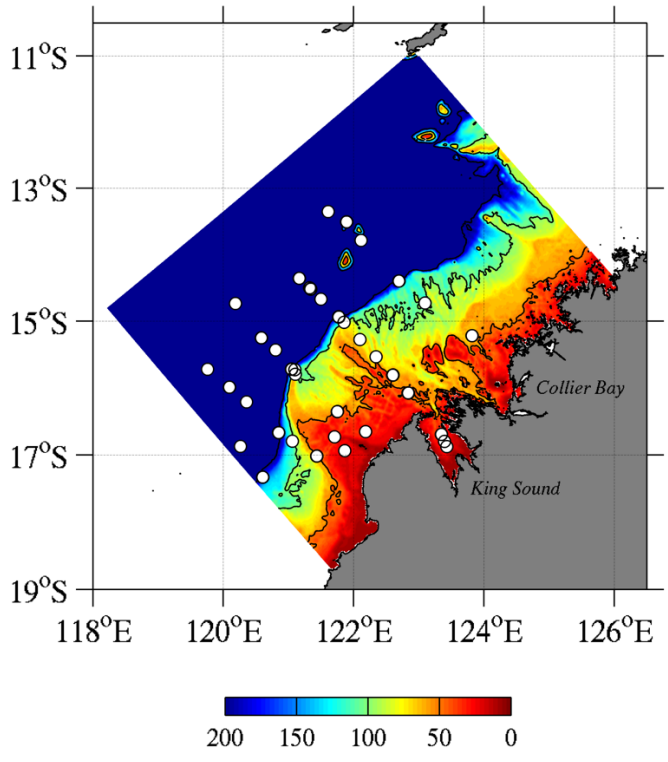

Figure 2.1. Location of 2010 CSIRO productivity stations within King Sound and on the adjacent Kimberley shelf (solid circles). Multiple stations along the central transect (five inside King Sound and two in the vicinity of each of the offshore locations) are omitted for clarity. Note that where multiple stations were undertaken these were occupied at different times (and slightly different locations) during the cruise and represent separate experiments and not duplicates. Contour lines indicate approximate position of sites on the 50, 200 and 1000 m isobaths.

January & October 2011: These two voyages led by AIMS can be seen in detail in the supplementary information for the McKinnon et al (2015) paper (link). Voyage tracks are provided as a kmz file, in addition to prepared plots of CTD casts and other monitoring data.

February/March 2013: Details as above. In addition, nine size-fractionated primary production experiments were carried out in Kimberley coastal waters between Napier-Broome Bay and Collier Bay on an AIMS cruise in March 2013 (Solander 5775). Daily production was estimated for the total population, the < 2 µm, 10 – 2 µm, and >10 µm size fractions. Details of methods are as summarised in subsequent Chapters.

2.2 Dry Season Cruise: Biological and Chemical Oceanographic Sampling

October 2013: The first cruise for the project was designed to capture dry season conditions; the chosen period was characteristic of a typical dry season with negligible river inflows entering the domain. Biological and chemical oceanographic sampling on Solander 5887 was primarily focused on three sites in Collier Bay (Figure 2) that typified conditions: on the seaward boundary of Collier Bay, the mid-bay, the inner-bay and an estuarine site in Walcott Inlet, one of the three large enclosed bays that exchanges water tidally with Camden Sound and Collier Bay. A number of additional stations were occupied within Collier Bay to resolve spatial distributions of plankton populations and hydrographic conditions and a longitudinal gradient of conditions within Walcott Inlet. Walcott Inlet (approx. 250 km^2) is the largest bay exchanging with Collier Bay and receives runoff from the largest catchment ultimately flowing into Collier Bay (the Isdell River).

Repetitive hydrographic sampling was carried out over a full diel cycle (26+ hours) at each of the four time-series sites to establish variability over a diel and tidal cycle. A range of sampling was carried out at these sites:

- CTD casts – every two (2) hours (see images below).
- Niskin water collection for dissolved and particulate nutrients – six (6) hourly (see images below).
- Phytoplankton community characterization – both using flow cytometry & cell counts undertaken and HPLC pigment analysis.
- Zooplankton community composition, standing crop and size structure (bongo net) – day, night.
- P vs I (Photosynthetron) experiment – daily P-I characteristics of coastal phytoplankton were measured at eight stations during the October 2013 cruise.
- Plankton community metabolism – sub-samples of metazooplankton from net tows were frozen for later analysis of ETS and AARS to estimate community metabolism and production rates.
- Plankton samples for stable isotope analysis (^{15}N, ^{13}C) analysis – at least once per site.
- Nitrogen uptake (^{15}N) – daytime.

Image 1: Deployment of the CTD rosette sampler in the inner part of Collier Bay (left) and mid-Walcott Inlet (right), demonstrating the sharp increase in turbidity (photo credit: Miles Furnas).

Image 2: Left: Nicole Patten filtering sample water for chlorophyll analysis aboard the RV Solander, October 2013 (photo credit: Thomas Nguyen). Right: Recovery of the bongo nets aboard the RV Solander 2013 (pictured: Miles Furnas, David McKinnon, Thomas Nguyen and Simon Spagnol). (photo credit: Nicole Patten).

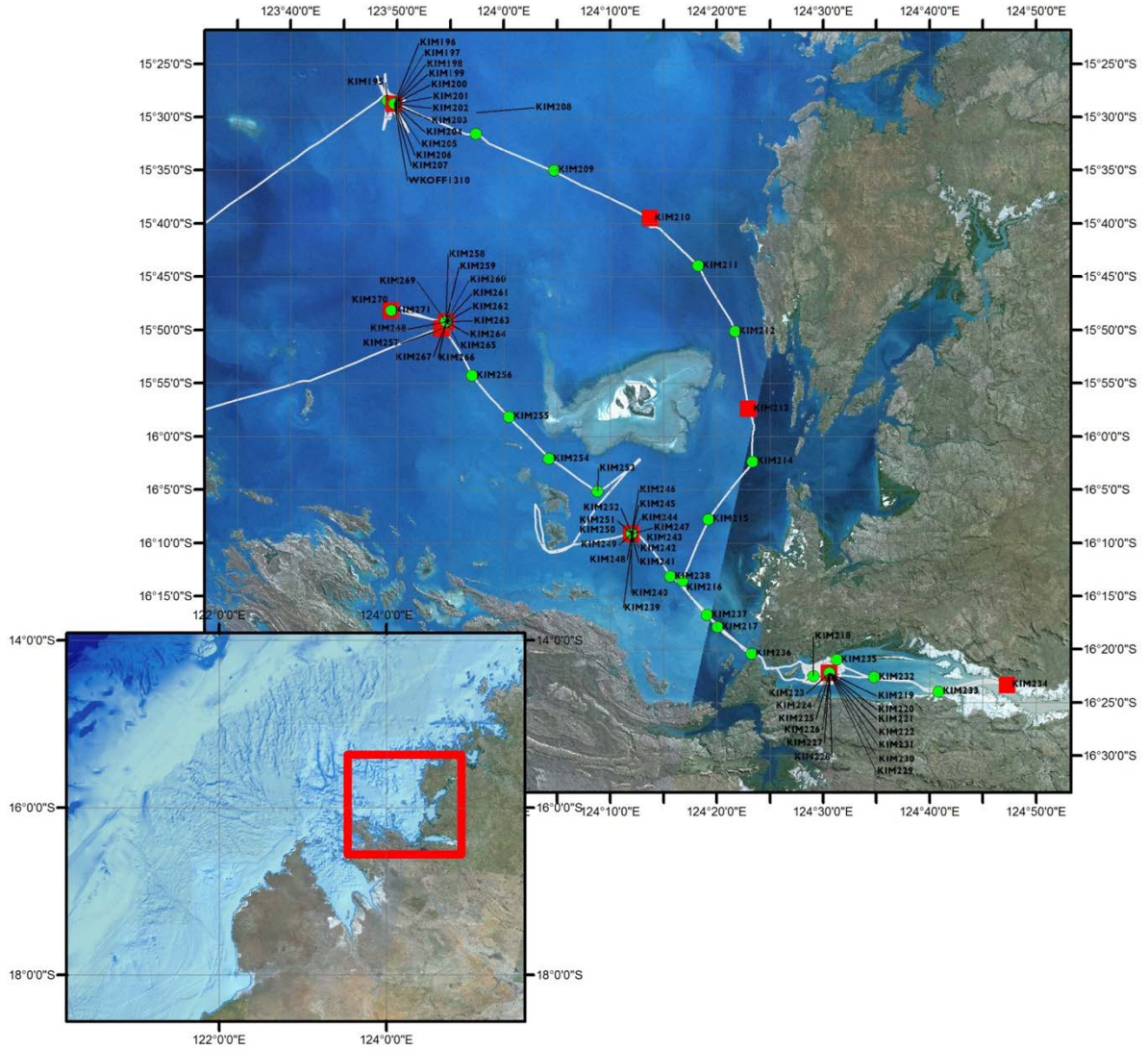

Figure 5.2. Locations of stations occupied in Collier Bay and Walcott Inlet during the October 2013 dry season cruise (Solander Voyage 5887).

2.3 Wet Season Cruise: Biological and Chemical Oceanographic Sampling

March 2014: The second cruise for the project was designed to capture the wet season and was completed in March 2014; the chosen period was characteristic of typical wet season river inflows, based on historic hydrologic analysis reported in Revill et al. (2017) for WAMSI KMRP Project 2.2.6. Similar to the dry season cruise, the geographic focus was along an estuarine-to-offshore transect from Walcott Inlet to outer Collier Bay, with sampling primarily clustered around four sites where 24-hour sampling (time interval ~ two hours) was undertaken, plus stations were spread throughout Collier Bay and Walcott Inlet. The sampling regime was similar to the above list of activities undertaken in the dry season, including completion of 98 CTD sampling stations, many of which also included water sampling stations for nutrients and many including plankton net tows. A series of P-I experiments was undertaken and water sampling and profiling was also undertaken in the Isdell River to support WAMSI KMRP Project 2.2.6. As for October 2013, concurrent photosynthesis/respiration measurements by high precision oxygen measurements were made during the cruise in Collier Bay, Walcott Inlet and northern Kimberley coastal waters. Sub-samples of metazooplankton from net tows were frozen for later analysis of ETS and AARS to estimate community metabolism and production rates (see Chapter 6).

Due to the final transit to Darwin we were also able to reoccupy sampling stations from earlier cruises along the central and Northern Kimberley, and were able to focus on stations at the entrance to bays/estuaries that receive large riverine inputs. Figure 2.3 summarizes the cruise tracks and mooring locations, and full details are in the AIMS Research Voyage Report Trip 5938.

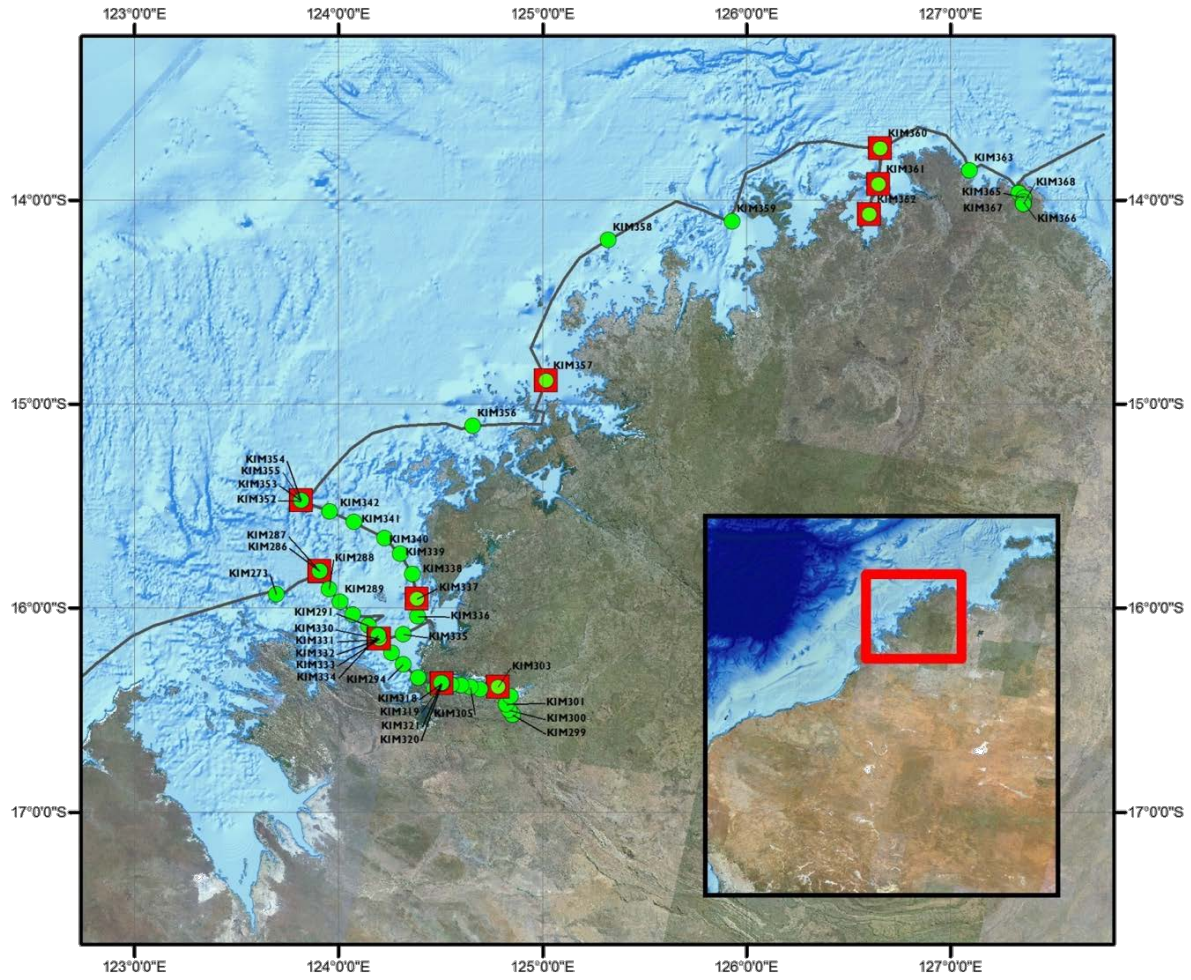

Figure 2.3. Locations of sampling sites occupied during the March 2014 wet season cruise (Solander Voyage 5938).

3 Kimberley Shelf and Coastal Biogeochemistry

3.1 Introduction

Before being able to identify key drivers of productivity within the Kimberley region, it is first necessary to describe the general biogeochemical features of the region. The range of past cruises and present cruises that have been undertaken allow for a general description of the spatial variation in salinity, nutrients, turbidity and light, both at the shelf-scale, and within the coastal embayments such as Camden Sound and King Sound. The aim of this Chapter is therefore to describe the variability in biogeochemistry, both across the domain and seasonally, to set the backdrop for subsequent Chapters. Further information of the Kimberley shelf physical oceanography is available from WAMSI KMRP Projects 2.2.1 and 2.2.7 reported in Espinosa-Gayosso et al. (2017) and Feng et al. (2017), respectively.

3.2 Data and analyses

3.2.1 CTD

For the Southern Surveyor cruise (see Table 2.1), the CSIRO conductivity, temperature, and depth (CTD) unit 21 was used with a Seabird SBE911 with dual conductivity and temperature sensors. The CTD was fitted with sensors for photosynthetically active radiation (PAR, 400 to 700 nm, Biospherical Instruments QCP-2300), fluorescence (Chelsea Instruments Aquatracka™ fluorometer), % transmission (Wetlabs C–Star™), dissolved oxygen (Anderra 3975 series optode) and nitrate (Satlanic ISUS sensor) concentrations. For the Solander cruises (see Table 2.1) CTD casts at each station were made with a SBE911plus CTD Rosette (Sea-Bird Electronics) fitted with a Wet Labs ECO FLRTD Fluorometer, Chelsea/Seatech C-Star Transmissometer.

3.2.2 Nutrients

All dissolved (NH_4^+, NO_2^-, NO_3^-, PO_4^{3-}, Si, DON, DOP, DOC) and particulate (PC, PN, PP) nutrient analyses were carried out at the AIMS laboratory using standard methods previously published (e.g., Furnas 2007). Prior to analysis, the following sample processing protocols were adopted at sea:

Dissolved nutrients – Sub-samples of water drawn from Niskin bottles were pressure-filtered (Sartorius Mini-sart, 0.45 µm) into 8 x 12 ml acid-washed polycarbonate screw-cap test tubes. Duplicates sets of tubes for analysis of dissolved inorganic nutrients (NH_4^+, NO_2^-, NO_3^-, PO_4^{3-}) and dissolved organic nutrients (DON, DOP) were frozen for later analysis ashore. One extra set of tubes of filtered water was also frozen as a backup for analytical troubles. Duplicate sets of tubes for analysis of silicate ($Si(OH)_4$) and dissolved organic carbon (DOC) were stored at 4°C until analysis. The DOC tubes were spiked with 100 µL of 12M HCl before storage.

Chlorophyll-a – Duplicate 100 or 250 ml sub-samples of water were filtered under subdued light onto 25 mm Whatman GF/F filters for fluorometric chlorophyll-a analyses (Total population). For size-fractionated phytoplankton samples, duplicate 250 ml aliquots were filtered onto 25 mm polycarbonate membrane filters (Poretics: 10, 5 or 2 µm pore size). The filters were folded, wrapped in (combusted) Al foil envelopes and frozen (-20°C).

Particulate nutrients – Duplicate sets of 250 ml sub-samples of water from the Niskin bottles were filtered onto (pre-combusted) 25 mm Whatman GF/F filters. The filters were folded, wrapped in (combusted) Al foil envelopes and frozen (-20°C).

Suspended particulate matter – Duplicate 1 L sub-samples were filtered onto pre-weighed 47 mm polycarbonate membrane filters (Poretics). The funnels and filters were washed with a small amount of deionized water to remove remnant saltwater, folded and returned to pre-labelled, pre-combusted scintillation vials.

Ammonia analyses – Because of contamination of filtered and frozen samples, analyses for ultra-low level in situ ammonia concentration (NH_4^+) were run at sea with unfiltered seawater samples using the fluorescence method of Holmes et al. (1999).

3.2.3 Light

To understand primary productivity the accurate parameterisation of sub-surface light, particularly photosynthetically active radiation (*PAR*), is essential. The characteristic gradients in colour of Kimberley waters make this an important factor that requires investigation, considering changes in seasonal river discharge and the strong tidal mixing that are expected to impact strongly on water transparency. Typically, sub-surface *PAR* varies according to an exponential decrease in the incident *PAR* according to:

$$I_{PAR} = 0.45\, I_0 e^{-K_d z} \tag{3.1}$$

where I_0 is surface irradiance, 0.45 is the fraction of sunlight that is photosynthetically active (Kirk 1994), z is the vertical depth (positive downwards), and K_d is the light attenuation rate. Variation of K_d is known to occur as a result of changing concentration of suspended solids (e.g. sediment and plankton), and coloured dissolved organic substances. Most models (including the ROMS-BGC and AED models used for this project) deal with this problem by splitting K_d into a number of separate components that each depend on the concentration of a different substance, for example:

$$K_d = K_w + K_{dA}[\bar{A}] + K_{dB}[\bar{B}] + \cdots \tag{3.2}$$

where K_w is the background attenuation in a clear uniform water column and A and B etc. are the depth-averaged concentrations of various solid or dissolved constituents, each are assigned a specific attenuation coefficient K_{dA}, K_{dB} etc. The values of K_w and the specific attenuation for particulates are well researched and typically given values of ~0.04 m^{-1}, and ~0.025 m^{-1} respectively. However, attenuation coefficients can vary widely and must be determined or adjusted based on local measurements. Estimates for the concentration of the various attenuating substances (e.g. chlorophyll *a*, suspended sediment etc.) are required to compute K_d, and in this study, measurements of submarine *PAR* (I_{PAR}), chlorophyll fluorescence ($\mathrm{Chl}a$), and total suspended solids (TSS) made in the vicinity of King Sound during May 2010 and in Collier Bay during October 2013 were analysed to ascertain and test parameters for Eq 2.

3.3 Salinity, temperature, oxygen and turbidity

This 2010 cruise data spans up to 400km off the coast and analysis of this dataset has demonstrated the variability in cross-shelf salinity, temperature and oxygen and turbidity (Figure 3.1). Slightly elevated salinity was evident in the shallow region closest to land by 0.1 – 0.3 psu. Temperature varied uniformly across the transects from ~30°C in the surface layer to ~14°C at 250 m depth, to ~5°C below 1000 m. Similarly, oxygen concentrations were at saturation for the upper 100 m, and below that dropped to <100 mmol/m^3, with the lowest concentration observed in the transects at ~750 m depth.

The 2013 and 2014 Collier Bay transects spans up to 200 km, but covering the estuarine portion of the embayment including into Walcott Inlet (Figure 3.2). The dry season plots show limited horizontal salinity stratification with a minor freshwater signal across the surface. At this time 2-3°C was noticeable within the embayment with evidence of both horizontal and vertical gradients. The wet season transects showed a more marked stratification signal in the salinity, with a freshwater pulse reducing salinity to 34psu 100 km offshore from the head of the estuary.

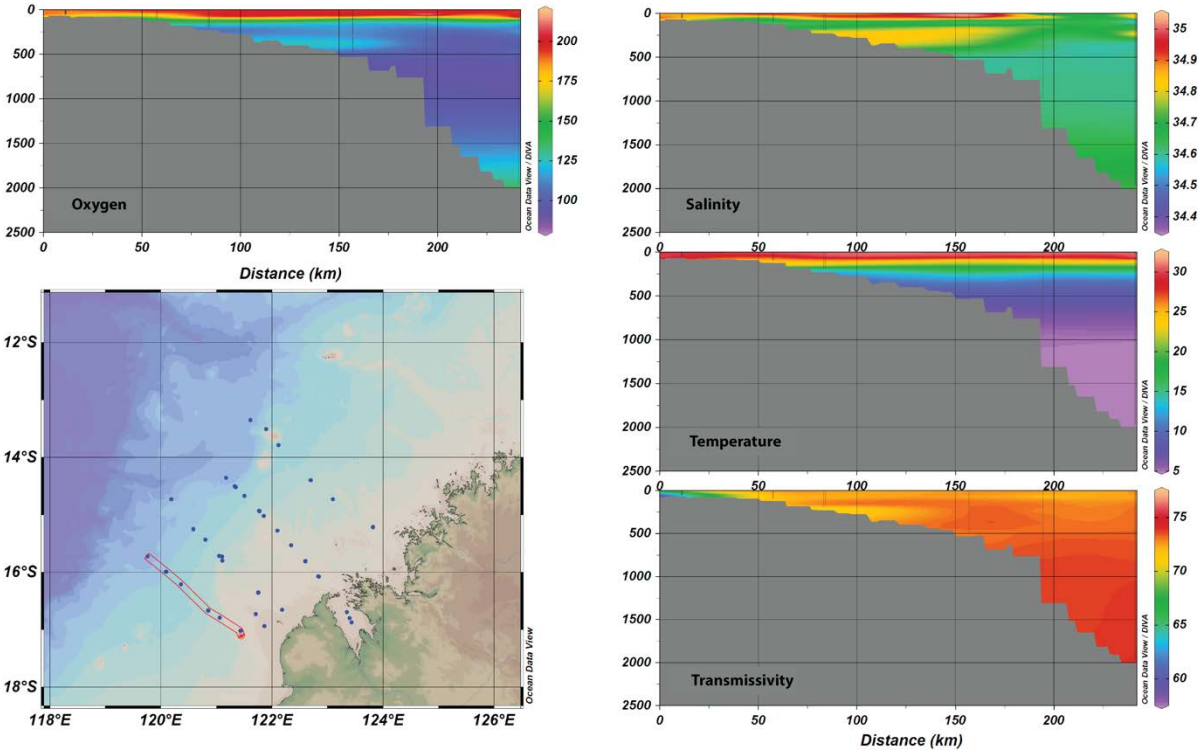

Figure 3.1a. Cross sections of salinity, temperature, oxygen and light transmission from the Transect A undertaken in 2010.

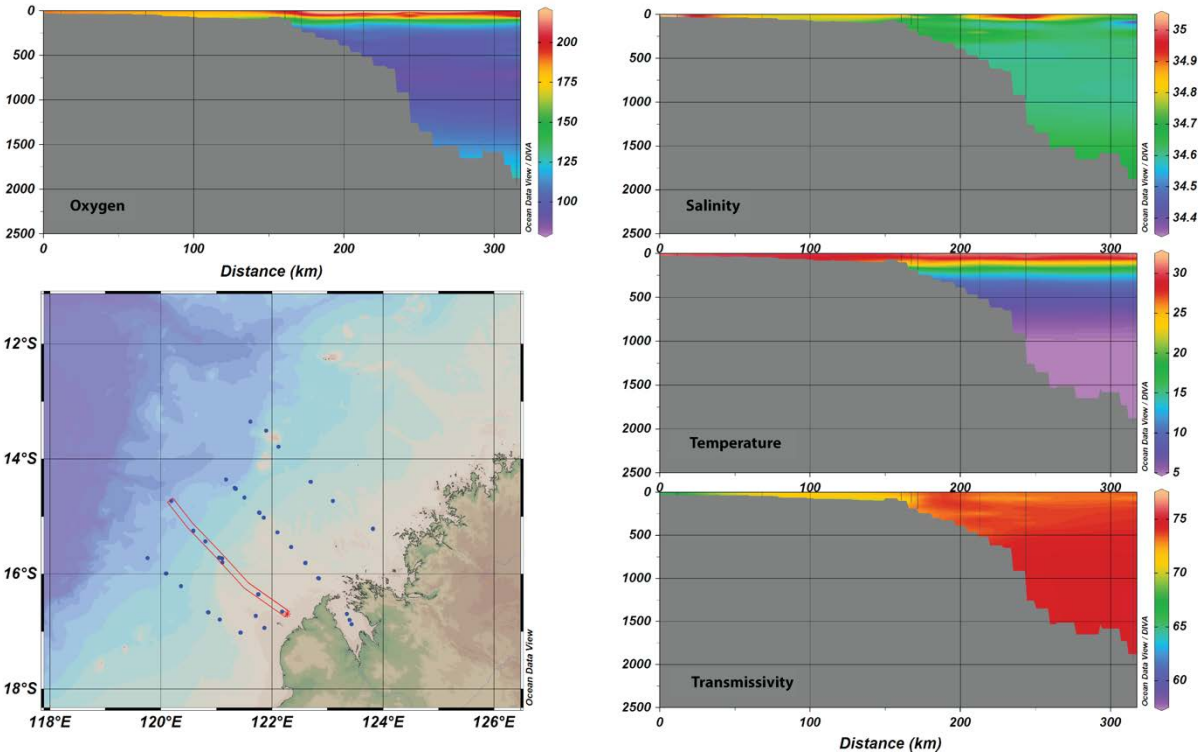

Figure 3.1b. Cross sections of salinity, temperature, oxygen and light transmission from the Transect B undertaken in 2010.

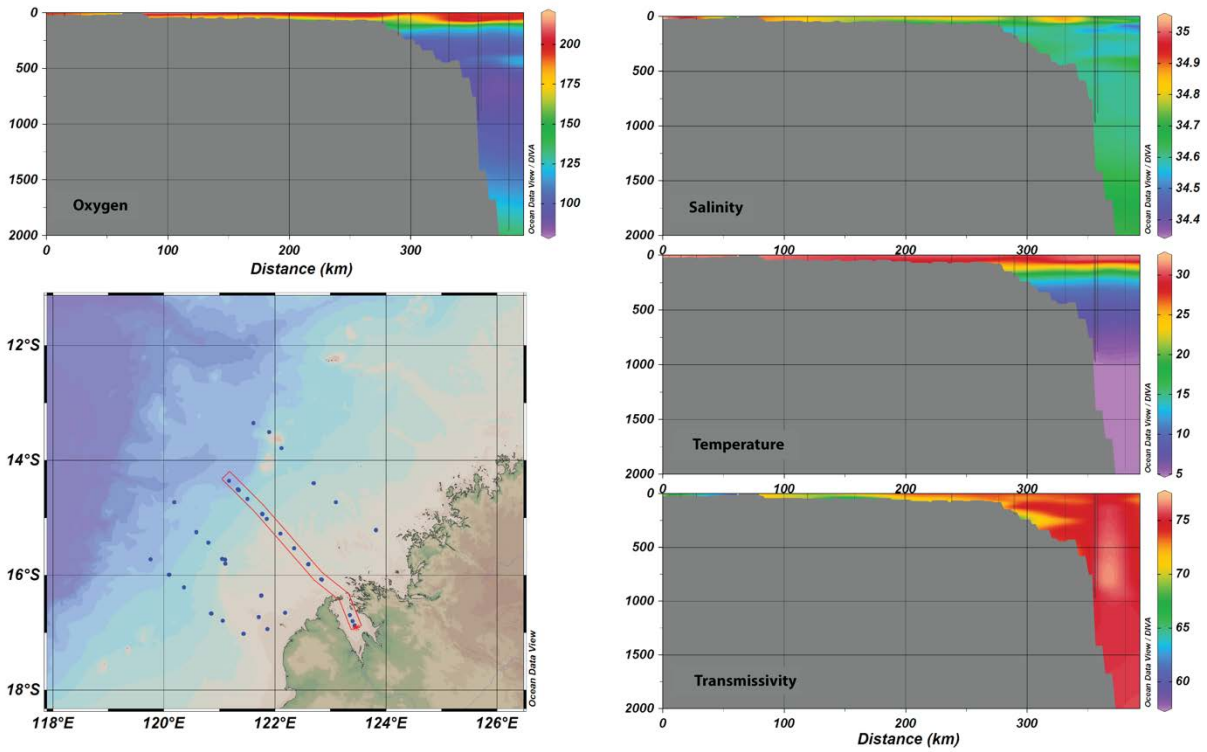

Figure 3.1c. Cross sections of salinity, temperature, oxygen and light transmission from the Transect C undertaken in 2010.

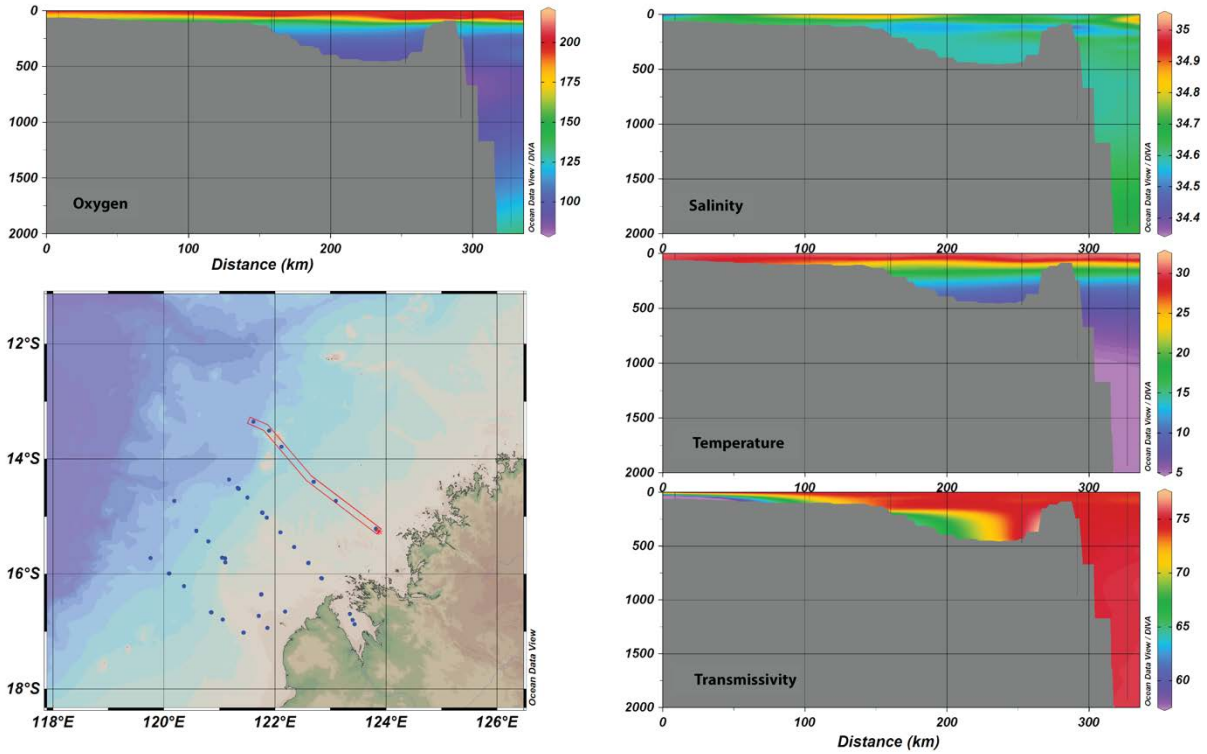

Figure 3.1d. Cross sections of salinity, temperature, oxygen and light transmission from the Transect D undertaken in 2010.

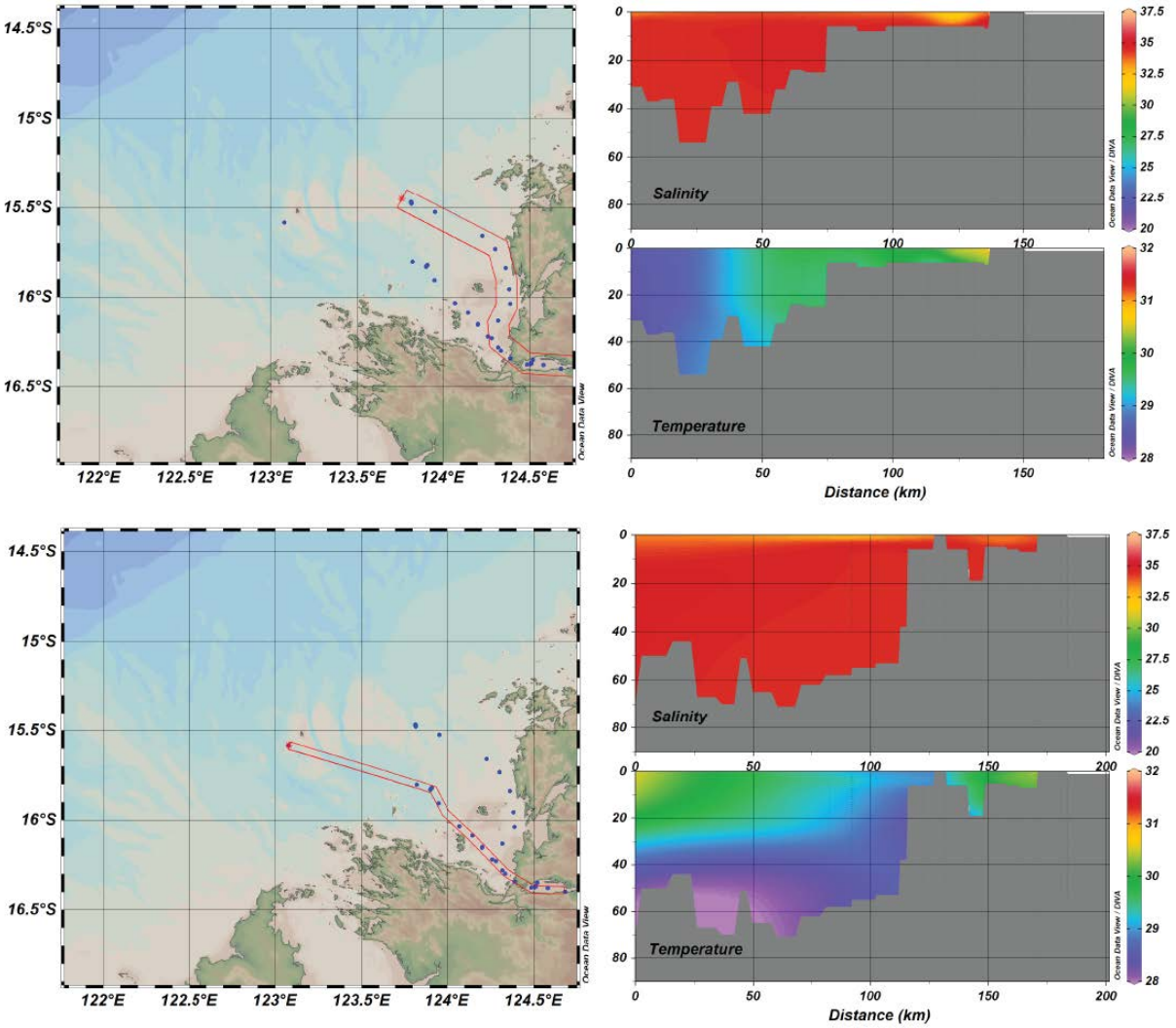

Figure 3.2. Cross sections of salinity and temperature undertaken within Collier Bay undertaken in 2013.

3.4 Nutrient and chlorophyll variation

From the 2010 cruise data, dissolved inorganic nitrogen concentrations integrated over the euphotic zone depth are observed to peak at the 200 m contour (Figure 3.3). The complete transects across the shelf show the 250-300 m deep surface mixed layer across the shelf, with nutrient deplete water in the surface, and nutrient rich water deeper below. In deeper waters this leads to a deep chlorophyll maxima, with limited biomass seen near the surface, expect in the shallow areas near the land interface, which show a chlorophyll peak throughout the water column. Some evidence for nutrient upwelling from the deep ocean to the shelf region is evident from the 2010 transects, with higher levels of PO_4, SiO_2, and NO_x towards the bottom of the shelf waters.

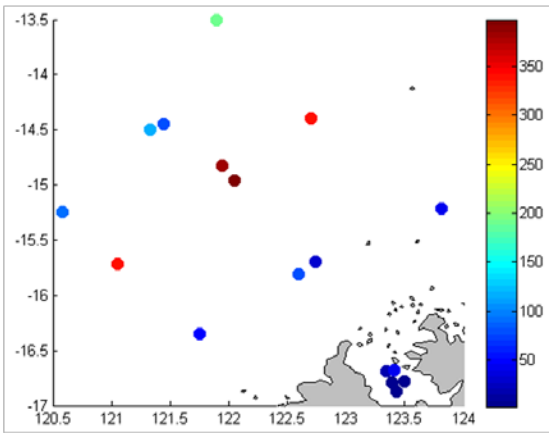

Figure 3.3. Depth-integrated (euphotic zone) dissolved inorganic nitrogen (DIN) concentration (mmol m^{-2}) in the King Sound and adjacent shelf region analysed based on the 2010 cruise data.

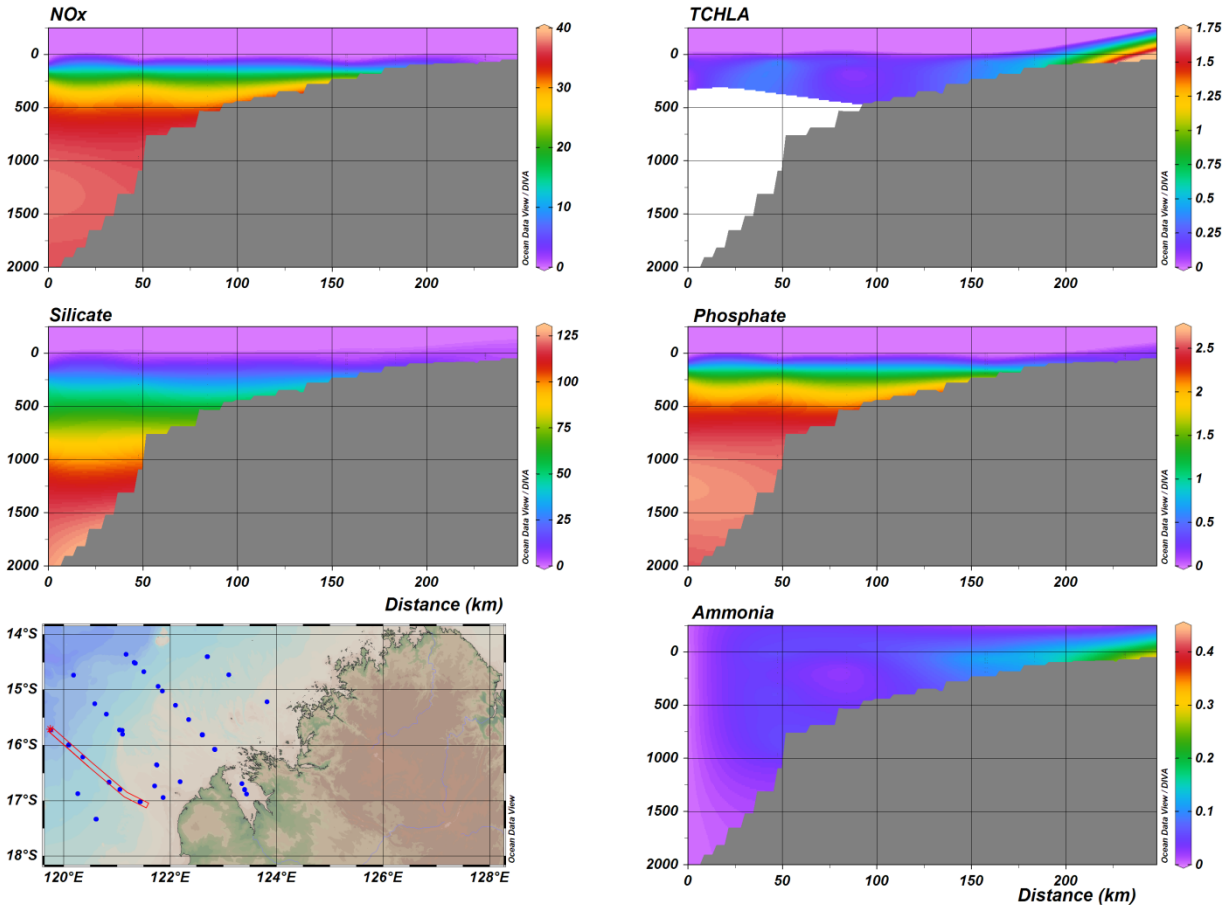

Figure 3.4a. Shelf-scale cross sections of NO_x, NH_4, Chl-a, reactive Si and PO_4 from the Transect A undertaken in 2010.

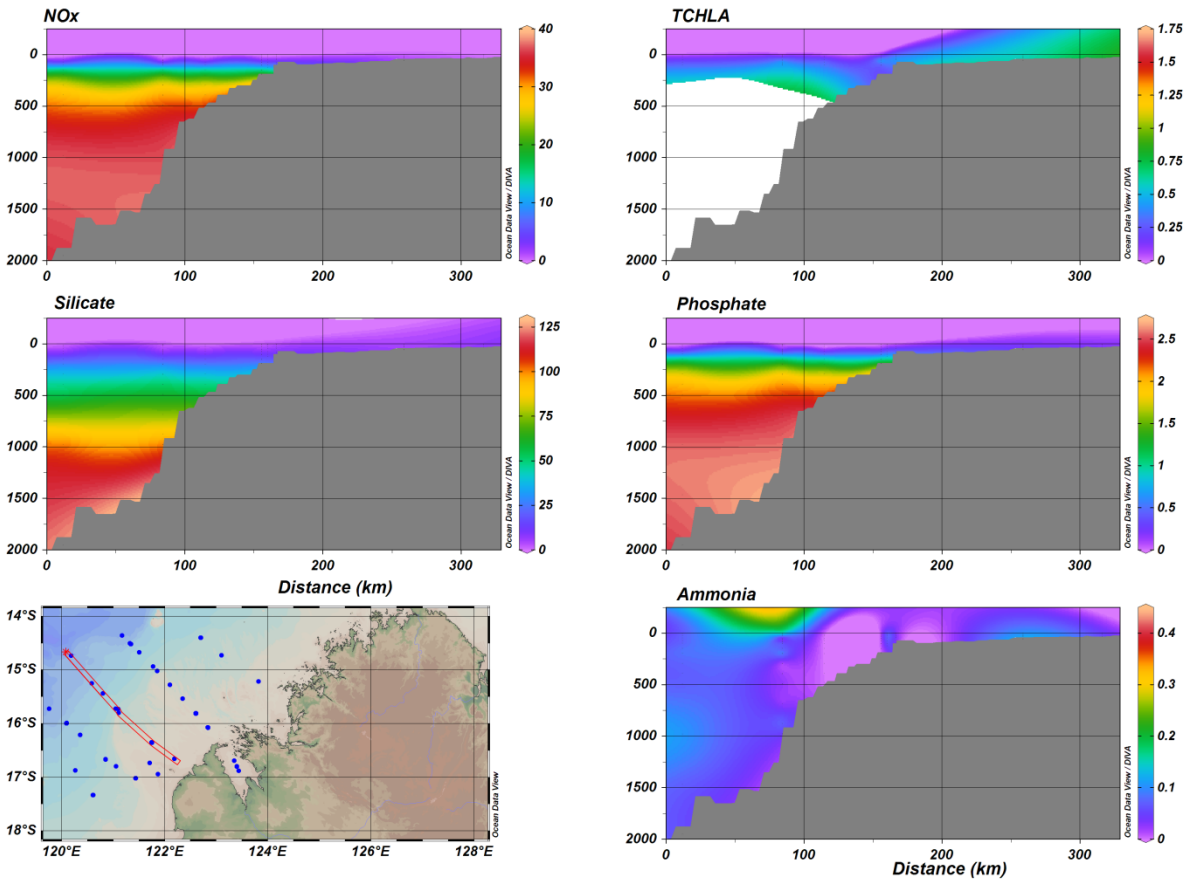

Figure 3.4b. Shelf-scale cross sections of NO_x, NH_4, Chl-a, reactive Si and PO_4 from the Transect B undertaken in 2010.

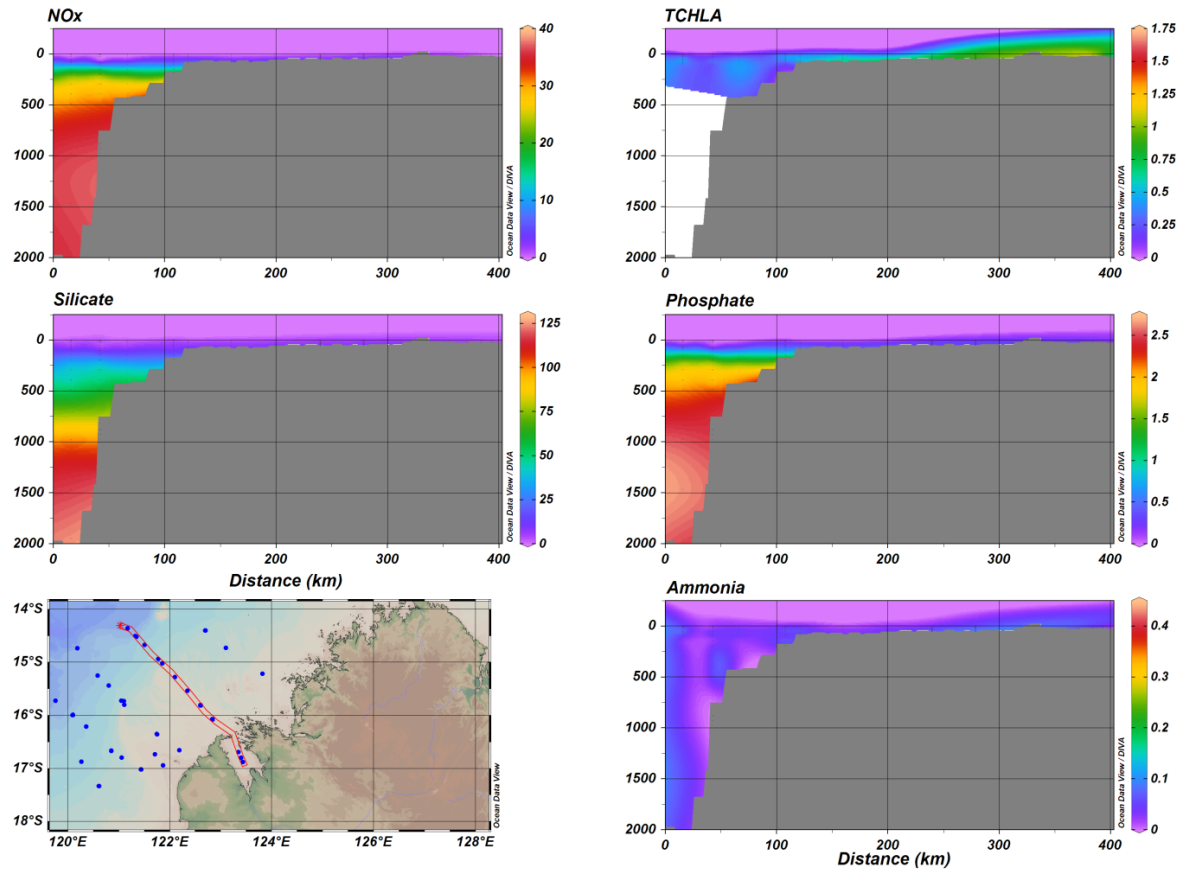

Figure 3.4c. Shelf-scale cross sections of NO_x, NH_4, Chl-a, reactive Si and PO_4 from the Transect C undertaken in 2010.

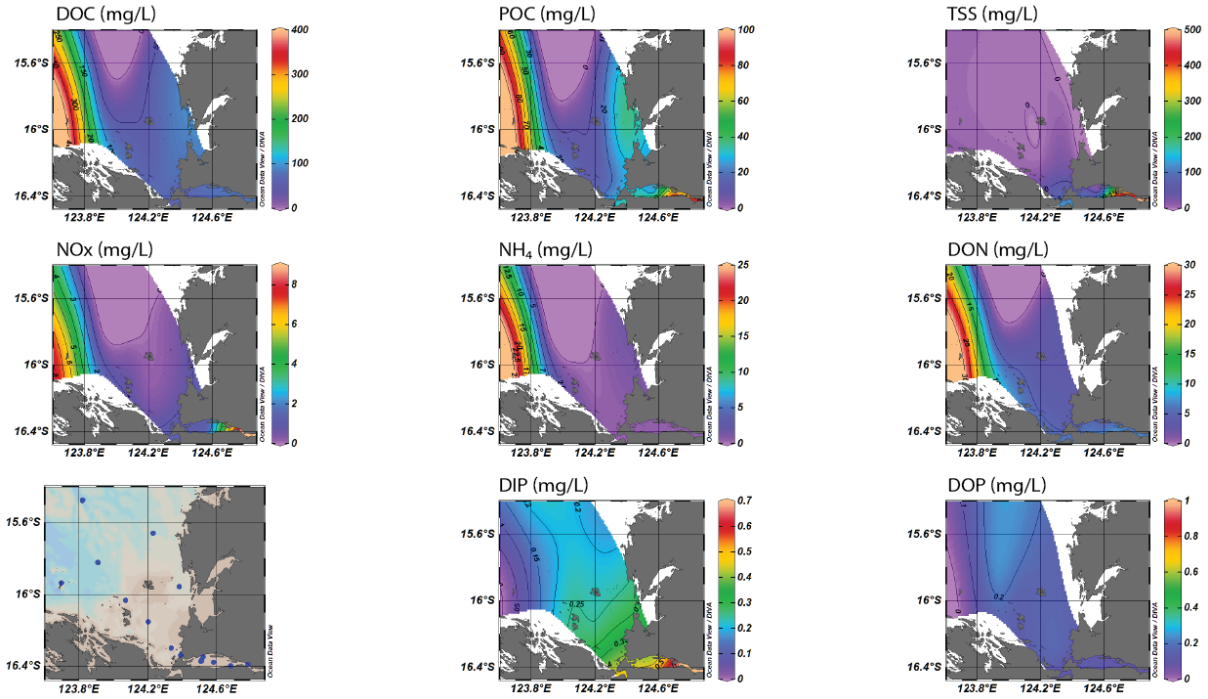

Figure 3.5a. Variation of inorganic and organic nutrients within Collier Bay based on samples taken during the October 2013 cruise.

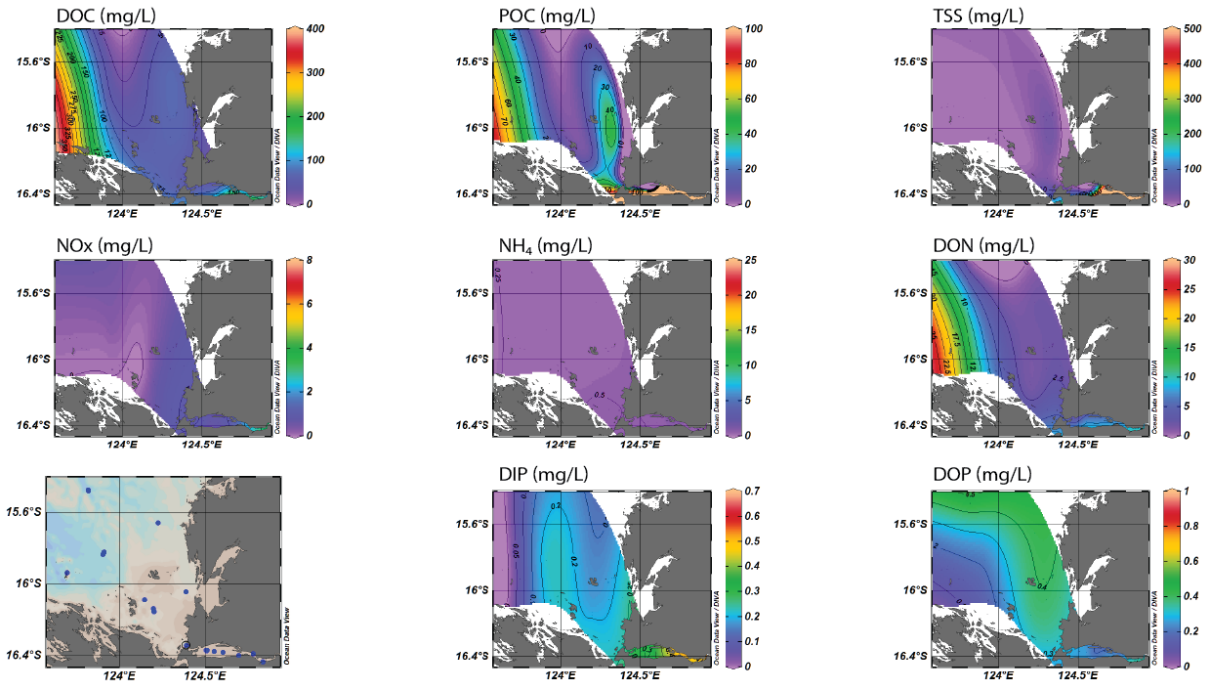

Figure 3.5b. Variation of inorganic and organic nutrients within Collier Bay based on samples taken during the March 2014 cruise.

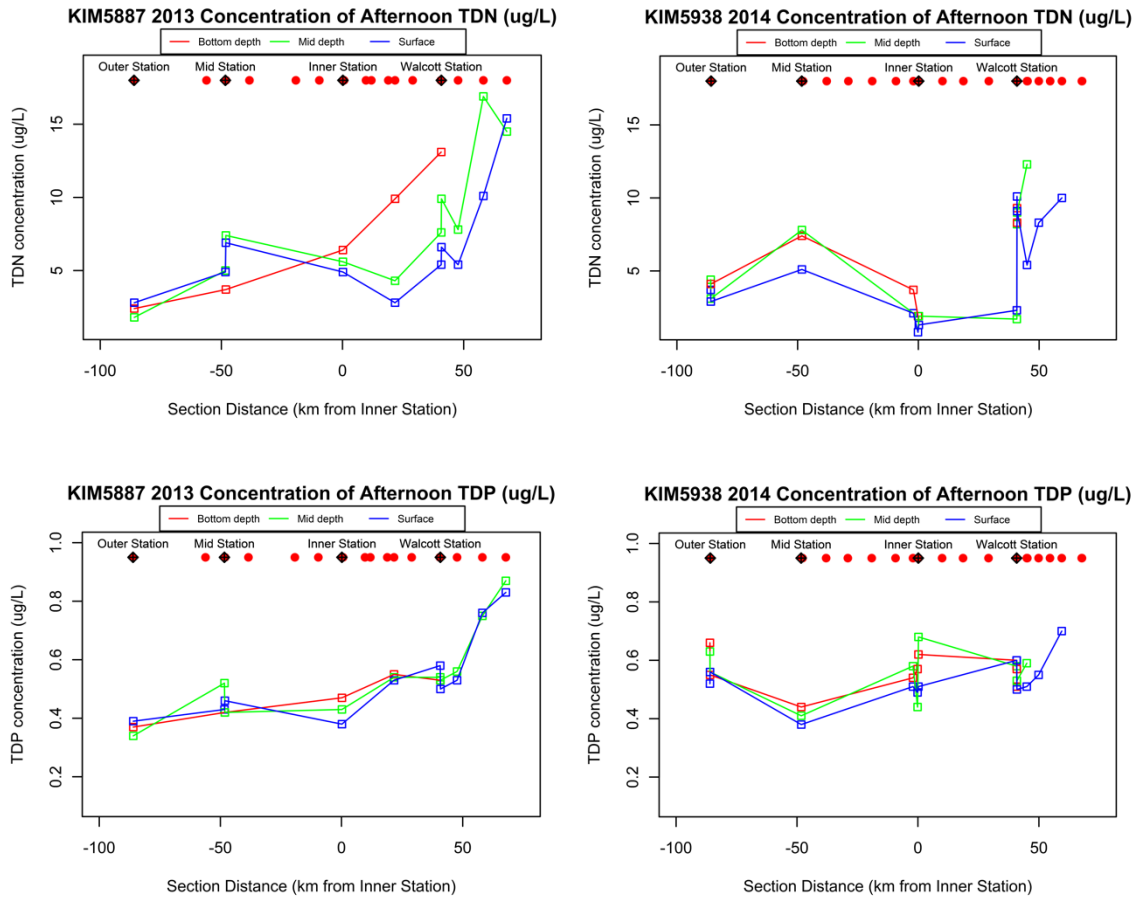

Figure 3.6. Total dissolved nitrogen (TDN; top) and phosphorus (TDP; bottom) variation in Collier Bay during the dry (Oct 2013) and wet (Mar 2014) season cruises, comparing surface, mid and bottom depths.

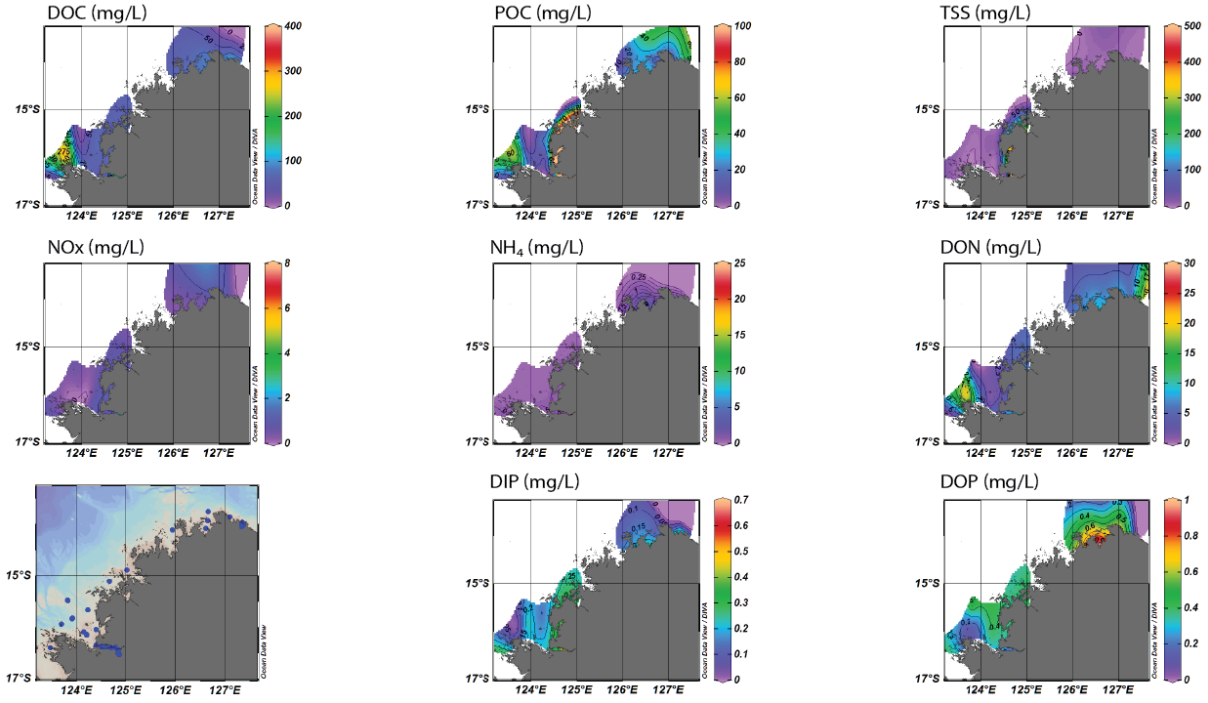

Figure 3.7. Variation of inorganic and organic nutrients along the wider Kimberley coast, based on samples taken during the March 2014 cruise.

3.5 Light climate variation

3.5.1 King Sound and adjacent shelf

Results from King Sound and the adjacent shelf region show a marked increase in light attenuation (K_d) toward the coast, with the highest rates of attenuation found inside the entrance to King Sound (Figure 3.7). Attenuation rate (K_d) was well predicted by:

$$K_d = 0.04 + 0.025\left[\overline{Chl}\right] + 0.12[TSS] \quad (3.3)$$

for shelf depths less than 50 m, where $\overline{Chl}$ is depth-averaged chlorophyll (mg m^{-3}) and TSS is the surface concentration of total suspended solids (g m^{-3}) (Figure 3.8). Further offshore (h > 50 m) attenuation rate depends primarily on chlorophyll concentration (not shown). The overall stronger dependence of attenuation on suspended solids suggests that some estimate of this quantity is necessary in subsequent modelling efforts (see Chapter 8).

Calculation of the depth of the euphotic layer (E_z, defined here by the depth level where 1% of the surface irradiance remains) reveals that despite the increase in attenuation rate toward the coast, the combined reduction in water-column height (h) ensures that the euphotic layer still extends to the seabed (Figure 3.9). Overall, very similar levels of light are predicted to reach the seabed for depths <100 m (Figure 3.9).

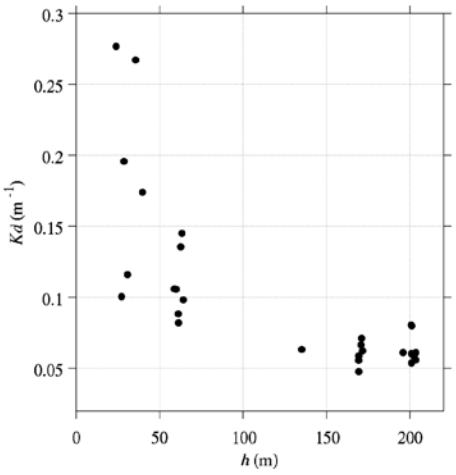

Figure 3.7. Variation of light attenuation rate (K_d) in King Sound and adjacent shelf region with shelf depth (h).

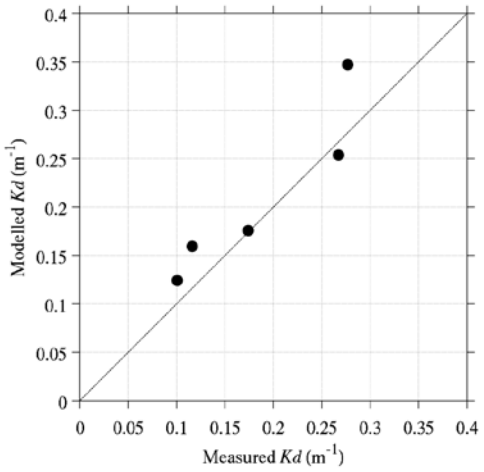

Figure 3.8. Comparison of attenuation rate (K_d) calculated from in-situ profiles ('Measured' K_d) with estimates made from Eq. 6 ('Modelled' K_d). Only data collected inshore of 50 m is shown.

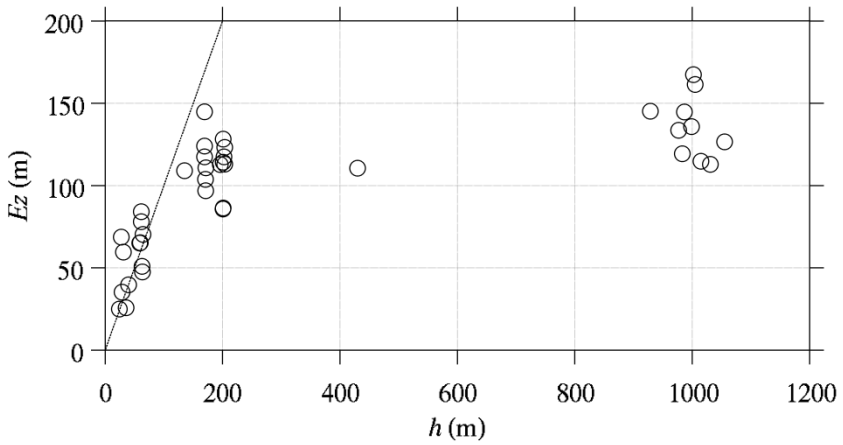

Figure 3.9. Variation in euphotic depth (E_z) with shelf depth (h) in King Sound and adjacent shelf region. E_z is defined by 1% of surface irradiance (E_z = -ln (0.01) / K_d). The solid line represents the condition E_z = h.

3.5.2 Collier Bay

The rates of attenuation observed across much of Collier Bay during October 2013 are generally higher than those observed in King Sound in May 2010, with most values between 0.2 and 0.5 m^{-1} (Figure 3.10). Even higher rates (~1.0 m^{-1} and greater) were observed in the vicinity of Walcott inlet, with rates approaching 100 m^{-1} recorded in the entrance to the inlet (Figure 3.10). In these extreme cases, 99% of surface irradiance is removed within a few cm of the surface, resulting in only a few data points and making accurate estimation of the attenuation rate from Eq. 1 difficult. Even so it is clear that very turbid conditions can occur in the innermost locations of Collier Bay and Walcott Inlet resulting in extremely thin euphotic layers. The results from Collier Bay also suggest that, in contrast to the outer King Sound area, very little light reaches the seabed anywhere within the bay, with euphotic depths that are typically 20 m or less, shallower than the seabed (Figure 3.11).

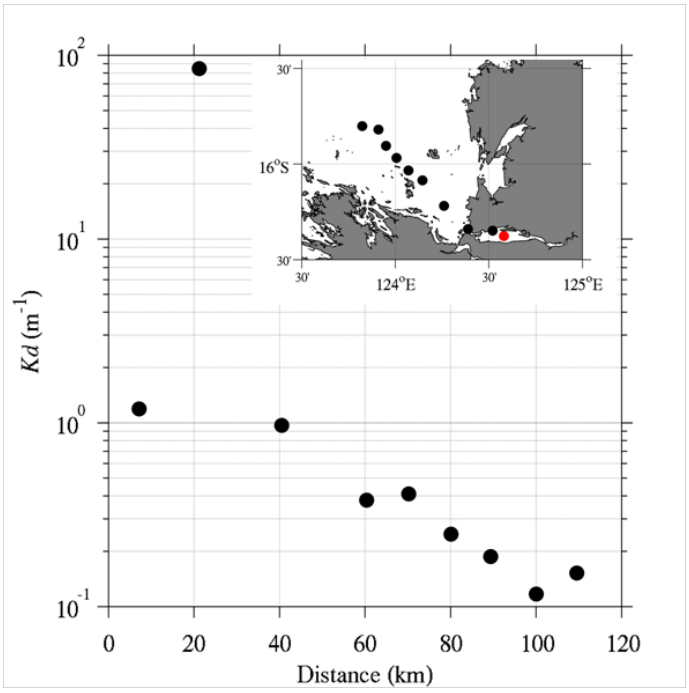

Figure 3.10. Variation of light attenuation rate (K_d) with distance along a cross-shore transect from ~20 km inside Walcott Inlet and out across Collier Bay. Inset map shows location for each K_d estimate (black circles) and point of zero distance (red circle).

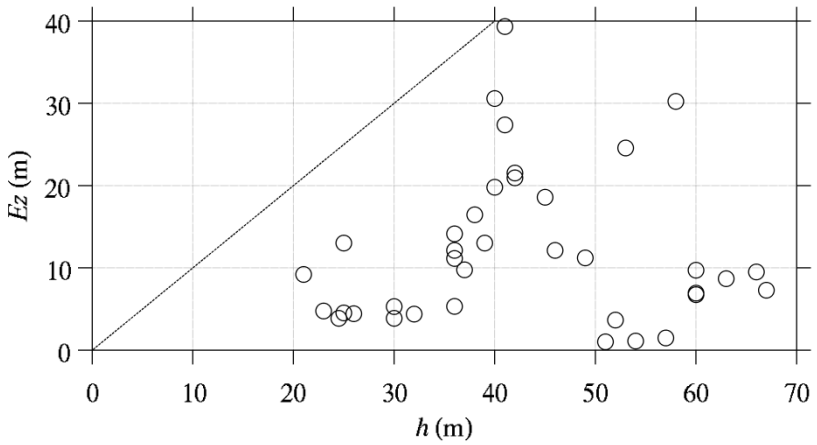

Figure 3.11. Variation in euphotic depth (E_z) with shelf depth (h) in Collier Bay and adjacent shelf region. E_z is defined by 1% of surface irradiance (E_z = -ln (0.01) / K_d). The solid line represents the condition E_z = h.

Variation in attenuation rate in Collier Bay is largely explained by changes in TSS, with a weak co-dependence on chlorophyll for the clearer waters at the outskirts of Collier Bay (Figure 3.12). The relationship is very similar to that already seen in the King Sound and summarized by Eq 3. Consequently, changes in euphotic depth in Collier Bay and in the vicinity of King Sound are accurately predicted using estimates of attenuation rate from Eq. 3.1 (Figure 3.13).

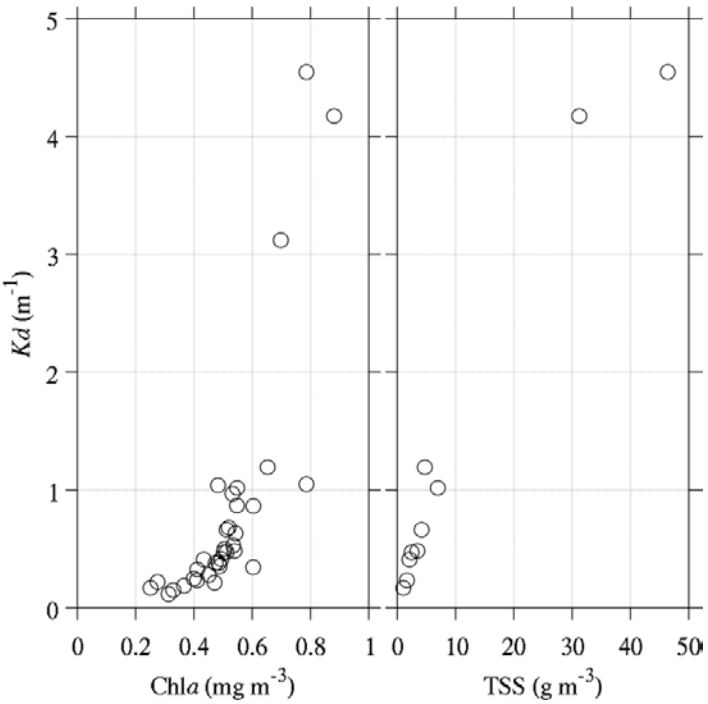

Figure 3.12. Variation of light attenuation rate (K_d) in Collier Bay with depth-averaged Chlorophyll (Chl$a$) and depth-averaged suspended solid concentration (TSS). Values of K_d greater than 10 m^{-1} have been omitted.

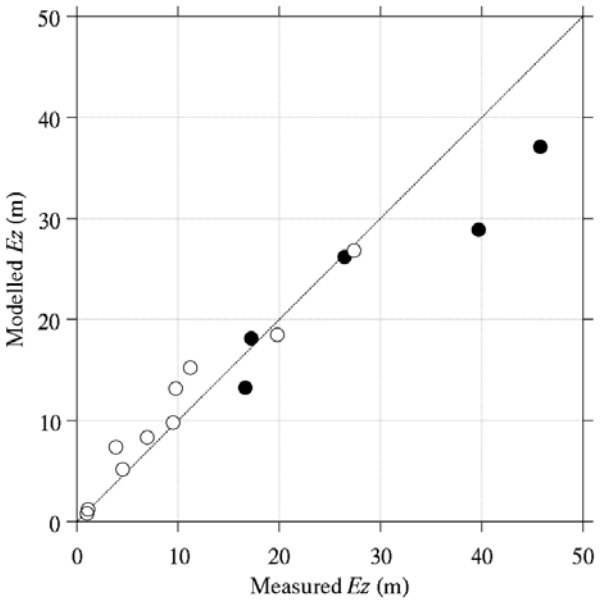

Figure 3.13. Comparison of euphotic depth in King Sound and adjacent shelf region (closed symbols) and Collier Bay (open symbols) calculated from in situ PAR ('Measured' E_z), and estimated from the attenuation model described by Eq. 3.1 ('Modelled' E_z).

3.6 Discussion

This analysis of the 2010, 2013 and 2014 cruise data has demonstrated the variability in cross-shelf salinity, temperature and oxygen, nutrients, chlorophyll, turbidity and light. The 2010 transects across the shelf show the ~250 m deep surface mixed layer across the shelf, with warm, nutrient deplete water in the surface, and cool, nutrient rich water deeper below. In deeper waters this leads to a deep chlorophyll maxima, with limited biomass seen near the surface, except in the shallow areas near the land interface, which show a chlorophyll peak throughout the water column. Some evidence for nutrient upwelling from the deep ocean to the shelf region is evident from the 2010 transects.

Within Collier Bay, high rates of vertical mixing mean there is little vertical structure in salinity or nutrients, and significant horizontal gradients in suspended sediment. This is similar to data presented in McKinnon et al. (2015) for the 2011 cruises (not shown here). In this region, relatively minor differences were seen in nutrient concentrations between the surface and bottom of the embayments, which is expected due to high rates of vertical mixing brought about by the large tides. Some vertical structure does occur when freshwater flows are high (Revill et al. 2017). The 2010 shelf-scale transects that extended further out from Collier Bay did indicate upwelling and a thin layer of elevated nutrients near the bottom, however, this did not extend all the way to Collier Bay, suggesting there is a distance off-shore where the effect of the vertical mixing no longer entirely dominates surface versus bottom differences water column properties.

The data showed the striking gradient in the light climate from the land-ward edge to the shelf edge of our study domain. Interestingly, the areas of very high light attenuation near the coast were coincident with high chlorophyll-a presence throughout the water column, suggesting a highly-adapted microbial community that is able to be maintained in this environment despite the high turbidities. The analysis of the sub-surface light data allowed us to parameterise the specific attenuation coefficients required to model the light field accurately for primary production estimation, as is required for the modelling work presented in later Chapters. To obtain further information about spatial and/or seasonal variability in TSS, it is desirable to be able to estimate TSS from satellite ocean colour. A procedure for extracting estimates of TSS from MODIS data to match-up with field measurements was explored and preliminary testing for the outer King Sound area has shown that a simple conversion factor (~2) may be adequate (Figure 3.14). It is noted though that these TSS concentrations

are relatively low and the relationship seen in Figure 3.14 may not necessarily hold at higher concentrations. Data collected in Collier Bay is expected to provide a more rigorous test of this approach as the TSS concentrations are considerably higher (Figure 3.10). Testing of in-situ versus satellite estimates of TSS for Collier Bay was undertaken in the WAMSI KMRPKMRP project 1.4?, and can further build upon relationships identified in this study.

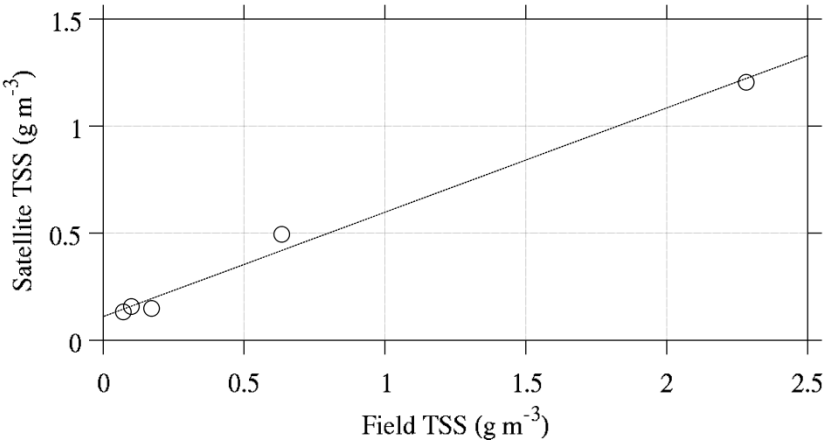

Figure 3.14. Comparison of field and satellite estimates of total suspended solid (TSS) concentration in the vicinity of the outer King Sound area.

4 Microbial Community Description

4.1 Introduction

The nature of the pelagic microbial community has had relatively little attention in Kimberley oceanic waters relative to comparable waters on the eastern edge of Australia, such as the Great Barrier Reef, or other waters of northern or southern Australia. The microbial community however forms the basis of biodiversity and fishery productivity for the region, and is potentially susceptible to changes brought about by climate change, or large-scale land-use development within Kimberley catchments. A focus on describing the microbial communities is therefore required to address Objective 1 of this project, and develop an underlying conceptual model.

Thomson and Bonham (2011) published an article based on the data from the 2010 Southern Surveyor, providing the most recent and comprehensive assessment of the Kimberley phytoplankton community to date. They identified that:

- >80% of the deep water phytoplankton were picoplankton (predominantly *Synechcoccus*),
- ~20% of the phytoplankton biomass was contributed to by coccolithophorids, and
- in the shallow waters close to shore, a decline in picoplankton was reported with a concomitant change in the phytoplankton community to be more dominated by medium to large diatoms.

Subsequently, McKinnon et al. (2015) undertook a detailed assessment of zooplankton within Kimberley waters based on data collected during the 2011 and 2013 (February) cruises. This analysis highlighted that:

- 78 species of copepods were identified, with marked changes in seasonal and spatial distributions across the region,
- distributions within embayments (particularly the southern embayments like Camden Sound) were mostly homogenous, owing to high rates of tidal-induced mixing, and
- relatively weak cross-shelf connectivity of groups was identified, relative to more noticeable along-shore connectivity.

This foundational understanding of the pelagic microbial community structure of the region has been built upon in this project, and new data collection efforts within the 2013 and 2014 cruises were undertaken to provide further detail and insight into the spatial heterogeneity in microbial groups along the Kimberley coast in particular, to identify how they vary seasonally, and also potential relationships among them. The aims of this Chapter are therefore twofold, to: a) address Project Objective 1 to describe the microbial community composition, and b) to address aspects of Project Objective 2 to ascertain the strength of food-web interactions. This is achieved through:

- collection of new picoplankton, phytoplankton and zooplankton size fraction data;
- plotting and analysis of phytoplankton and zooplankton data sourced from both cytometry, microscopy and including both newly collected and past datasets; and
- stable isotope analysis of particulate organic matter and zooplankton size fractions.

4.2 Data & Analyses

4.2.1 Historical data collation

The historical phytoplankton data presented in Thomson and Bonham (2011) for the 2010 cruise is curated and available via the *Australian Phytoplankton Database* initiative (Davies et al. 2016). This additionally includes other data sources spanning back to 1958 (albeit sparse), and contains over 9500 individual cell count entries for the north-west region. Zooplankton data as described in McKinnon et al. (2015) were also compiled.

4.2.2 Microbial community composition and abundance using flow cytometry

Samples were collected at all 24 h stations (every 2-6 h) as well as select stations throughout the region. Sample water was collected in 50 mL conical vial from each depth, homogenized and 1 mL collected in cryovials

with EM grade paraformaldehyde (0.5% final concentration). Sample and preservative were homogenized and left to fix for 10 min before being snap frozen in liquid nitrogen. Duplicate samples were collected at each station. Samples were run for viral, bacterial, and picoplankton enumeration sequentially.

Virus and Bacterial Quantification – Samples were thawed at 37°C for 2-3 min, homogenised and diluted 1:5 in Tris EDTA (pH = 8) into a 96 well plate. The diluted samples were stained with SYBR green at a final concentration of 5 x 10^{-5} v/v, mixed on a shaker plate and incubated in the dark at 80°C for 12 min (Patten et al. 2008). Fluorescent beads (Fluoresbrite YG Carboxylate Microspheres 0.5 µm) were added as an internal standard. Samples were run on a BD FACSCANTO II flow cytometer at a flow rate of 0.5 µl s^{-1} for 2 min. discriminating on SYBR fluorescence. Factors collected for each event include: forward scatter, side scatter, SYBR fluorescence (BP 530/30), phycobillin fluorescence (BP 585/42), and chlorophyll a fluorescence (LP 670).

Autotrophic Picoplankton Quantification – Samples were thawed at 37°C for 2-3 min and aliquots added to a 96 well plate. Fluorescent beads (Fluoresbrite YG Carboxylate Microspheres 1.0 µm) were added as an internal standard. Samples were run on a BD FACSCANTO II flow cytometer at a flow rate of 1 µl s^{-1} for 2 min. discriminating on chlorophyll a fluorescence. Factors collected for each event include: forward scatter, side scatter, SYBR fluorescence (BP 530/30), phycobillin fluorescence (BP 585/42), and chlorophyll a fluorescence (LP 670).

Post processing determination of groups was performed with Kaluza Flow Cytometry software v1.2 (Beckman Coulter, Inc.) using various gates and biplots of fluorescence to fully separate microbial sub-populations.

4.2.3 Phytoplankton community composition using High Performance Liquid Chromatography

Sub-samples of water drawn from Niskin bottles were filtered onto pre-combusted 25 mm glass-fibre filters (Whatman GF/F). The filters were placed in 3 ml cyro-vials and snap-frozen in liquid nitrogen. Samples were analysed in an automated UPLC system following the general protocols of Van Heukelem and Thomas (2001).

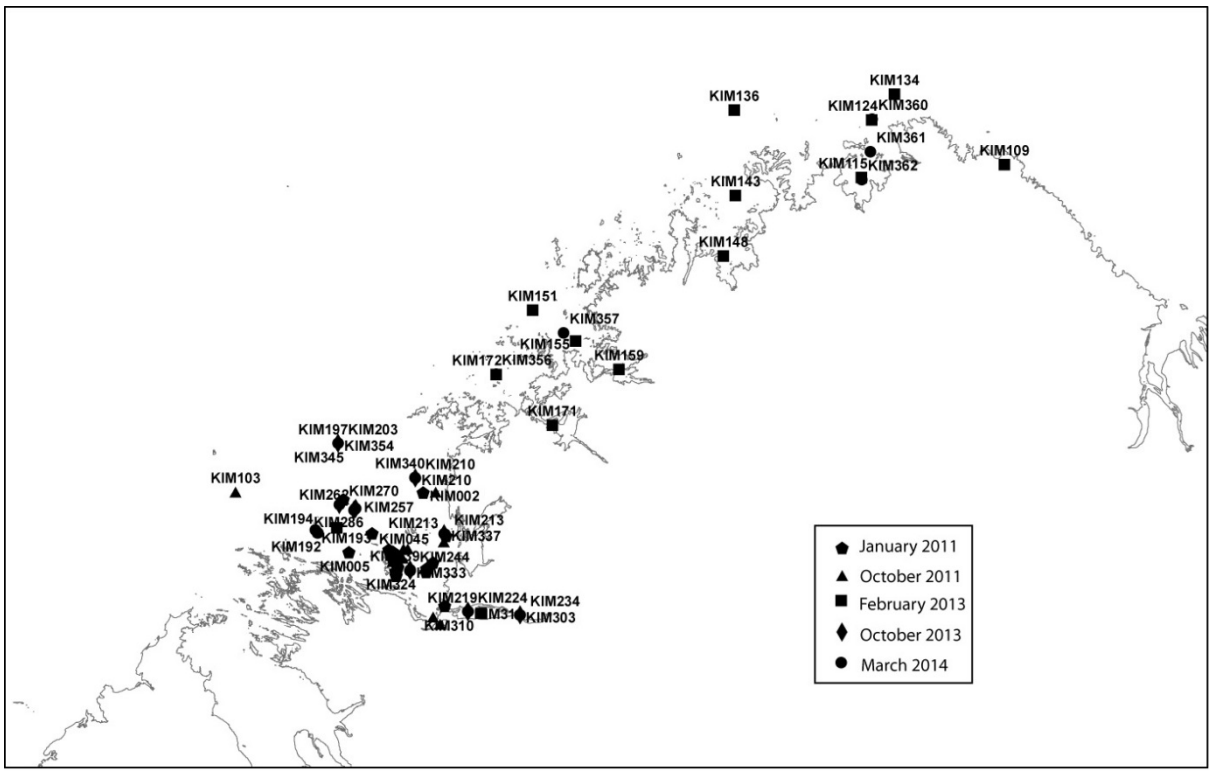

Figure 4.1. Stations occupied during the 5 Kimberley cruises for zooplankton enumeration.

4.2.4 Zooplankton biomass

Plankton samples were collected with a purpose-built bongo net that size-fractionates the *sample in situ* to more fully describe the size distribution of the zooplankton community (McKinnon et al. 2005). One side of the bongo net was fitted with a WP-2 net of 350 μm plankton mesh, and the other side with a 150 μm plankton net of 34cm diameter nested inside a 73 μm net of 50cm diameter. Therefore, this bongo net array allowed us to collect zooplankton samples fractionated *in situ* into the >350 μm, >150 μm and 73-150 μm size ranges. Hydrobios electronic flowmeters were mounted off-centre in the mouths of the 150 μm and 350 μm nets (Gehringer & Aron 1974). Each net sample was split into three portions: half was transferred into cryovials and frozen in liquid nitrogen for subsequent enzymatic assays, one quarter which was preserved in formaldehyde for analysis of community composition, and one quarter filtered on to a pre-weighed disk of 73 μm mesh and frozen. The frozen mesh was subsequently dried (65º) and re-weighed to estimate zooplankton community biomass as dry weight. The dried plankton was subsequently ground and analysed for C and N content on a Shimadzu CN analyser. Biomass in the 73-150, >150 and >350 μm size ranges was calculated directly from the samples taken from the respective nets, and the total biomass >73 μm was then calculated by summing the samples collected from the 73 and 150 μm nets.

4.2.5 Stable isotope analysis

2010 sample collection – Samples were collected using the CTD/Rosette from surface waters and zooplankton and POM were analysed for stable isotopes ($\delta^{13}C$ and $\delta^{15}N$) at the West Australian Biogeochemistry Centre, University of Western Australia.

2013 and 2014 sample collection – For both the dry and wet season experiment, sample water was collected using the CTD/Rosette from surface and near bottom depths at the three (near shore, mid, offshore) 24 h stations as well as from Walcott Inlet.

Size Fractionated POM – 2010, 2013, and 2014 – 2 L was sampled for the two size fractions (< 5 μm and >5 μm) were collected onto precombusted GF/Fs. Filters were snap frozen in liquid nitrogen aboard the vessel and transported back to the laboratory for processing and analysis. Samples were dried (60°C), acidified in fuming HCl (32%) for <12 h to remove calcium carbonate (Armitage and Fourqurean 2009). Acidified samples were dried again at 60 °C, then weighed and packaged into tin boats with the optimal N load of 50 μg. Samples were analyzed at the University of California (Davis) Stable Isotope Facility. Samples were run using Elementar Vario EL Cube or Micro Cube elemental analyzer (Elementar Analysensysteme GmbH, Hanau, Germany) interfaced to a PDZ Europa 20-20 isotope ratio mass spectrometer (Sercon Ltd., Cheshire, UK) with a long term standard deviation of 0.2 ‰ ^{13}C and 0.03 ‰ ^{15}N.

Size fractionated zooplankton - 2010, 2013, and 2014 – Zooplankton were collected using 100 μm and 350 μm bongo nets deployed off the stern of the ship. In 2010 the slurry was thoroughly rinsed with surface seawater and immediately passed through a series of screens, separating organisms at 4000, 2000, 1000, 500, and 200 μm. In 2013 and 2014 they were size fractionated into 73 μm, 150 μm and 350 μm. Slurry from cod end was transferred to a clean bucket and screened through a 37 μm sieve to remove seawater. One ml from each size class was snap frozen in liquid nitrogen aboard the vessel and transported back to the laboratory for processing and analysis. Samples were dried (60°C), acidified in fuming HCl (32%) for <12 h to remove calcium carbonate (Armitage and Fourqurean 2009). Acidified samples were dried again at 60 º?C, ground to a fine powder using a ball mill (7 min at high speed) then weighed and packaged into tin boats with the optimal N load of 50 μg. Samples were analyzed at the University of California (Davis) Stable Isotope Facility. Samples were run using Elementar Vario EL Cube or Micro Cube elemental analyzer (Elementar Analysensysteme GmbH, Hanau, Germany) interfaced to a PDZ Europa 20-20 isotope ratio mass spectrometer (Sercon Ltd., Cheshire, UK) with a long term standard deviation of 0.2 ‰ ^{13}C and 0.03 ‰ ^{15}N.

Representative zooplankton samples - 2010, 2013, and 2014 – Additional zooplankton samples were collected using a 500 μm bongo net. The slurry was transferred to a bucket and representative samples of common zooplankton groups were picked and snap frozen in liquid nitrogen. Target groups include: chaetognaths, larval

fishes, copepods, ostracods, zoea/juvenile crabs, siphonophores, isopods, ctenophores, lucifers, amphipods, shrimp, prawn, mysid, krill, other crustaceans, salps, polychaetes, pluteus, appendicularians, cnidarians, phyllosoma, puerulus, other groups may be collected depending on community composition at the station. Samples were dried (60°C), acidified in fuming HCl (32%) for <12 h to remove calcium carbonate (Armitage and Fourqurean 2009). Acidified samples were dried again at 60 ºC, ground to a fine powder using a ball mill (7 min at high speed) then weighed and packaged into tin boats with the optimal N load of 50 µg. Samples were analyzed at the University of California (Davis) Stable Isotope Facility. Samples were run using Elementar Vario EL Cube or Micro Cube elemental analyzer (Elementar Analysensysteme GmbH, Hanau, Germany) interfaced to a PDZ Europa 20-20 isotope ratio mass spectrometer (Sercon Ltd., Cheshire, UK) with a long term standard deviation of 0.2 ‰ ^{13}C and 0.03 ‰ ^{15}N.

Larval fish – 2010 – Larval and juvenile fish were also collected from the above net hauls. Using a dissecting microscope, larval fishes were sorted from the zooplankton and identified to the best possible taxonomic resolution. Fish larvae/juveniles were then placed into cryovials and frozen in liquid nitrogen. Where larvae were small (< 5 mm), more than one individual of the same species was included to ensure that there was enough biomass for the isotope analysis. In the laboratory, for fish larvae/juveniles that were < 5 cm, the whole fish sample was processed. When larvae/juveniles were ~≥ 5 cm, tail tissue was processed for isotope analysis by removing tail tissue from both sides of the fish and ensuring no bones, scales or skin were attached to the tissue. Fish larvae/juveniles were then oven dried, acid fumed and oven dried again as above for mesozooplankton, ground with a ball mill, weighed (ca. 0.5 – 0.6 mg) and packed into a tin boat for elemental and isotopic analysis as above.

Marine sediments – 2010 – Marine sediments were collected using a benthic sled from the 200 m isobath along Transect A. Samples were transferred to cryovials and frozen in liquid nitrogen until analysis. In the laboratory, marine sediments were dried at 60°C for 24 hrs, the sample grinded with a mortar and pestle, half the sample transferred to a vial and concentrated HCl added to the sediments until no bubbles were observed. All sediments were then dried at 60°C for 24 hrs, ground with a ball mill and sub samples (ca. 50 mg from the untreated samples for N analysis and 10 mg from acid fumed samples for C analysis) were weighed and packed into a tin boat for elemental and isotopic analysis as above.

Other samples of marine origin – 2010 – In addition to mesozoplankton and larval/juvenile fish samples, Sargassum sp. and Green filametous algae (species unknown), were also collected from the waters of King Sound, frozen and processed as for marine zooplankton. An adult *Euthynnus affinus* (Mackeral) was also caught by line fishing at the 50 m isobath along Transect B. Adult fish tissue was processed as above for fish ≥ 5 cm.

Riverine and terrestrial samples – 2010 – Coastal and terrestrial samples were collected from various locations (along the shore and inland) at Derby (latitude 125ºE 35.5 and longitude 17ºS 16 min), while riverine and terrestrial samples were further collected from the nearby Fitzroy River region. Water samples collected from Derby shore (30 ml) and Fitzroy River (400 ml), were filtered through pre-combusted GF/F filters, frozen and processed for elemental isotope analysis as described above for marine POM samples. Mesozooplankton samples were collected using a 120 and/or 350 µm mesh net , samples transferred to cryovials and frozen and processed in the same way as size fractionated (marine) mesozooplankton (above) except that ca. 1.4 – 1.5 mg sub-samples were weighed and packed into tin boats. Sediments were collected from Fitzroy River, frozen and processed as outlined above for marine sediments, except that for the treated samples for C analysis, sub-samples of ca. 20 mg were weighed and transferred into tin boat. Additional animals were also collected and frozen; a Clupeiform larvae was collected from Derby shore, a Mudskipper (from Derby Shore), a Mysid (from Derby Jetty) and an Intertidal Fly (from Derby). These animals were processed as above for mesozooplankton and larval fish except that 0.6 – 0.7 mg was weighed and transferred into tin boats. Leaves and grass were collected from various plants from Derby and on the banks of the Fitzroy River. Frozen samples were dried at 60°C for 24 hrs, leaves broken down in a coffee grinder and further homogenised using a ball mill. Sub-samples (1.0 – 1.1 mg) were then weighed and packed into tin boast for elemental analysis of C and N.

4.3 Phytoplankton distribution

4.3.1 Historical cell count data

Historical data entries from the Australian Phytoplankton Database that sit within the study region were collated and are displayed in Figure 4.1. These plots summarise five main groupings of species in the database, indicating the frequency (number of unique entries), the relative biovolume, and the cell counts recorded.

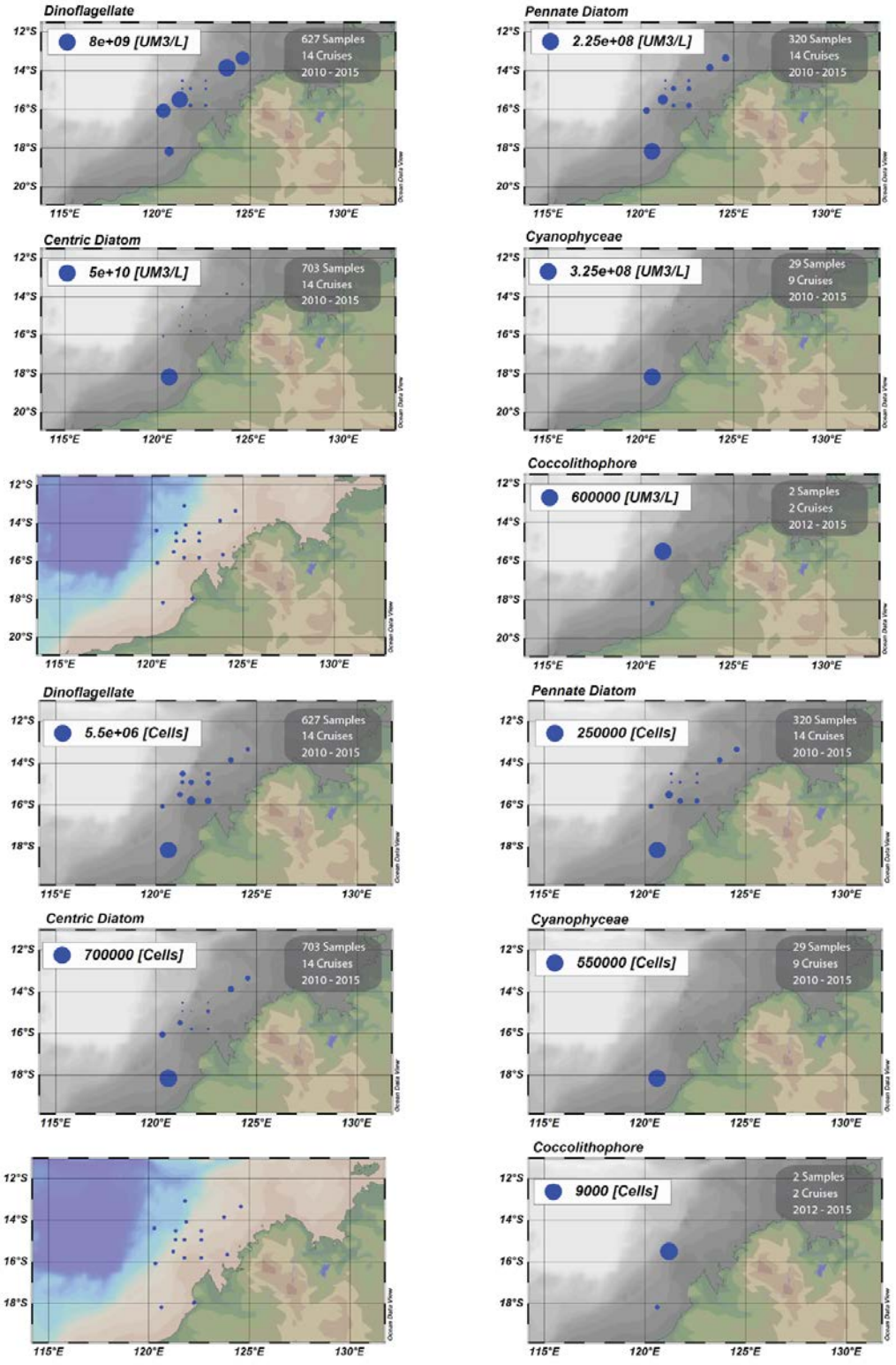

Figure 4.2. Summary of entries in the Australian Phytoplankton Database for the Kimberley, presented as biovolumes (top panels) and cell counts (bottom panels) for five key groupings. Sampling locations are indicated in the bottom left panel.

4.3.2 Regional variation in phytoplankton size fractions

The size fractionated chlorophyll-a data is shown in Figure 4.3. Overall, the biomass was not found to be considerably higher along the coast than elsewhere, as might be expected from the chlorophyll flouresence shown in Chapter 3, however, note these are depth-averaged outputs. The data shows the transition from dominance by the <2 um size fraction at the shelf-edge to a dominance of the >10 um size fraction along the coastal margin, with an intermediate community across the shelf, and this is generally consistent with the earlier reports of Thompson and Bonham (2011). Notably, the picophytoplankton fraction is still consistently present in the samples taken from the bays and areas near the coast, albeit as a smaller relative fraction. These are explored in more detail in the next section.

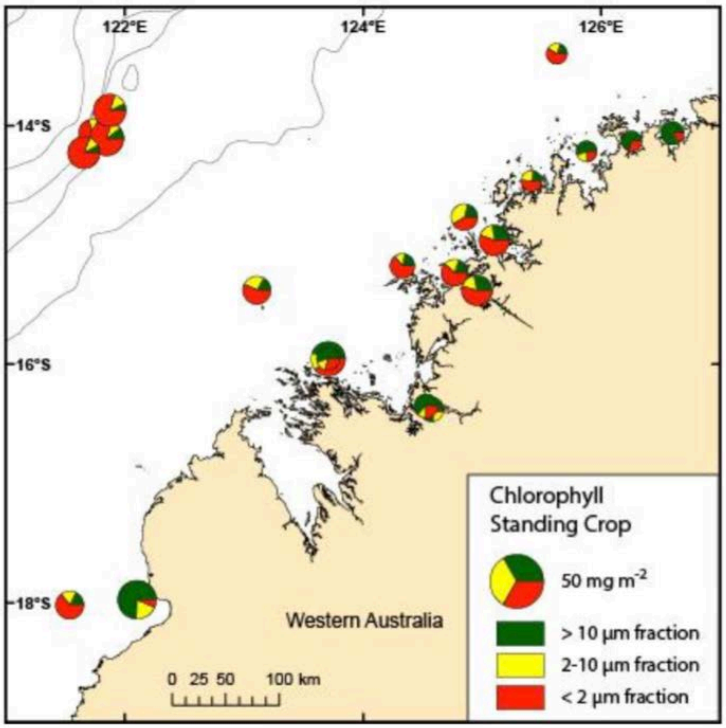

Figure 4.3. Spatial variability in size fractions and chlorophyll biomass, as measured using HPLC. Symbol size indicates overall biomass, and the <2um (red) fraction refers to picophytoplankton.

4.3.3 Picoplankton community

The picoplankton community was assesed in more detail within Collier Bay using flow cytometry and demonstrated high variability and weak trends in most of the enumerated populations (Figure 4.4). The counts of bacteria and viral particles were of a simialr magnitude (~10^3 cells/60 uL), with lower conceptrations of picocyanobacteria (approximately $5x10^2$ and $1x10^2$ cells/60 uL for *Prochlorococcus* and *Synechococcus*, respectively), and lower concentrations still of picoeukaryotic algae (~1 cell/60uL).

Statistical assessment of the relationship between cell concentrations of the picoplankton community and environmental factors was undertaken using PRIMER, however no statistically significant relationships were identified within the dataset and hence are not shown. It therefore remains difficult to conclude what are the dirvers of population variability in the region based on this dataset.

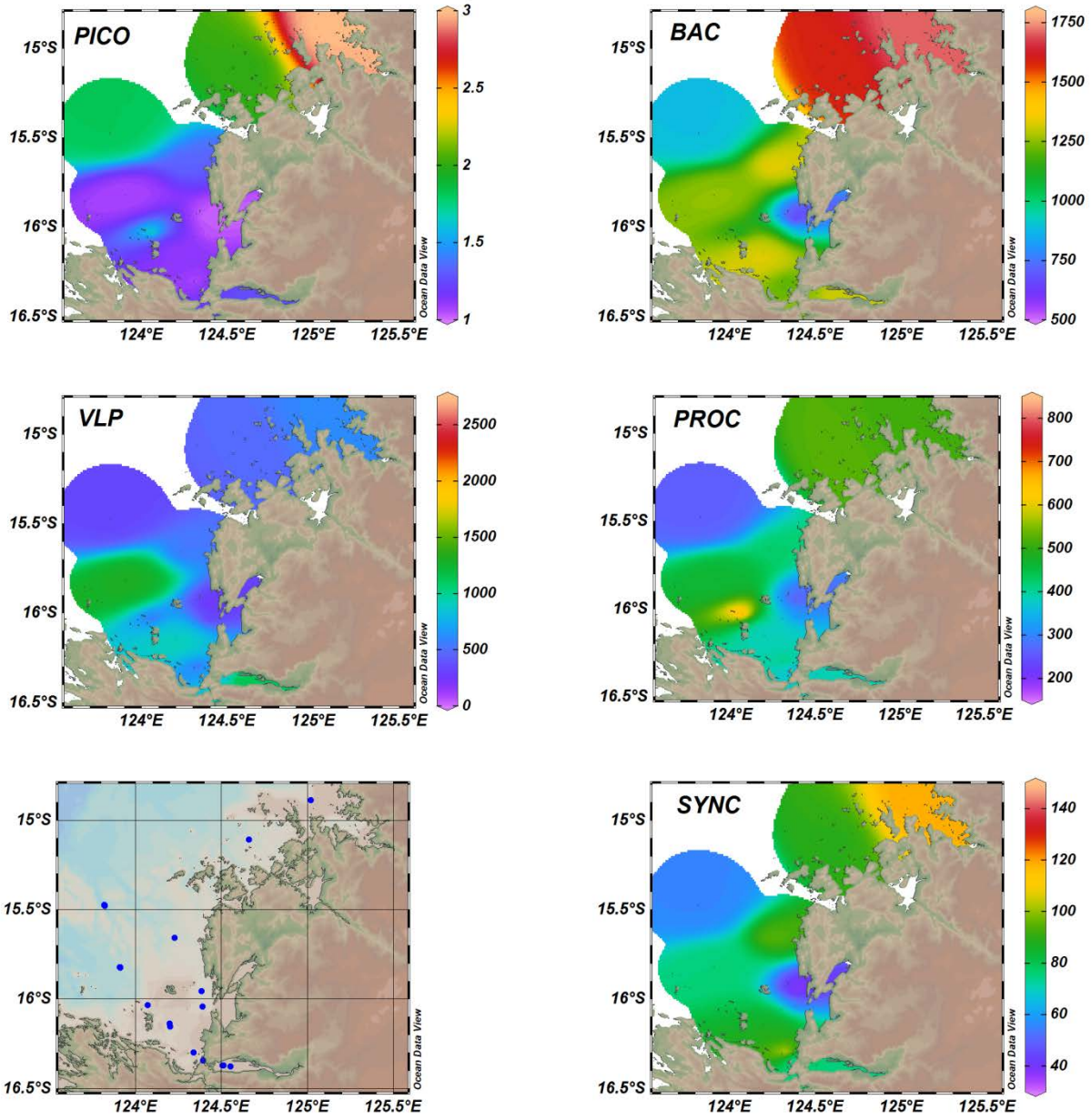

Figure 4.4. Variation of concentrations (#/60uL) of picoeukaryotes (PICO), bacteria (BAC), virus-like-particles (VLP), *Prochlorococcus* (PROC) and *Synechococcus* (SYNC) within the Collier Bay region, taken during the 2013/2014 cruise. Data are based on averages of samples taken at the bottom, mid and surface depths, and different times of the sampling.

4.4 Zooplankton distribution

4.4.1 Community composition

The zooplankton community composition has been described for the Kimberley coast on the basis of the 2011, 2013 and 2014 research voyage datasets, and this has been compared to earlier studies conducted in adjacent regions (North West Cape, Scott Reef and the Arafura Sea). This work is described in some detail in McKinnon et al (2015), to which readers are referred; a summary of the compiled dataset for the region is shown here for completeness, and is outlined in Figure 4.5.

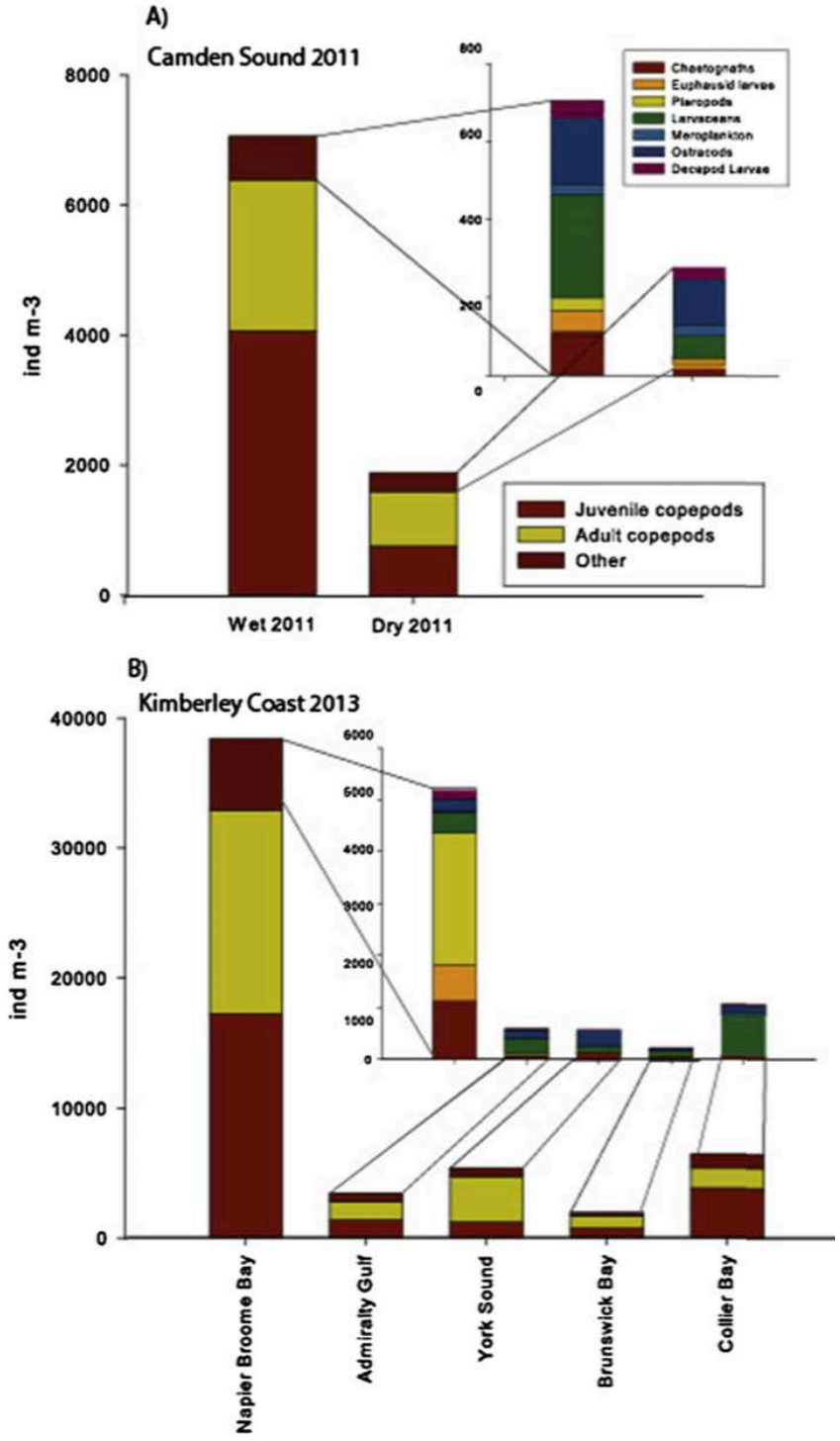

Figure 4.5. Zooplankton community composition of the Kimberley coast. (taken from McKinnon et al. 2015). Note the non-copepod fraction is expanded.

4.4.2 Zooplankton biomass

Overall, the average >73 μm biomass was 148.24 mg DW m^{-3} (Table 4, as sum of the 73-150 and >150 μm size fractions). The small size fraction (73-150 μm) comprised <9% C and <2% N, indicating that there was a substantial inorganic component in this fraction, probably re-suspended fine sediment. The larger fractions comprised ~18% C and 4.5% N, indicating that they included mostly organic material, putatively zooplankton, with a C:N ratio ~4. For comparison, (Harris et al. 2000) report the dry weight of small zooplankton is 14.8-42.8 % C, and 1.8-5.6 % N, and the average C:N ratio of copepods, the most common component of the Kimberley zooplankton samples, is 5.16. Given the low C:N ratio of the >150 μm and 350 μm size fractions in our samples, the N-content is probably the best indicator of live zooplankton biomass in these turbid waters.

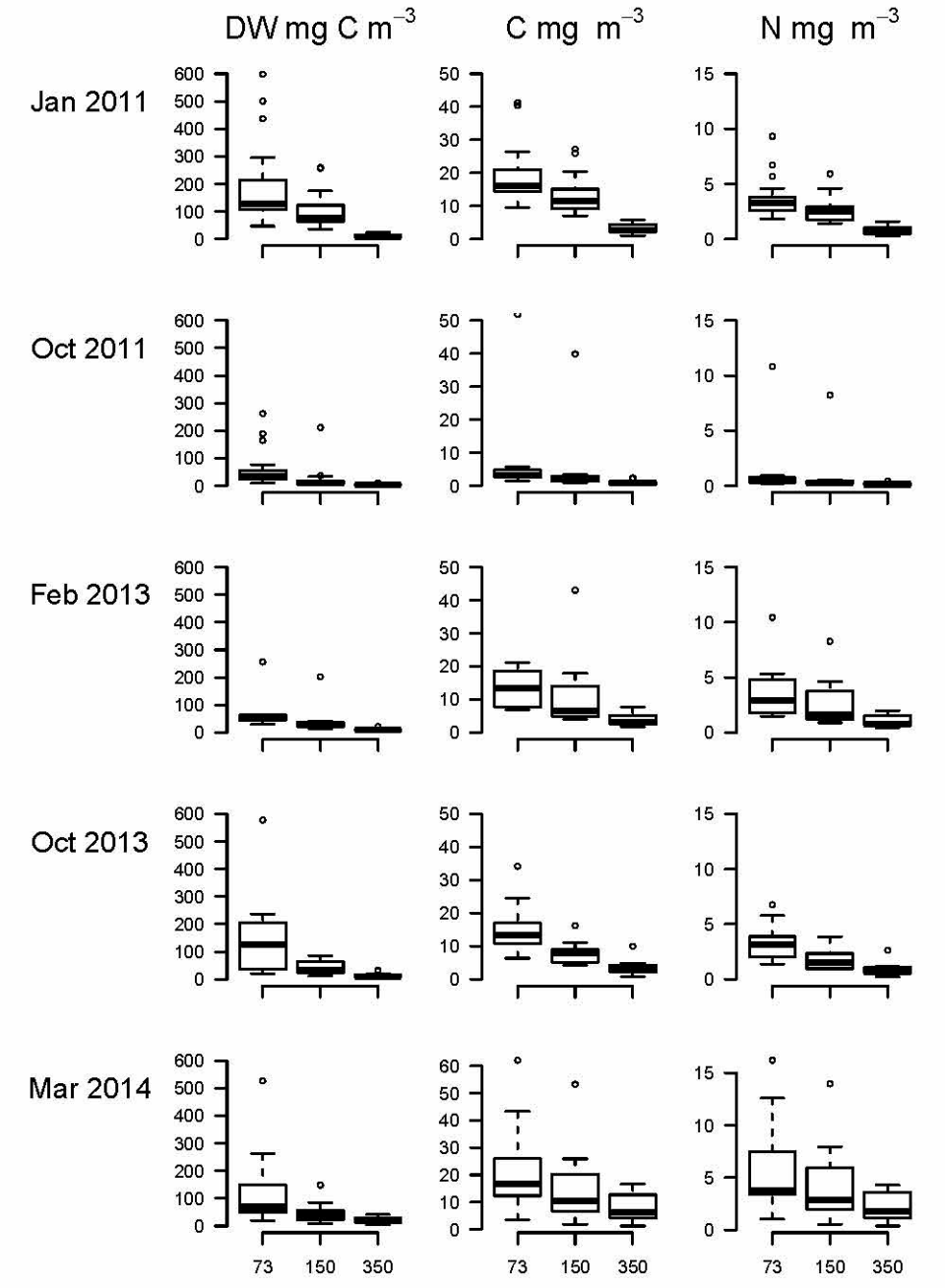

Figure 4.6. Zooplankton biomass in three size fractions (>73 µm, >150 µm, >350 µm) aggregated over all stations shown in units of dry weight (DW), carbon (C) and nitrogen (N).

Box plots of the biomass data highlight the occurrence of extreme outliers in the data. For example, samples taken at KIM064 in Camden Sound in October 2011 and at KIM175 in Walcott Inlet in February 2013 far exceed the values seen on other occasions (Figure 4.6). The cause of the high values observed at KIM064 is unclear, but might have resulted from the accumulation of plankton as a result of physical processes around the Kingfisher Islands. In the case of KIM175, there was a massive diatom (*Dactyliosolen* sp.) bloom in Walcott Inlet that resulted in the finer nets clogging and retaining particles of a size that would normally pass through. In neither of these cases was there an outlying value in the >350 µm size class.

Table 4.1. Mean values of zooplankton dry weight (DW), plus carbon, nitrogen (as mg m^{-3}) and protein aggregated over all stations in each of the three size fractions sampled by the bongo net, and their ratios by weight.

Mesh	*DW*	*C*	*N*	*Protein*	*C:DW*	*N:DW*	*C:N*
73-150µm	66.25	5.79	1.27	1.08	0.087	0.019	4.542
>150 µm	81.99	14.62	3.63	3.51	0.178	0.044	4.025
>350 µm	41.36	7.26	1.94	3.06	0.175	0.047	3.749

4.5 Stable isotope analysis

Stable isotope assessment can reveal the relative strength of connections within the food web and potentially the dominant sources of nutrition (Middleburg 2014; Espinasse et al. 2014; Yang et al. 2017). The range of samples processed for stable isotope assessment (refer to section 4.2.5) in this project was substantial, creating a novel dataset for the region.

The carbon and nitrogen concentration of each sample was plotted to determine any initial differences in the C:N relationship between samples from different trophic levels, or location within the domain (Figure 4.7). The results indicate a separation in the C:N ratio of the Collier Bay samples relative to those from the shelf and King Sound waters, and therefore the relative N enrichment in the embayment samples.

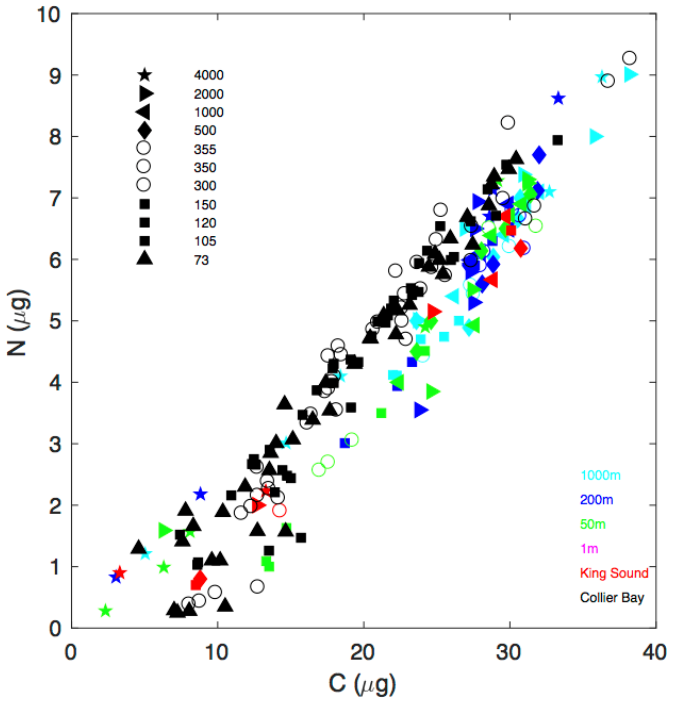

Figure 4.7. C:N relationship from all the zooplankton samples sent for stable isotope analysis, classified according to the location (1, 50, 200, and 1000m depth contour, plus King Sound and Collier Bay), as well as planktonic size fraction, ranging from <73µm to >4000µm). Note the Collier Bay data was from the 2013 and 2014 cruises, and all other data was from the 2010 cruise (refer to Chapter 2).

Stable isotope results are shown in Figure 4.8 for the POM and zooplankton samples. POM $\delta^{15}N$ is greatest for samples collected from the 50 m isobath, indicating a regenerated source of nutrients, which is potentially associated with shelf upwelling. This increased $\delta^{15}N$ signature is less apparent in the samples collected further offshore (200 m isobath), and the smaller size fraction at 1000 m. The only significant size fractionation in $\delta^{15}N$ POM signatures is found in the samples furthest offshore. Lower $\delta^{15}N$ signatures in the smallest size fractions of phytoplankton has been observed in the Sargasso Sea and is attributed to the smaller size fractions utilizing newer nitrogen sources (Fawcett et al. 2011). Zooplankton $\delta^{13}C$ and $\delta^{15}N$ differ among all samples (King Sound to 50 m, 200 m and 1000 m, and Collier Bay). When looking specifically at the smaller zooplankton from the

2010 Southern Surveyor transects, $\delta^{13}C$ and $\delta^{15}N$ show an onshore to offshore trend with $\delta^{13}C$ and $\delta^{15}N$ heavier in shallow water.

Collier Bay samples have reported values of $\delta^{13}C$ between -6 – -26 ‰ with many of the total POM samples > -15‰. This potentially indicates samples contaminated with carbonate, which could occur if sample acidification did not fully remove the inorganic material prior to analysis. By averaging the dataset (Figure 4.8c&d), the enrichment of zooplankton relative to POM becomes apparent, and a tendency for more enrichment of the shelf samples. Some of the >4000 µm zooplankton samples show depletion in their carbon content relative to the smaller size fractions, however, most of the larger zooplankton size fractions >500 µm are located in the centre indicating their integrating role and utilization of diverse food sources.

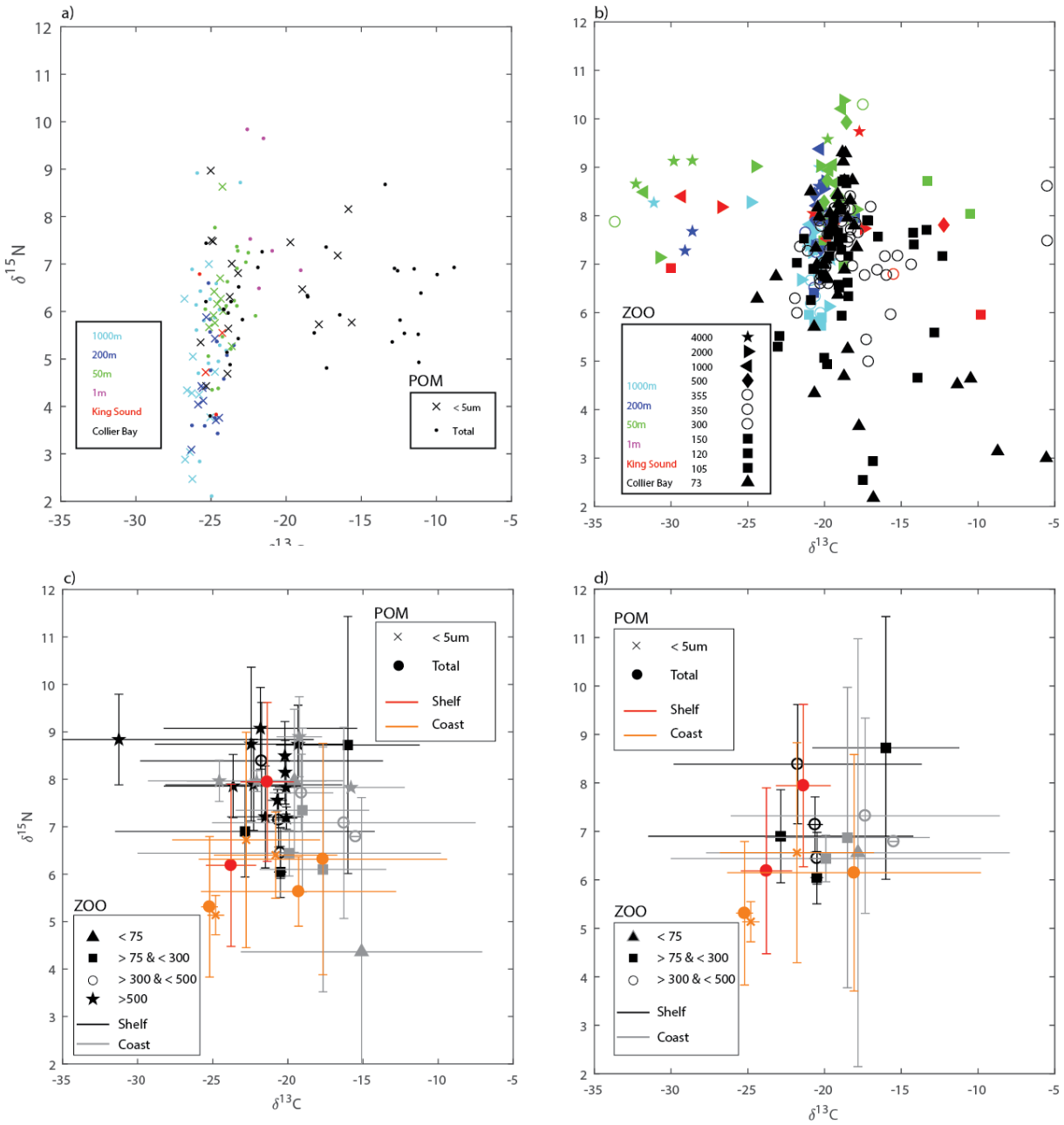

Figure 4.8. (a) Carbon and Nitrogen isotopic composition of POM of the <5 µm filtered and total fractions, as a function of distance offshore, b) zooplankton (ZOO) according to location / isobath depth, for the various size fractions captured over the three cruises, c) both POM and zooplankton average ratios lumped according to size and classified as being a “coast” (King Sound, Collier Bay and 1m) or “shelf” (50m, 200m and 1000m) sample, and d) as for c but without the larger planktonic groups for clarity.

4.6 Summary and conceptual model

This Chapter has provided a general overview of the microbial community on across the Kimberley shelf and provided new insights into the planktonic community, particularly within the embayments and near the coastal margin. Based primarily on the 2010 cell count data during the Southern Surveyor voyage, the phytoplankton groupings had previously been characterised to be mainly comprised of the picoplankton *Synechococcus* in the deeper waters with diatoms increasingly dominant inshore of the 50 m contour (see Thompson and Bonham 2011 for a more detailed discussion). Whilst the cyanobacteria *Trichodesmium* was identified this was relatively sparse in the available sampling. The additional size-fractionated data for the region collected subsequent to 2010 confirms the general trend, and shows the transition from <2 µm organisms at the shelf-edge to a dominance of >10 µm size fraction along the coastal margin, with an intermediate community across the shelf. Depth-integrated chlorophyll concentrations were largely comparable within the near-shore and shelf samples. The cytometry data that was collected during 2013 and 2014 within Collier Bay indicated the presence of *Synechococcus* and *Prochlorococcus*, in addition to providing information on the typical cell counts of bacteria and virus-like particles. Together these datasets allow us to partition biomass into relevant classes and develop a functional classification for model design that should separate primary producers into discrete groupings including diatoms, and picocyanobacteria, and potentially also considering the flagellates.

Zooplankton were demonstrated to be consistently partitioned across the size distributions with the greatest mass in the 75-150 µm fraction, less within the 150-350 µm fraction, and the least within the >350 µm size (Figure 4.6). Notably, the total zooplankton biomass is ~3–4-fold higher in the Kimberley than on the GBR in all three size classes (see McKinnon et al. 2016), highlighting the productive nature of Kimberley waters. The C:N ratios of POM and zooplankton highlighted higher nutritional content of samples collected near the coast across the size spectrum.

To advance our conceptual understanding of the main pathways to production we can use this dataset to better define the dominant pools of biomass within the water column, and when interpreted in light of the inter-relationships between the identified groups, this can be used as a basis for subsequent biogeochemical modelling. The stable isotope analysis has provided empirical insights into the potential strength of connections and source of nutrition to help us define these inter-relationships. The isotope data was difficult to interpret but did provide evidence of upwelling of deep nutrients as a source of nutrients in the shelf samples and a more terrestrial supported food web in the near-shore regions. Further analysis however is suggested for unravelling this data.

Based on interpretation of these data sets, a (purposefully) simplified conceptual model of interactions along the Kimberley coast is depicted in Figure 4.9. Chapters 5 and 6 provide estimates of the strength of pathways in this diagram, with a focus on primary and secondary rates of production, respectively. Chapters 7 and 8 then implement simplifications of the depicted relationships within the numerical hydrodynamic-biogeochemical models.

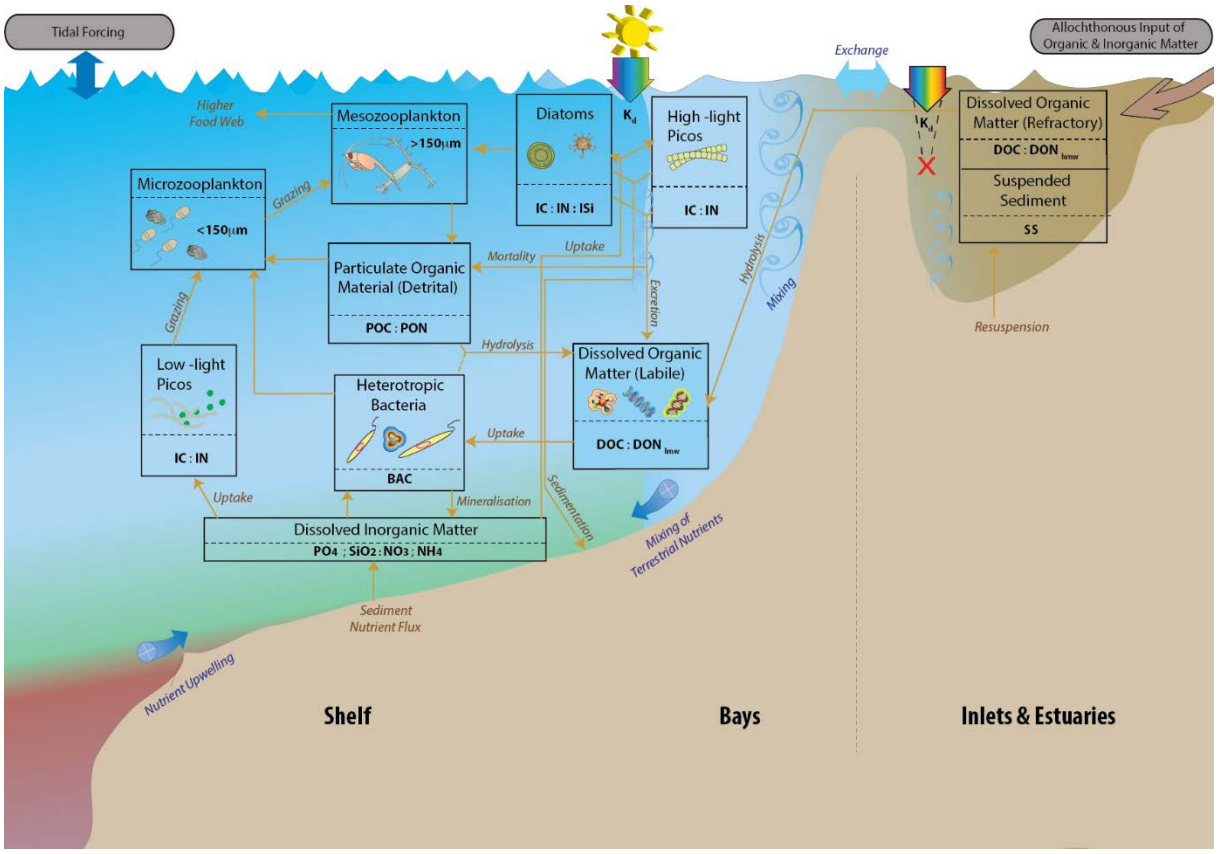

Figure 4.9. Conceptual model depicting main flow of carbon and nitrogen in Kimberley waters, considering the gradient in conditions from the coastal inlets to the shelf-edge.

5 Primary Production

5.1 Introduction

The presence of primary producers in Kimberley waters is described in the previous Chapter, however, to allow an understanding of ecosystem function and to develop modelling tools it is necessary to directly estimate the rates of primary production observed in the field. Prior work by Furnas and Carpenter (2016) reported a summary of estimates of daily primary production (in the context of chlorophyll a standing crop), and the contribution of picoplankton measured at primary production stations across a broad range of continental shelf waters spanning northern Australia. From this dataset the first estimates of spatially integrated productivity were provided with results ranging from 600-1800 mg /m^2 /d in the Kimberley region, which were similar to values reported to the north of and east of Australia. However, from this data it is not possible to generalize these estimates given for the Kimberley since there were a limited number of stations sampled, and only one station sampled from a "coastal" environment. Furthermore, questions remain as to the drivers of productivity over the region, for example, the sensitivity of productivity to light in both deep and coastal phytoplankton populations, and also how productivity is impacted by the high tidal range and vertical mixing rates. Therefore, in this study, field and numerical experiments were conducted with the aim to quantify productivity across a wider range of coastal habitats/environments, and secondly to resolve the main drivers of pelagic phytoplankton productivity in near-shore and shelf waters. Productivity experiments were conducted at selected stations during three cruises (see Section 2 for cruise details) covering the region of Walcott Inlet and Collier Bay and King Sound, and the adjacent shelf region. The productivity experiments consisted of on-deck incubations of unfiltered water from different depths, and under controlled light conditions. This provided sets of productivity versus irradiance (P-I) curves for each location that were used for the parameterization of light-limited phytoplankton growth, and to calculate depth integrated productivity rates. To help understand the photosynthesis-light relationship in the context of the large vertical mixing rates in the Kimberley, we also examine the vertical distribution of phytoplankton and nitrate at several locations in Collier Bay using a one-dimensional (vertical) model to elucidate how vertical mixing and turbidity influence pelagic productivity.

5.2 Methods

Different experimental techniques, described in the following two sections, were used for the photosynthesis versus irradiance experiments conducted either during the RV Southern Surveyor 2010 cruise (King Sound and adjacent shelf; Figure 5.1), or during one of the RV Solander 2013 and 2014 cruises (Collier Bay/Walcott inlet; Table 5.1).

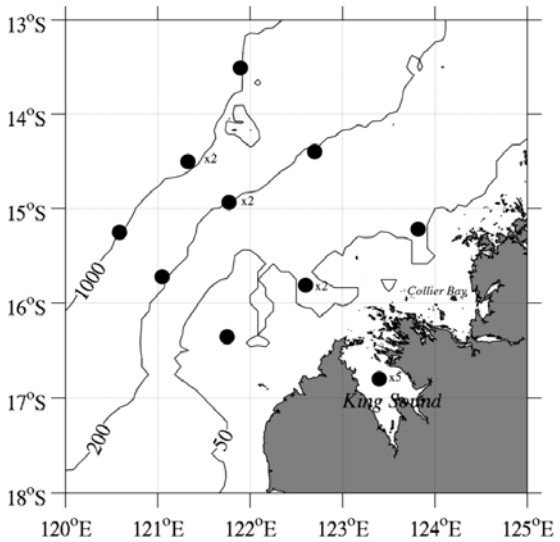

Figure 5.1. Location of 2010 productivity stations within King Sound and on adjacent shelf (solid circles). Multiple stations along the central transect (5 inside King Sound and 2 in the vicinity of each of the offshore locations) are omitted for clarity where the labels 'x#' indicates the number of repeated stations occupied at each approximate location. Note that where multiple stations are indicated these were occupied at different times (and slightly different locations) during the cruise and represent separate experiments and not duplicates. Contour lines indicate approximate position of the 50, 200 and 1000 m isobaths.

Table 5.1. Stations where size-fractionated primary production experiments (March 2013) and P vs I experiments (October 2013, March 2014) have been undertaken on AIMS cruises. See Figures 2.2 and 2.3 for station locations.

Expt #	*March 2013* *Size-fractionated production*	*October 2013* *P vs I*	*March 2014* *P vs I*
1	115 (Napier-Broome Bay)	196	283
2	135	210	292
3	151	219	297
4	161 (Hunter River)	231	316
5	173 (Walcott Inlet)	235	321
6	175 (Walcott Inlet)	251	330
7	180 (Walcott Inlet)	254	336
8	192 (outer Collier Bay)	268	351
9	194 (outer Collier Bay)		356
10			361
11			362

5.2.1 RV Southern Surveyor 2010 productivity incubation methods

This sub-section describes the method used to estimate phytoplankton productivity during the 2010 Southern Surveyor cruise. A small sample volume (7 mL) ^{14}Carbon (^{14}C) uptake method was used with a photosynthetron incubator. Water samples collected during night-time casts were stored at cool temperature in the dark until processing and incubation on the following day. A working solution for each depth was created by inoculating sample water with ^{14}C (as $NaH^{14}CO_3$) to a final concentration of 1.0 µCi per 1.0 mL seawater. Duplicate aliquots from each sampling depth were incubated for approximately 1 h at seven main light levels, ranging from 0 to 750 µE m^{-2} s^{-1} determined via a Biospherical Instruments Inc. 2100 PAR logger, by using combinations of spectrally resolving blue filters. Within each main light level, duplicates were exposed to slightly different irradiance levels by variability in the light output through distance between the light tubes in the incubator resulting in a total of up to 12 separate light levels (plus dark) per experiment. Two 100 µL aliquots of spiked water from each depth were analysed to determine the total initial ^{14}C activity, as were duplicate 7 mL time zero samples. Continuous surface seawater flow through the photosynthetron was used to regulate the temperature for all incubations. Experiments were terminated through the addition of 0.25 mL of 6M HCl, and placing the samples in an orbital shaker at ~180 revs min^{-1} for ca. 24 h to drive off any excess ^{14}C as CO_2. All samples were counted on-board the ship using an LKB Rackbeta liquid scintillation counter the following day.

5.2.2 RV Solander 2013 - 2014 productivity incubation methods

Photosynthesis versus irradiance (P-I) experiments conducted onboard the RV Solander during October 2013 were carried out using a solid-state LED-based photosynthetron. Irradiances between 0 and 750 µE m^{-2} s^{-1} were set by placing the scintillation vials (36) used for incubations in close proximity (<10 mm) to individual high-intensity cool-white LED's. The maximum intensity (approx. 750 µE m^{-2} s^{-1}) was determined by the distance between the brightest LED at full voltage (12V DC) and the incubation vial. This distance was originally set as a compromise between maximum irradiance intensity (as close as possible) and the need for an air gap to allow fan cooling of the bottom of the vials. In all, 36 individual samples could be incubated in the photosynthetron at one time. Three 'dark' vials (light excluded) and three poisoned vials (controls) were incubated separately (described below). At full intensity, the LED's produced very little heat, so air cooling and an aluminium heat sink were found to be sufficient to keep samples at ambient temperature during incubations. Irradiances across the range used were set by regulating the voltages to twelve banks of three LED's. Variability in the light outputs of individual LED's within each bank produced a spread of incubation intensities across the range used. Incubation light intensities produced by each LED were measured with a LICOR PAR sensor pressed against the

bottom of each incubation-well. Because of the high turbidity of Kimberley coastal waters, spectral influences on attenuation of PAR underwater are minimized. As a result, direct 'cool-white' light from the LED's was felt to be more representative of the coastal light regime than light from blue LED's or blue-filtered white light.

For the incubations 10-ml aliquots of raw seawater were dispensed into 42 clean glass scintillation vials. The vials were spiked with 1 µCi of 14C-bicarbonate and incubated for four hours. Three vials were incubated in the dark (dark control) and three vials were poisoned with formalin (killed control). At the end of the incubation, the photosynthetron lights were turned off and the contents of each vial quickly killed with 100 µL of formalin. The vial contents were then acidified (< pH 2) with 100 µL of full-strength HCl and gently sparged with air for 1 hour to drive off all DIC. The vials were then tightly closed and returned to AIMS for scintillation counting.

Prior to the March 2014 cruise, the photosynthetron was modified to increase the maximum irradiance to approximately 1600 µE m^{-2} s^{-1}. No significant heating of incubation vials was observed at the highest light intensities. All other procedures were the same as used in 2013, as described above.

5.3 Regional variation in primary productivity

Analysis of the productivity data collected along the across shelf transects during the 2010 cruise is shown in Figure 5.2a. These values are normalized by chlorophyll concentration at each location, and indicate that the coastal phytoplankton are relatively more efficient than the off-shore phytoplankton, with a rapid decline in areal productivity with increasing distance off-shore (Figure 5.2b). The productivity rates are able to be put in context with others taken from Northern Australia by comparing against the historical summary of rates by Furnas and Carpenter (2016). This highlights that the productivity rates are as high as other locations in northern Australia, despite the relatively high rates of light attenuation.

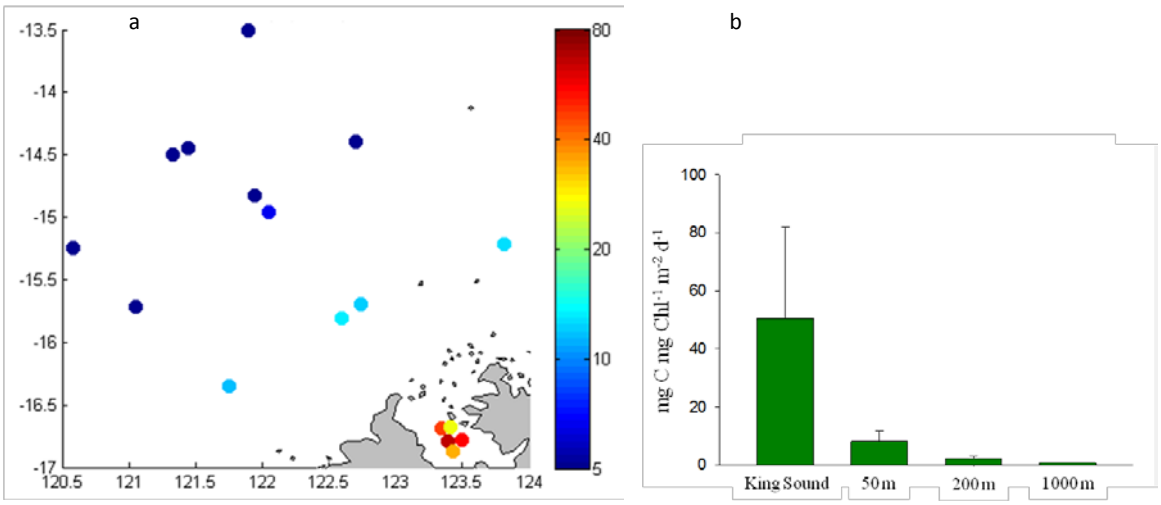

Figure 5.2. (a) Map of depth-integrated productivity rates (mg C mg Chl^{-1} m^{-2} d^{-1}) for King Sound and adjacent shelf region. Approximate station position in relation to shelf bathymetry is as shown in Figure 5.1. (b) Comparison of depth-integrated productivity by shelf position for the 2010 data.

When looking at the size-fractionated productivity undertaken in subsequent cruises, it is evident that the <2 µm fraction is able to contribute a sizeable amount of the overall productivity, exceeding 60% in many of the sites. Collier Bay however, did show high productivity of the large size class, >10 µm. As with the 2010 data, these data also indicate a general trend of high productivity closer to the coast, with lower rates off-shore.

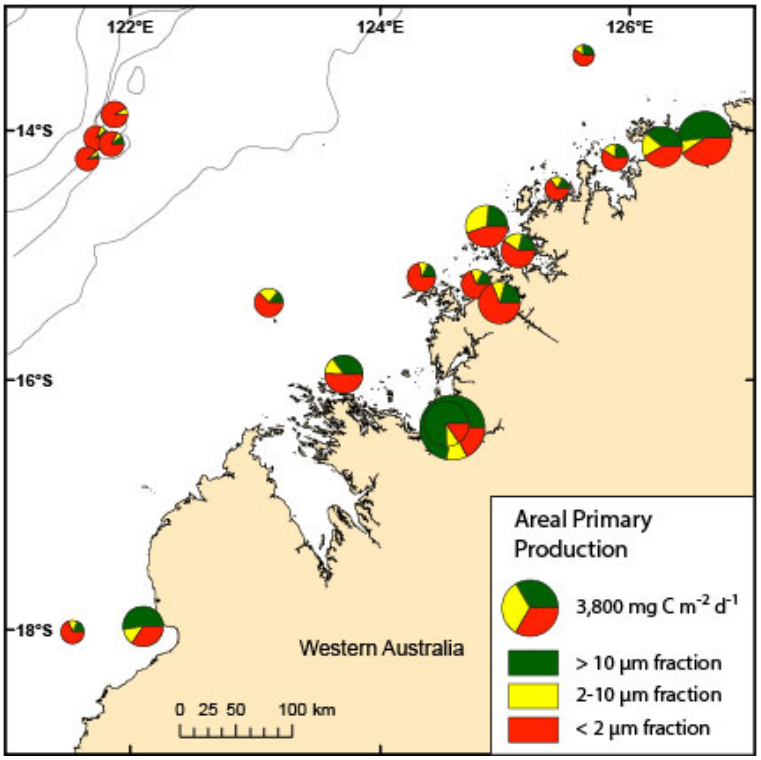

Figure 5.3. Summary of all size-fractionated areal primary production data. Note size of symbol correlates with primary production intensity of the total community.

5.4 Photosynthesis-Irradiance results

5.4.1 King Sound and adjacent shelf

Photosynthesis-irradiance data collected for King Sound and the adjacent shelf (a total of 75 curves) were fitted (using the Matlab © function `nlinfit`) to the model of Platt et al. (1980), using the equation:

$$P = P_s\left(1 - e^{-\alpha I/P_s}\right)e^{-\beta I/P_s} \tag{5.1}$$

where P_s is the light saturated photosynthetic rate in the absence of photoinhibition, α is the initial slope of the productivity irradiance response, β is an index of photoinhibition, and I is irradiance. The maximum photosynthetic rate, P_{max} is calculated as:

$$P_{\max} = P_s\left[\alpha/(\alpha+\beta)\right]\left[\beta/(\alpha+\beta)\right]^{\beta/\alpha} \tag{5.2}$$

A strong cross-shelf trend in phytoplankton-irradiance response was identified, with phytoplankton communities closer to the coast, and especially within King Sound, exhibiting lower initial slopes, higher maximum photosynthetic rates, and little evidence of photo-inhibition (Figure 5.2). The results for King Sound showed very little variation in irradiance response with water-column depth (Figure 5.3). For stations outside of King Sound the maximum photosynthetic rate (P_{max}) decreased, photo-inhibition (β) increased, and the initial slope of the curves (α) was largely unchanged, with water-column depth (Figure 5.3).

Daily rates of chlorophyll-adjusted, depth-integrated primary production were calculated from the photosynthetic parameters (P_{max}, α, β), chlorophyll-*a* measurements, and in-situ light conditions. Depth integration was from the surface to the base of the euphotic layer defined by 1% of the surface irradiance. To estimate the in-situ light conditions, deck board irradiance data collected at 5 minute intervals (via a Li-Cor LI-192SB Quantum Sensor in air) and a theoretical sine curve of "cloudless" irradiance based on date and latitude was corrected for wind roughening, solar elevation and zenith angle to provide 24 hour in-water surface irradiance estimates. Attenuation of surface irradiance was made according to measured PAR profiles at each

location. Highest productivity rates (mg C mg Chl^{-1} m^{-2} d^{-1}) were observed in King Sound (Figures 5.4), despite relatively turbid conditions and low levels of dissolved nitrogen.

5.4.2 Collier Bay

A total of 12 photosynthesis-irradiance data sets collected at various locations within Collier Bay during October 2013 and March 2014 have been examined. Results from Collier Bay showed no obvious sign of photo-inhibition, allowing an immediate simplification of Equation 3 by *setting β* equal to zero:

$$P = P_s\left(1 - e^{-\alpha I / P_s}\right) \tag{5.3}$$

In this case, P_{max} is numerically equal to P_s, and α retains its earlier meaning as the initial slope. The Collier Bay data were fitted to Equation 5, using the MATLAB function `nlinfit`.

Results from October suggest that P_{max} was not reached in one of the experiments (Figure 5.5a), and only barely reached in several others, within the range of irradiance measured (Figures 5.5b-f). This makes estimation of P_{max} potentially risky (or not possible at all in the case of Figure 5.5a). Nevertheless, results were found to be reasonably consistent between sites with estimates of P_{max} ranging from 5.27 to 10.18. Estimates of α (ranging from 0.01-0.04) are less likely to be affected by this problem and are expected to be more reliable.

Following the suspected truncation problem encountered in the Oct 2013 experiments, the irradiance range was doubled for the March 2014 experiments to try to obtain a better estimate of P_{max}. Unfortunately, in three cases (Figures 5.6a, c and f), scatter in productivity rates estimated at the highest irradiances, still compromised the estimation of P_{max}. For the March 2014 data set, values of P_{max} were generally higher (ranging from 10.21 to 19.70) than estimated for October. The highest estimate of 19.70 appears to result from two unusually high readings made toward the end of the experiment (Figure 5.6d) and could be rather misleading (note that for that reason it is omitted from averaged values presented later in Table 5.2). One of the six experiments in Collier Bay during March sampled sub-surface water at 26 m (Figure 5.6). This result shows little difference from the others that were conducted with water sampled from 2 m water depth.

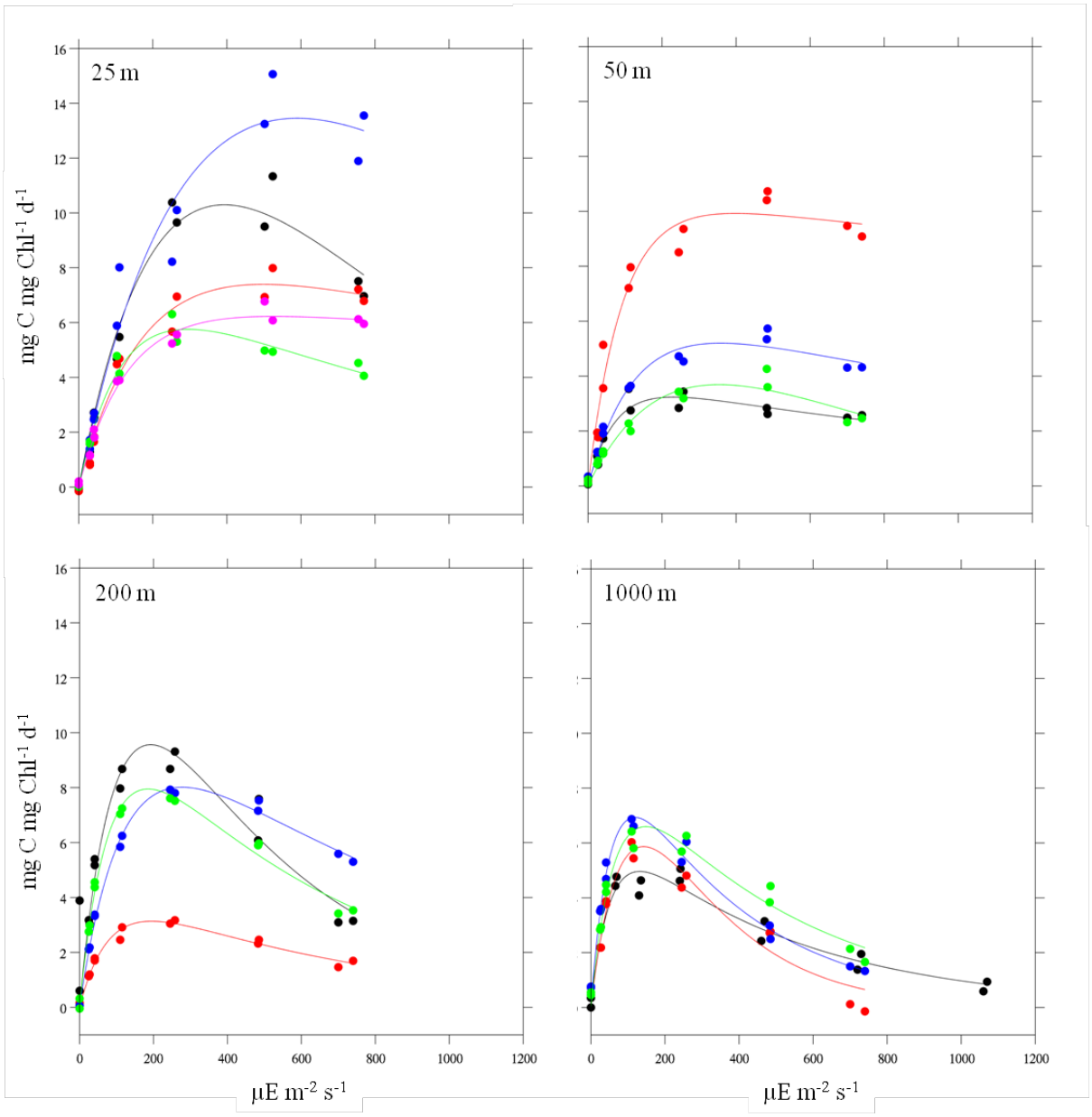

Figure 5.2. Photosynthesis-irradiance response measured at 10 m water depth for shelf positions with seabed depths of 25 m (i.e. King Sound), 50 m, 200 m and 1000 m. At each cross-shelf position the colours represent separate sample stations (4 for each of the mid and outer shelf positions, and 5 for King Sound). The solid lines represent non-linear fittings of equation 5.1.

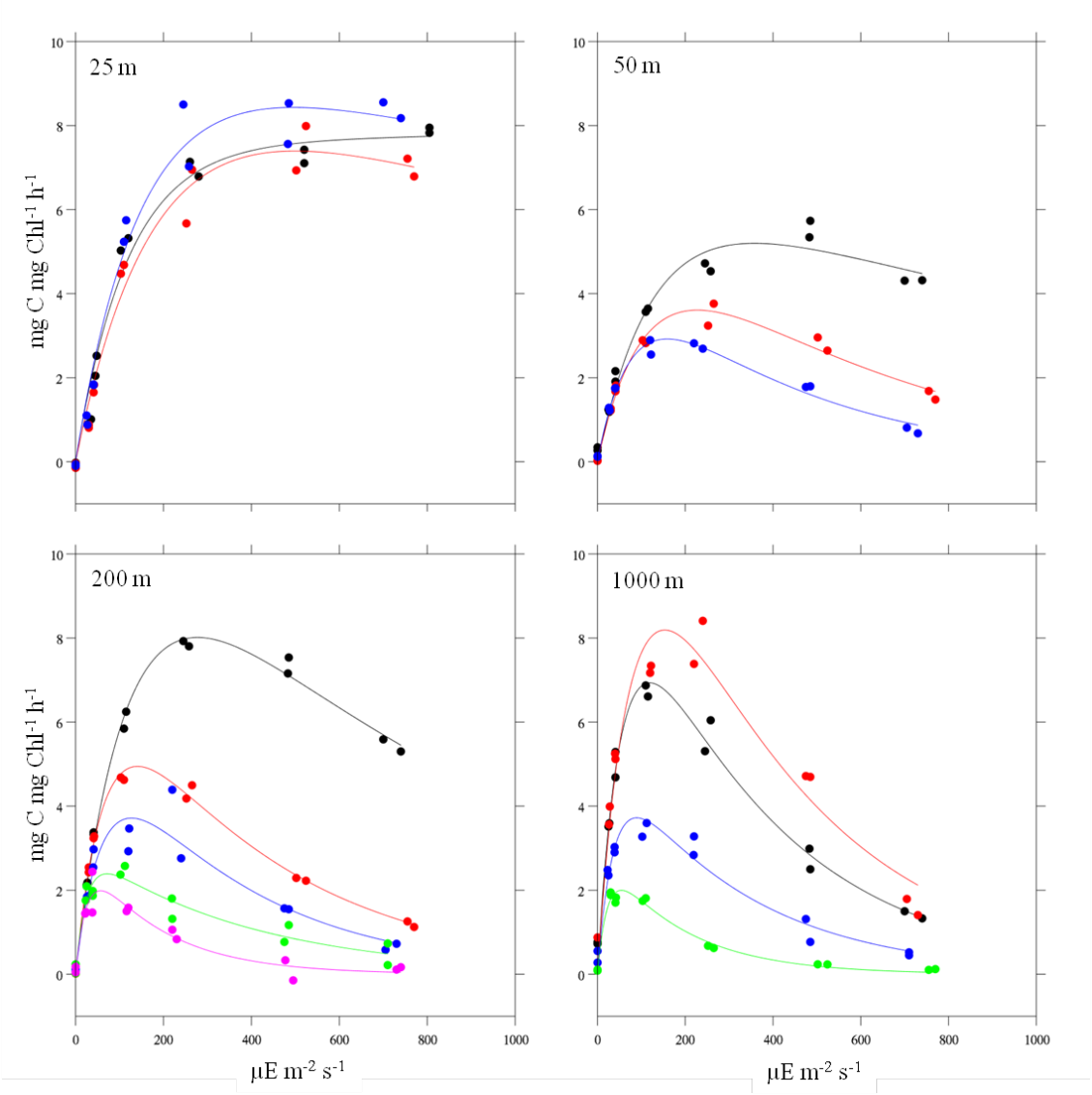

Figure 5.3. Typical variation in irradiance response with water-column depth at each shelf position. For King Sound (25 m) colours represent water-column depths of 0 (black), 25 (red), and 50 m (blue). For the other three shelf locations (50, 200 and 1000 m) colours represent water-column depths of 10 (black), 25 (red), 50 (blue), 75 (green) and 100 m (magenta). The solid lines represent non-linear fittings of Equation 5.1.

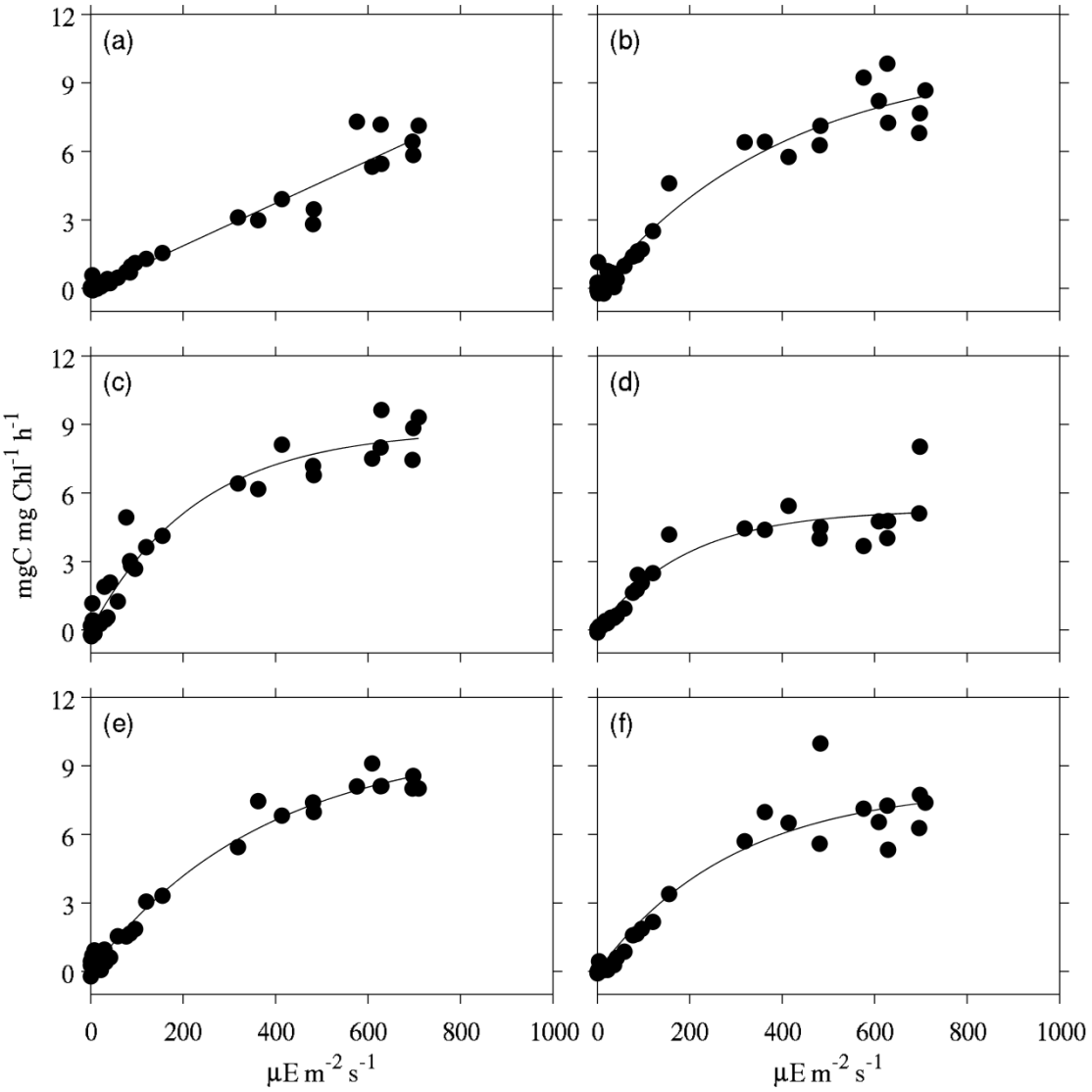

Figure 5.5. Photosynthesis irradiance response in Collier Bay (2 m below the surface) during October 2013. Each panel represents a separate location in Collier Bay. Solid line represent non-linear fitting of Equation 5.3. Note that P_{max} could not be estimated for (a).

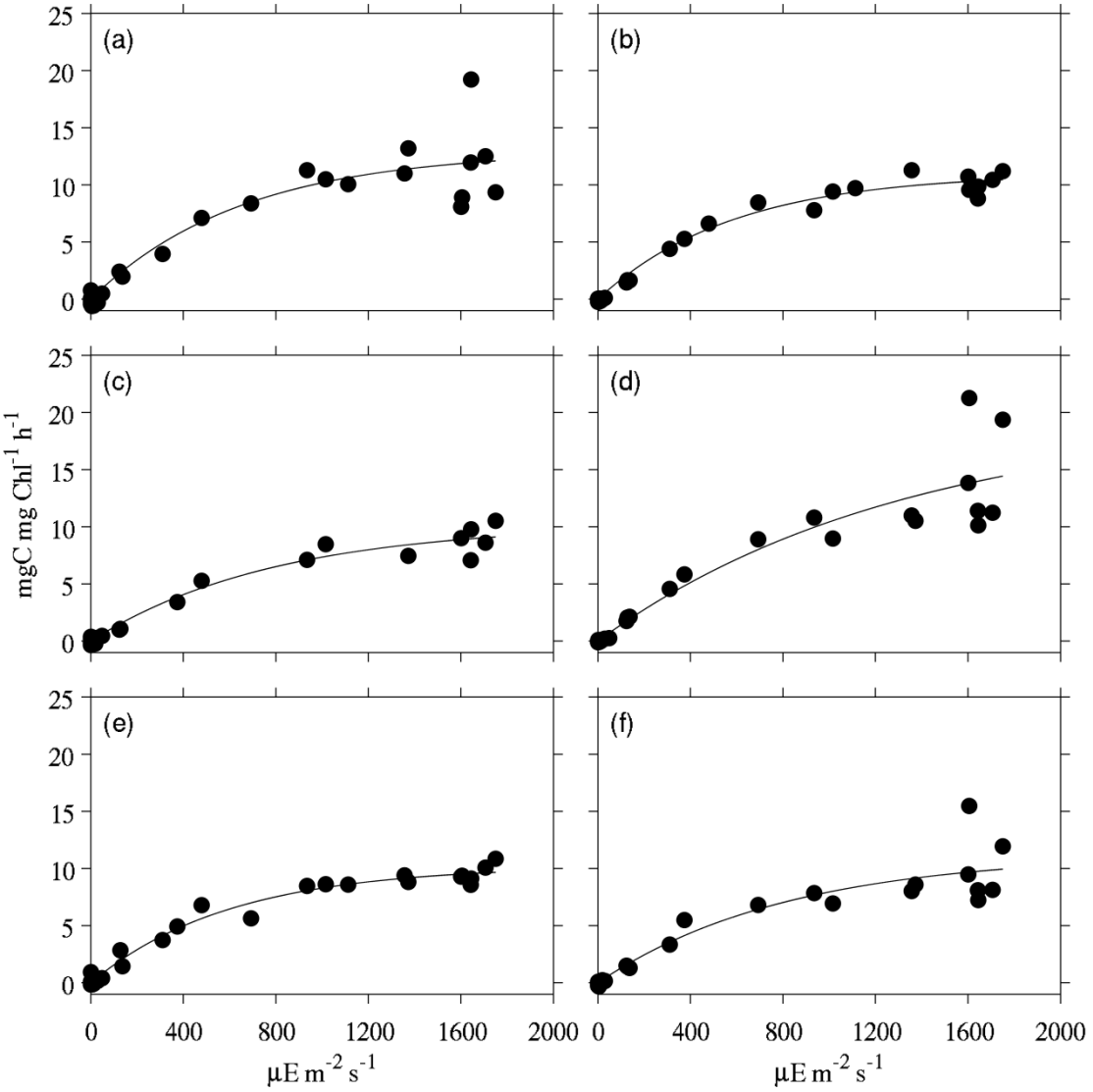

Figure 5.6. Photosynthesis irradiance response in Collier Bay during March 2014. Each panel represents a separate location in Collier Bay. The experiment reported in panel (b) was conducted at 26 m water depth. All others were conducted at 2 m water depth. Solid lines represent a non-linear fitting of Equation 5.3.

5.5 Controls on the vertical distribution of productivity within Collier Bay

In this section, we examine repeat vertical profiles of temperature, salinity, chlorophyll florescence, nitrate concentration and total suspended solid (TSS) concentration collected at three locations in the vicinity of Collier Bay, representing the Inner Bay (40 m water depth), Outer Bay (40 m water depth) and Shelf (70 m water depth) sub-regions (Figure 5.7). A steady-state one-dimensional (vertical) model (Greenwood and Craig 2014) is then employed to help understand how changes in underwater light and vertical mixing impact on the vertical distribution of phytoplankton and nitrate in the bay.

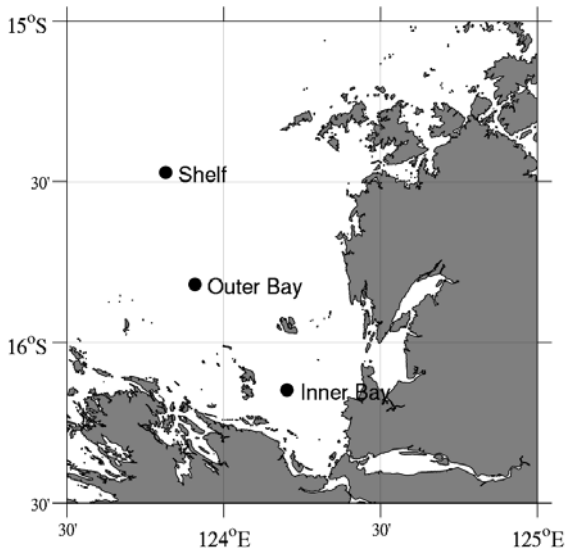

Figure 5.7. Position of repeat measurement stations representing the Inner Bay, Outer Bay and Shelf, sub-regions.

5.5.1 Observations

At each site (Figure 5.7) measurements of temperature, salinity, and chlorophyll were made approximately every two hours, while measurements of nitrate and TSS were made less frequently. The frequent measurements of temperature, salinity and chlorophyll are expected to resolve any changes in the vertical structure related to tides. This reveals that relatively little change takes place over the course of one day, with the main differences being observed either between sites or at different times of the year (Figure 5.8).

Both the inner and outer bay sites show evidence of strong density stratification in March (wet season). This results mainly from vertical variation in salinity (not shown) presumably as a result of freshwater runoff. We suspect that the continuous addition of freshwater at the surface in the wet season maintains the vertical density gradient at the bay sites despite tidal stirring which acts to overcome it. In contrast, during the dry season (October data set) reduced freshwater input is associated with close to uniform vertical density profiles at both bay sites (Figure 5.8). Vertically uniform density profiles in both data sets at the shelf site suggest that relatively strong mixing extends throughout the whole water column in dry and wet seasons. This condition is also reflected in the close to uniform profiles of chlorophyll, nitrate and TSS observed at the shelf site.

One of the most interesting biological differences between the two bay sites is that nitrate concentration increases more rapidly with depth at the inner bay site than it does at the outer bay site (Figure 5.8). However, despite the difference in nitrate, at least in the October data set, total phytoplankton biomass (inferred from chlorophyll concentration) at the two sites is very similar. The other important point is that water clarity is reduced at the inner bay site with a vertical light attenuation rate of ~0.2 m^{-1} compared with ~0.1 m^{-1} at the outer bay. It was our hypothesis that the two results are connected, and this is therefore tested with a simple model. We also investigate whether a combination of decreased water clarity (vertical light attenuation of 0.35 m^{-1}) and enhanced mixing at the shelf site can explain the vertical profiles of chlorophyll-a and nitrate.

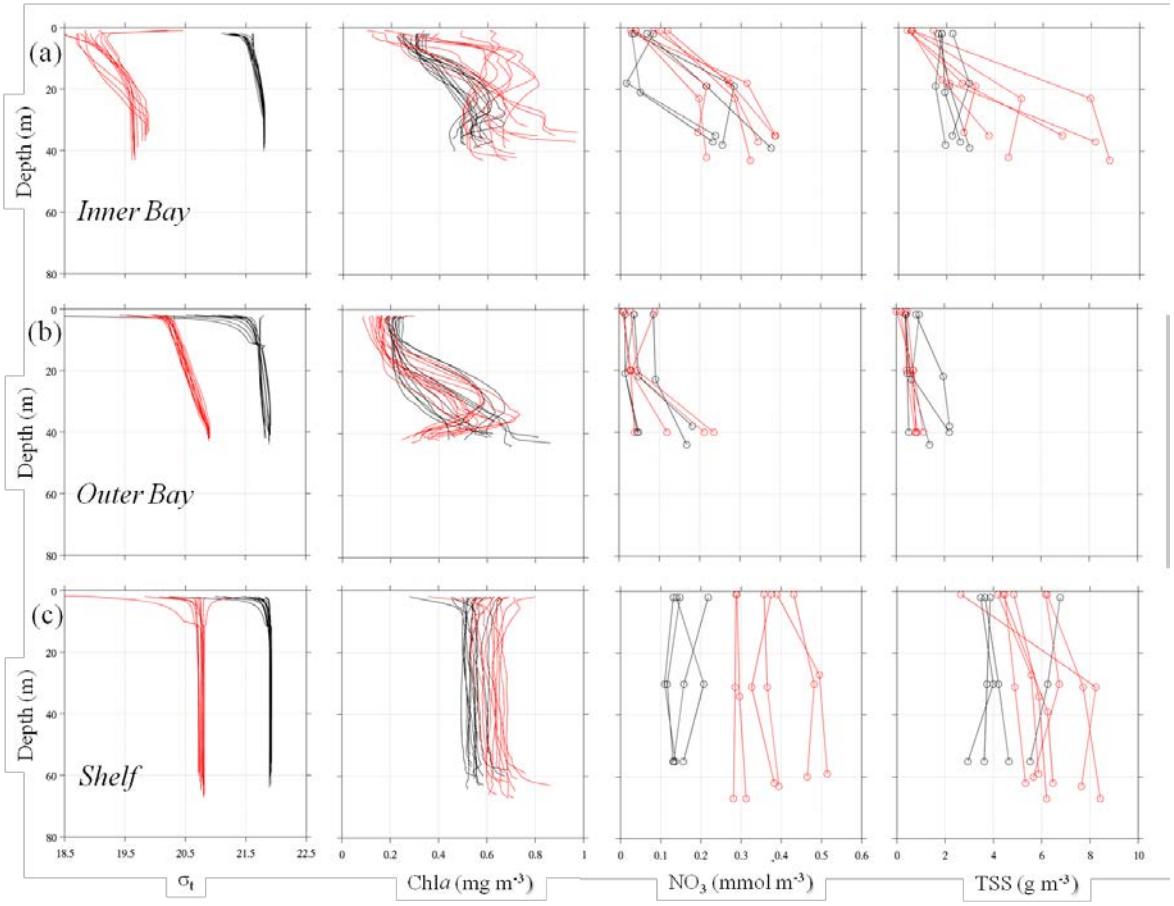

Figure 5.8. Vertical profiles of sigma-t density (σ_t), chlorophyll-a biomass (Chl*a*), nitrate concentration (NO_3), and total suspended solid concentration (TSS) collected in different regions of Collier Bay during October 2013 (black) and March 2014 (red).

5.5.2 Modelling

In this sub-section we apply a one-dimensional coupled physical/biological model to test some basic ideas about the vertical distribution of phytoplankton and nitrate at the three sites discussed above (Figure 5.7). We consider the simpler non-stratified dry season condition where mixing is assumed to be constant with depth. The model is nitrogen-based, to suit the nitrogen-limited WA ecosystem, and for simplicity consists of only two compartments, phytoplankton P and nitrate N (Figure 5.9).

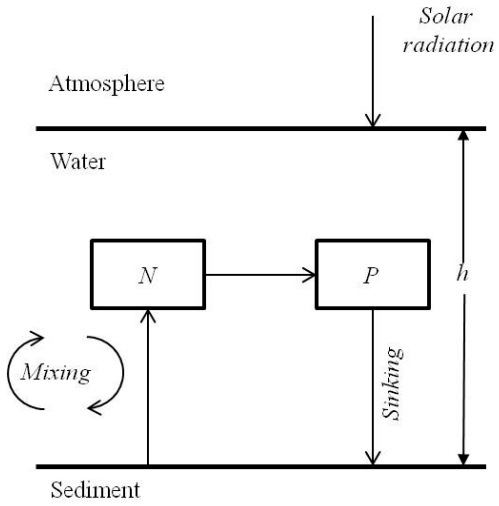

Figure 5.9. Schematic of the model showing major fluxes (arrows) and compartments (boxes).

The time dependent rate of change of P and N is described by the coupled differential equations:

$$\frac{\partial P}{\partial t} = \mu(I,N)P - mP - w\frac{\partial P}{\partial z} + A\frac{\partial^2 P}{\partial z^2} \quad (5.4)$$

$$\frac{\partial N}{\partial t} = -\mu(I,N)P + mP + A\frac{\partial^2 N}{\partial z^2} \quad (5.5)$$

where μ and m are the growth rate and mortality rate, respectively, of phytoplankton, I is the photosynthetic light intensity, w is the settling velocity, A is the vertical diffusivity (constant with depth), and z is the vertical coordinate (zero at the surface and decreasing downward). The growth and mortality terms determine the transfer of nitrogen between the two compartments. Photosynthetic light is modelled to decline exponentially with depth (z) at a rate determined by a pre-defined attenuation constant.

The phytoplankton growth rate μ as a function of light, I, and nitrate, N is given by

$$\mu(N,I) = \left(P_s\left(1 - e^{-\alpha I / P_s}\right)e^{-\beta I / P_s}\right).\left(N/\left(N + K_N\right)\right) \quad (5.6)$$

where P_s is the light saturated photosynthetic rate in the absence of photoinhibition, α is the initial slope of the productivity irradiance response, β is an index of photoinhibition, and K_N is a half-saturation constant. At steady-state, Equations 5.4 and 5.5 reduce to a pair of ordinary differential equations that can be solved numerically as a boundary value problem. We use the Matlab © "bvp4" solver with the boundary conditions:

$$wP - A\frac{\partial P}{\partial z} = A\frac{\partial N}{\partial z} = 0 \text{ , at } z = 0 \quad (5.7)$$

$$A\frac{\partial N}{\partial z} - wP = 0 \text{ , at } z = -h, \quad (5.8)$$

together with specification of P at $z = -h$, where h is the total water depth. The surface boundary condition (Equation 5.7) specifies no flux of P or N through the surface. The flux condition at the bottom boundary (Equation 10) is the so-called 'reflective boundary condition' recommended for elementary coupling of pelagic and benthic biogeochemical ocean models (Soetaert et al. 2000). It is the condition that the efflux of *N* from the in-sediment pore-water is matched by the deposition flux of particulate *P* from the water column. The conversion of P to N in the sediments is mediated by bacterial processes that do not need to be explicitly represented in the model.

The water depth is set to 40 m for the inner and outer bay sites and 60 m for the shelf site, and the lower boundary concentration of P is fixed at 0.25 mmol N m^{-3} consistent with concentrations of chlorophyll at all the sites (Figure 5.8), and by applying a chlorophyll-a to nitrogen ratio of 2:1. Vertical eddy diffusivity (A) is treated as a calibration parameter and adjusted to obtain the best result. The value of surface incident PAR, I_0, is based on a daily mean value of 1000 µE m^{-2} s^{-1}, and the light attenuation rate constant is determined from the average vertical light profile collected at each of the sites. Parameters used to determine settling velocity and loss in the model are based on commonly used values (Greenwood and Craig 2014), while phytoplankton light-limited growth parameters are taken from measurements reported in Section 5.4.2.

By adjustment of the vertical light attenuation and mixing rates, profiles of chlorophyll and nitrate can be closely matched by the model for each of the sites. All other parameters in the model are fixed across the sites. Importantly, the difference in the rate of increase in nitrate with depth, and the shape of the chlorophyll profile between the two bay sites is reproduced by the model by adjusting only the light attenuation rate (Figure 5.10). This is explained by a reduction in downward light penetration at the inner bay site that results in the build-up of nitrate near the seabed that cannot be accessed by the growing phytoplankton. Meanwhile growth is favoured toward the upper water column where both light and nitrate are optimal, and combines with gravitational settling to result in a sub-surface maximum in chlorophyll. Relatively slow rates of vertical mixing

play an important part in this by allowing vertical structure to develop in both properties. By applying stronger light attenuation and vertical mixing rates, the observations at the shelf site are also reproduced. Note that it is the combined adjustment of these two parameters that is necessary to match the shelf conditions. For example, increasing only the vertical mixing rate but keeping the light attenuation rate set for the adjacent outer bay site, results in a drop of 0.1 mmol N m^{-3} in the depth-averaged nitrate concentration, and a mismatch between the model and observations.

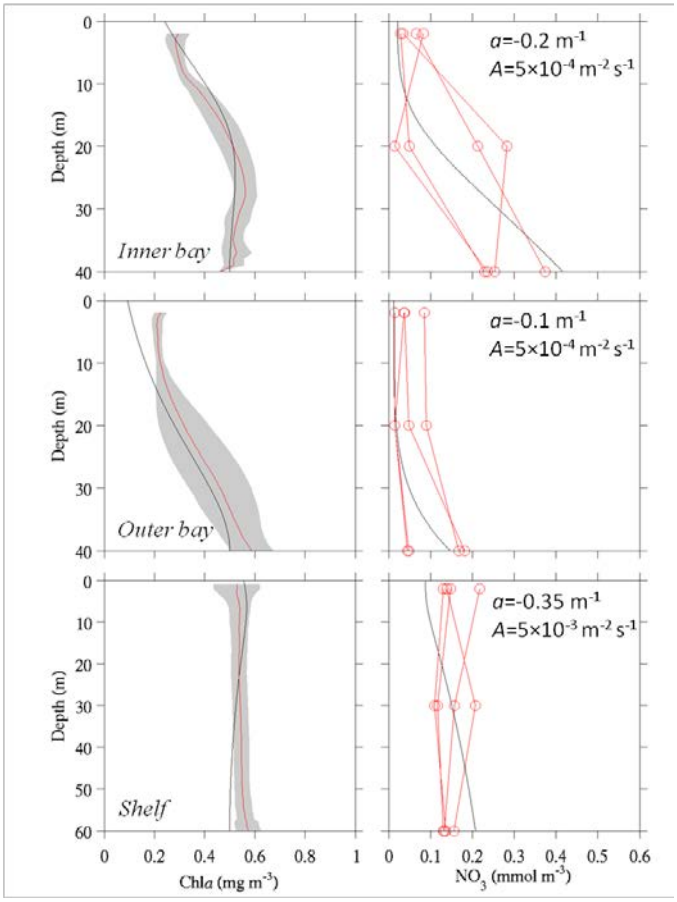

Figure 5.10. Comparison between modelled (black) and observed (red) profiles of chlorophyll (Chl*a*) and nitrate (NO_3) for each site. Observed chlorophyll is shown as the mean (solid red line) ± 1 standard deviation (shaded grey area). The rate of vertical light attenuation (*a*) and vertical mixing (*A*) is shown in the right-hand panel for each site.

5.6 Discussion

Some striking cross-shelf trends in the response of phytoplankton to irradiance are summarized in Table 5.2 and Figure 5.11. Phytoplankton in King Sound and Collier Bay have relatively low initial (α) and high maximum (P_{max}) photosynthetic rates compared with those further offshore (Table 5.2). They also show little, if any, sign of photo-inhibition. These characteristics determine a quite distinct predicted irradiance response in comparison to phytoplankton collected further off-shore.

The comparatively small values of α in King Sound and Collier Bay, suggest that phytoplankton in these areas are not particularly well adapted to low light conditions. Compared with the phytoplankton sampled further offshore (that had much higher α values throughout the water-column), they seem to be relatively inefficient at utilizing low light intensities. This is somewhat curious given the relatively high turbidity in these coastal waters. Rather than adapting to high-turbidity / low-light conditions, it seems, from the high P_{max} values and general absence of photo-inhibition, that the coastal phytoplankton have specialized in being able to maximize growth under high intensity light conditions near the surface at the expense of growth further down the water column. This growth strategy only seems viable in well-mixed water-column conditions where excursions to the surface are frequent. This raises questions concerning the daily light history of phytoplankton and variability in vertical mixing. Absence of any noticeable trend in irradiance response with depth either in the King Sound

data or in Collier Bay (Figure 5.6), further suggests that the phytoplankton population is vertically homogenous, consistent with relatively strong mixing.

The consistency in irradiance response across Collier Bay suggests that a simple (i.e. single phytoplankton) model of this region would be appropriate. Results from King Sound and the adjacent shelf suggest that parameterising a biological model for the whole shelf would present a considerably greater challenge due to variation in phytoplankton light response between the inner and outer shelf regions. Even so, the transition in light response moving away from the coast is surprisingly smooth (see Table 5.2 and Figure 5.11) suggesting that parameter estimation as a function of seabed depth (*h*) might be feasible. Otherwise, inclusion of at least two phytoplankton groups in the model is recommended to capture the contrast between inner and outer shelf response.

Table 5.2. Average photosynthesis-irradiance parameters at various shelf positions

Shelf position	***P_{max} (hr^{-1})***	***α (initial slope)*** *(mgC mg Chl^{-1} hr^{-1} μE^{-1} m^2 s)*	***β (inhibition parameter)*** *(mgC mg Chl^{-1} hr^{-1} μE^{-1} m^2 s)*
Collier Bay	9.82	0.02	-
King Sound	8.91	0.08	0.001
50 m	5.06	0.06	0.006
200 m	4.23	0.11	0.013
1000 m	5.77	0.16	0.032

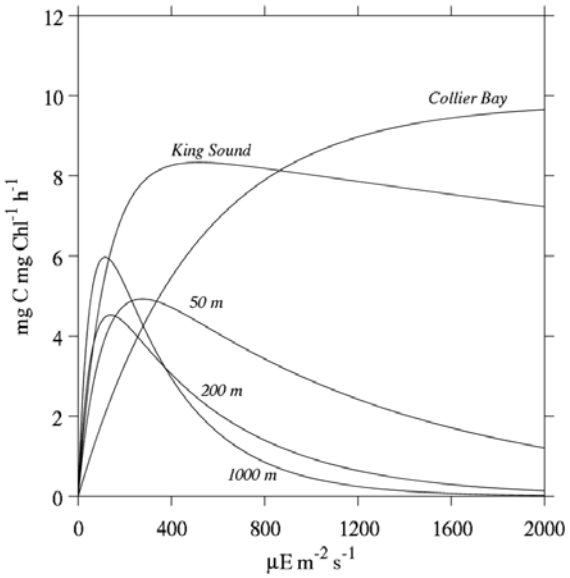

Figure 5.11. Predicted photosynthesis-irradiance response at various shelf locations based on parameters in Table 5.2, highlighting the significant transition in light sensitivity of phytoplankton with distance off-shore.

The coupling between chlorophyll-a and nitrate in the one-dimensional model means that there are fairly tight constraints on the range of parameters that will give a good fit to both properties. The fact that we have been able to obtain reasonable fits to the data by adjusting only the vertical mixing and light attenuation rates in our model, suggest that these are key parameters in determining changes in the vertical distribution of phytoplankton and nitrate across the bay.

6 Secondary Production and Community Metabolism

6.1 Introduction

It has been estimated that ~40% of the primary production that occurs in coastal regions is consumed by secondary producers, ~40% is re-mineralised within the water column, ~16% is exported off-shore to deeper water, and ~4% is deposited to the sediments. The transfer of carbon from primary production to upper trophic levels (i.e. fish) via mesozooplankton involves many microbial linkages at the lower end of the food web, the strength of which is poorly established in Australian waters. Specifically, few measurements of zooplankton production in Australian waters have been undertaken, making it difficult to clearly quantify the exact relationship between primary production, grazing, and ultimately fish productivity, and as a result we therefore have inadequate information on grazing rates that are needed to parameterize coastal biogeochemical models. Furthermore, the extent to which this partitioning of primary production into secondary production occurs within the macro-tidal environments of NW Australia remains essentially unexplored. In this environment, grazing is likely to account for a larger proportion of the primary production that is not respired, and it is hypothesized that the grazing rate may be less for open water areas, but may be comparable for semi enclosed embayments relative to other regions. To better understand how nutrients and primary productivity are converted into secondary production (and fisheries), we must therefore ascertain the specific rates that typify Kimberley waters, and identify how they vary seasonally. The aim of this chapter is therefore to address Project Objective 2, to characterise actual rates of secondary productivity across the Kimberley coast, and understand how grazing rates are defined by seasonal trends.

In marine waters, community metabolism is able to provide a bulk measure of total zooplankton respiration, which can be used as a measure of their overall activity. However, it is also desirable to understand the degree to which specific functional groups of zooplankton are driving secondary production, and the nature and strength of linkages between them. The three size groups described in Chapter 4 for the Kimberley coast include the 75-150 µm, 150-350 and >350 fractions. The important grazers for the picoplankton community are the protists in the smaller size class, and the larger mesozooplankton graze upon larger phytoplankton cells (herbivory) and also include copepods that predate upon smaller zooplankton and flagellates. Mesozooplankton grazing, is difficult to measure directly as the standing stock of phytoplankton is very low, meaning that the main trophic resources available to mesozooplankton are either protistan grazers or detrital flocs or aggregates. Copepod growth is usually measured using cohort development or egg production methods. To estimate their grazing rate, several methods can be adopted, including feeding experiments and/or gut inspection methods. These methods are highly controlled and may differ from that *in situ*. Biochemical indices related to increases in structural growth and respiration of organisms are therefore becoming a more attractive alternative as they are based on *in situ* conditions prior to the time of collection, thereby eliminating both the necessity for incubations in the field and the problem of bottle effects. Moreover, biochemical indices represent instantaneous rates in a period shorter than that estimated by traditional methods. Specifically, Aminoacyl-tRNA synthetases (AARS) catalyze the first step of protein synthesis and their activity is significantly related to somatic growth in freshwater and marine crustaceans. The activity of AARS can be used as an index of copepod somatic growth (Yebra and Hernández-Léon 2004). AARS activity can be complemented with by quantifying the electron transport system (ETS), which is nearly ubiquitous in mitochondrial membranes, and can be used as an indicator of organic matter remineralisation, as it consists of a complex chain of cytochromes, flavo proteins and metabolic ions that transport electrons from catabolised foodstuffs to oxygen. ETS activity is correlated to in vivo respiration, so that ETS activity can be used as an estimate of mesozooplankton respiration rate. In this Chapter, the specific activity of aminoacyl-tRNA synthetases (spAARS), and the electron transport system (spETS), were measured as an index of growth and respiration, respectively, for each of the three zooplankton size fractions (73–150 µm, >150 µm and >350 µm) at numerous sites across the Kimberley during five cruises. These measurements were undertaken in conjunction with traditional community metabolism estimates, with a view to providing novel insights into secondary production within Kimberley waters.

6.2 Methods

6.2.1 Community metabolism

Measurements of water column community respiration (CR) and net community production (NCP) based on oxygen fluxes were conducted at stations within Camden Sound in January and October 2011, February 2013 and March 2014. In February 2013 additional measurements were taken in Napier Broome Bay, York Sound and Prince Regent Sound. A single experiment was conducted in Napier Broome Bay in March 2014 (at site KIM361). Figures 6.1 – 6.2 show the locations where metabolism was measured for the different cruises.

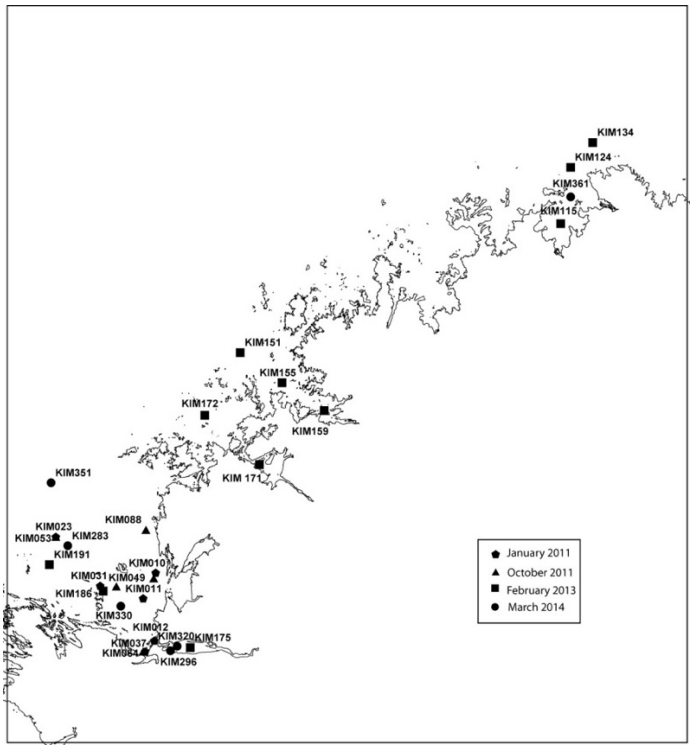

Figure 6.1. Kimberley stations at which (dark) community metabolism was measured.

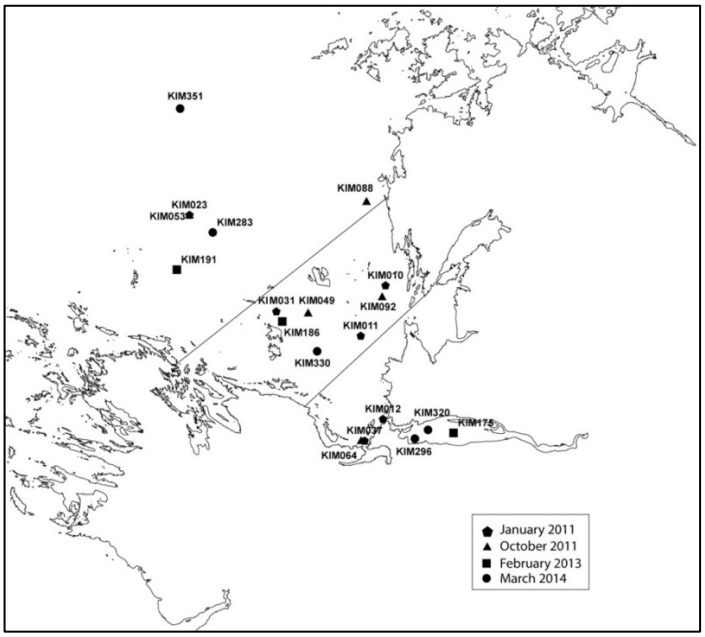

Figure 6.2: Stations at which (dark) community metabolism was measured within Camden Sound. Lines indicate the division between Inner, Mid, and Outer bay locations.

Samples were taken from CTD-rosette casts at a subset of the stations occupied for water quality measurements. Immediately after retrieval of the CTD on board, seawater from the Niskin bottles was used to fill calibrated acid-washed iodine flasks with a nominal volume of 125 mL. At every station and at least 2 depths, sets of 4 Pyrex iodine flasks were filled for measurement of initial oxygen concentration (zero-time samples), respiration (incubated in the dark for 24 h) and production (placed in deck incubators for 24 h, under neutral density mesh to simulate light levels occurring at appropriate isolumes throughout the euphotic zone. The entire set of flasks from each experiment was titrated as a single batch within 24 h of completion of the experiment.

Dissolved oxygen concentration was determined with an automated high-precision Winkler titration system developed at the Oceanographic Data Facility, Scripps Institution of Oceanography, University of California, San Diego, and which uses the absorption of 365 nm UV light for endpoint detection. Net community production (NCP) and dark community respiration (CR) were estimated as the change in oxygen concentration during a 24 h period in flasks incubated in the light and dark respectively. Gross primary production (GPP) was calculated as the sum of NCP and CR, and the P:R ratio calculated as the ratio GPP:CR. We computed area-specific community NCP rates by trapezoidal integration of volumetric data at each isolume down to the 1% light level. The depth of each isolume was estimated from light profiles obtained from the CTD casts. Area-specific CR was calculated in a similar fashion, but to the sea bottom.

6.2.2 Zooplankton growth and respiration

Growth and respiration were estimated at each station of the 5 cruises as shown in Figure 4.1. The specific activity of AARS (spAARS) was measured using the method of Yebra & Hernández-León (2004), and was corrected for the *in-situ* temperature with an activation energy of 10.5 kcal mol^{-1} (Guerra 2006). The ETS activity (spETS) was assayed using the method of Packard (1971), as modified by Gómez et al. (1996). ETS activity was corrected for the in-situ temperature at each depth using the Arrhenius equation with an activation energy of 15 kcal mol^{-1}, as given by Packard et al. (1975).

The community respiration rates (R; mg C m^{-2} h^{-1}) were assessed from specific ETS activities (ml O_2 mg $prot^{-1}$ h^{-1}) and integrated biomass (mg protein m^{-2}), assuming a respiratory quotient of 0.97 (Omori and Ikeda 1984) and a theoretical R : ETS ratio of 0.5 (Hernández- León & Gómez 1996; Ikeda et al. 2000). We assessed the community potential ingestion (I; mg C m^{-2} h^{-1}) from respiration rates (R), assuming an assimilation and a gross growth efficiency of 70 and 30%, respectively, and applying the equation proposed by Ikeda and Motoda (1978): I = 100 R/(70 - 30) = 2.5 R.

6.3 Results

6.3.1 Community metabolism

In Camden Sound, volume-specific CR was higher during the wet season than during the dry season: 2.46 ± 1.76 (SD) and 1.78 ± 0.90 mmol O_2 m^{-3} d^{-1}, respectively (Figure 6.3). Spatially, rates of CR tended to be higher at stations nearest the coast: 2.91 ± 1.05 mmol O_2 m^{-3} d^{-1} at inner locations, 2.37 ± 1.31 in the mid-reaches of Camden Sound, and 1.70 ± 0.65 offshore.

In February 2013 we conducted single experiments on three station transects comprising inner bay, mid bay and outer bay locations in each of Napier Broome Bay, York Sound, Prince Regent Sound and Camden Sound (Figure 6.1). There was a general trend of CR being highest inshore, and highest at the shallowest depth sampled. Surface waters at the innermost station at Napier Broome Bay yielded the highest value of CR recorded, twofold higher than any recorded elsewhere.

Within Camden Sound, the highest rates of volume-specific NCP were measured in January (up to 26 mmol O_2 m^{-3} d^{-1}) compared to October (maximum of 20 mmol O_2 m^{-3} d^{-1}). Over the entire study, the highest proportion of surface NCP measurements fell between 10 and 20 mmol O_2 m^{-3} d^{-1}), but one extremely high value (90.6 mmol O_2 m^{-3} d^{-1}) was measured in Walcott Inlet in February 2013 (Figure 6.4).

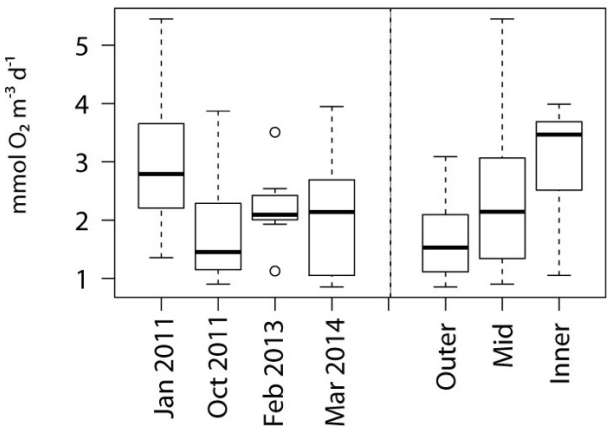

Figure 6.3. Boxplot of community respiration (CR) in Camden Sound for each cruise (left panels) and at stations in the outer bay, mid bay, and inner bay (Collier Bay and Walcott Inlet).

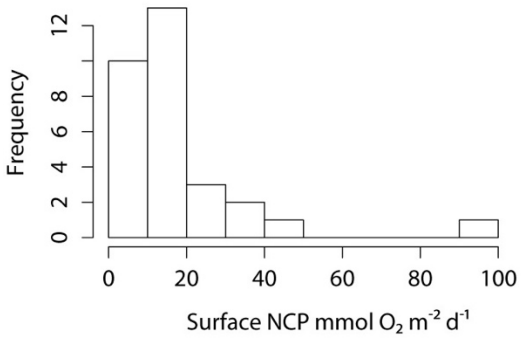

Figure 6.4. Frequency of binned measurements of volume-specific oxygen production from near-surface samples.

Table 6.1. Community respiration (mmol O_2 m^{-3} d^{-1}) on the Kimberley transects from 2013.

Inner		*Mid*		*Offshore*	
Napier Broome Bay					
2m	11.031	2m	1.987	2m	2.710
5m	4.826	5m	4.000	7m	2.152
18m	7.759	30m	turbid	57m	2.192
York Sound					
3m	3.464	3m	3.969	2m	3.179
6m	2.281	9m	1.442	9m	1.268
57m	1.504	38m	1.545	47m	1.665
Prince Regent Sound					
		2m	3.509	3m	3.308
		9m	1.768	6m	1.634
		39m	1.429	20m	1.411
Camden Sound					
2m	3.509	2m	2.540	2m	2.094
		9m	2.308	4m	2.085
		57m	1.125	56m	1.929

Area-specific metabolic rates demonstrated that all stations were net autotrophic, with P:R ratios between 1.1 and 6.0 (Figure 6.5). The very high P:R ratio and high area-specific value of NCP observed at KIM175, in Walcott Inlet in February 2013, was coincident with a diatom bloom. Area-specific NCP ranged from 7.2 – 213.5 mmol O_2 m^{-2} d^{-1}, based on the integration of production rates to the 1% light level, and respiration rates to the sea bottom. Assuming a photosynthetic quotient of 1, the highest rate of net production observed was equivalent to 2.6 g C m^{-2} d^{-1}. Area-specific CR was high, especially during the wet season, with rates up to 382 mmol O_2 m^{-2} d^{-1}. There was no consistent pattern in the area-specific data, though wet season measurements were more variable than in the dry season.

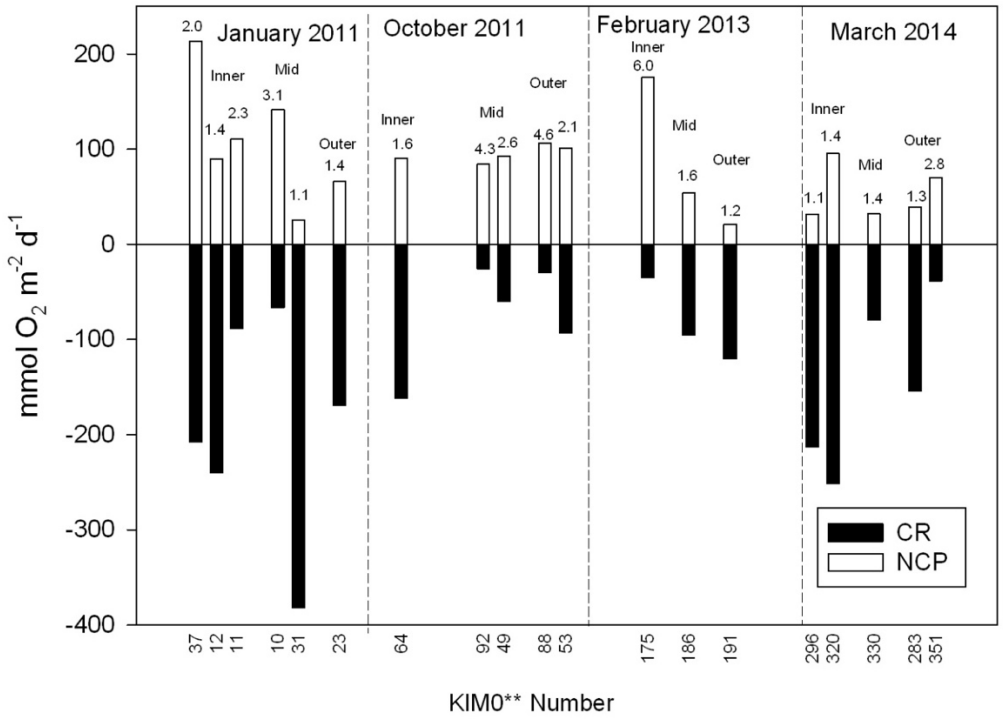

Figure 6.5. Area-specific metabolism in Camden Sound. White bars represent NCP, black bars CR, and the total bar length GPP. The number above each bar is the P:R ratio. Numbers along the x-axis represent the Station number in the KIM series.

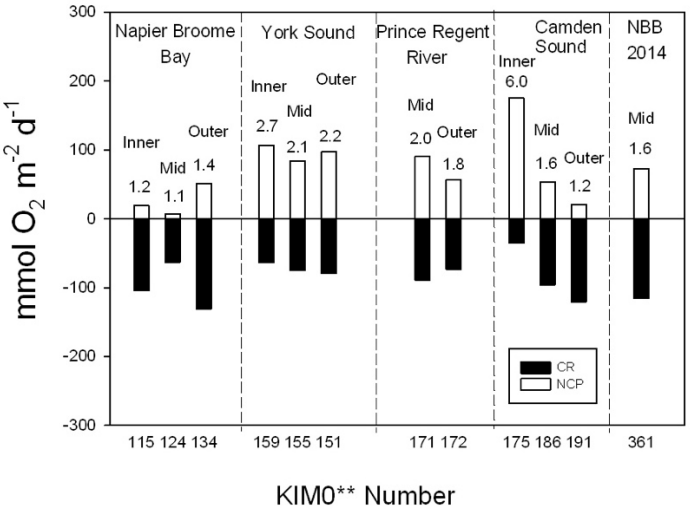

Figure 6.6. Area-specific metabolism as for Figure 6.5, but measured on 3-station transects in four Kimberley inlets during February 2013. The single measurement in Napier Broome Bay (NBB) in 2014 is included for comparison.

Area-specific rates of net community production measured in February 2013 were lower in Napier Broome Bay than at other locations, despite higher respiration rates both in volume-specific (Table 6.1) and area-specific terms (Figure 6.5). This was most likely caused by the very overcast and stormy conditions prevailing during the time of sampling.

The grand mean of NCP, aggregated over all stations occupied, is 79.54 ± 46.61(SD) mmol O_2 m^{-2} d^{-1}, and that of CR 117.95 ± 80.87. Assuming carbon-specific primary production, as normally measured using ^{14}C, is equivalent to 45% of GPP (Bender et al. 1999), this is approximately equivalent to a primary production rate of 1 gC m^{-2} d^{-1}.

6.3.2 Zooplankton growth and respiration

The results of the enzyme analysis for AARS and ETS show differences across the Kimberley coast, and between size fractions (Figure 6.7), with some changes in activity notable between cruises (Figure 6.8 and 6.9). Some interesting points include that the AARS activity in both the 73-150 μm and >150 μm fraction were lower in the January 2011 cruise than on other cruises. If AARS reflects secondary production, it is not expected that it is lowest on the cruise with the highest primary production and possibly this is a reflection of the most important phytoplankton being unavailable to mesozooplankton grazers, either because of toxicity (e.g., *Trichodesmium*) or size (*Coscinodiscus*). The October 2011 cruise had the highest AARS activity, but low ETS activity. These results seem inconsistent, but this does confirm that the two enzyme systems measure different metabolic processes. ETS activity in the >150 μm fraction, which contains the dominant copepod fraction of the mesozooplankton, was higher during wet season cruises than the dry season cruises, which seems reasonable since respiration should scale with temperature. Furthermore, there did not seem to be consistent seasonal trends in the enzyme data (Figure 6.9). It may be that these measurements are a reflection of the zooplankton communities present at the time, or of trophic conditions at the time of sampling. For example, the October 2011 cruise had the highest AARS values in all three size fractions and consistently high P:R ratios in the metabolism data, which might indicate high phytoplankton growth rates. Other anomalies include high ETS rates in the 73-150 and >150 size fractions in February 2013 in Walcott Inlet, and high ETS and AARS rates in the >350 size fraction in February 2013 (at KIM115 in Napier Broome Bay), occured where there was a bloom of the pteropod *Creseis* sp.

By interpreting the enzyme data it is possible to estimate typical rates of secondary productivity. Based on the equation of Herrera et al. (2012), the median growth rates based on AARS are 0.78 for the 73-150 μm fraction, 1.05 for the >150 μm fraction, and 1.18 for the >350 μm fraction. Considering only the >150 μm fraction, and applying the growth rate of 1.05 to a biomass of 3.63 mgN m^{-3}, yields a production rate of 3.81 mgN m^{-3} d^{-1}. Assuming, an average water column depth of 35 m, this equals a secondary production rate of 133 mg N m^{-2} d^{-1}. Taking a growth efficiency of 33% (Harris et al. 2000), this is equivalent to a grazing rate of 404 mg N m^{-2} d^{-1}. Taking an average primary production rate of 1 gC m^{-2} d^{-1} as above, (=150 mgN m^{-2} d^{-1}, assuming a Redfield ratio of 6.6C:1N), then the theoretical maximum grazing rate is 2.7 times the primary production rate. It is therefore reasonable to assume that zooplankton are food-limited in these environments.

Calculation of mesozooplankton respiration rates from the ETS data result in median (aggregated over all stations) rates of 5, 8 and 2 mg C m^{-3} d^{-1} in the 73-150 μm, >150 μm and >350 μm size fractions respectively. Assuming an average water depth of 35 m and applying the equations of Ikeda & Motoda (1978) as above, we calculate the median grazing rates of each of these size fractions as 405, 737 and 185 mg C m^{-2} d^{-1} respectively. However, these numbers are based on the assumption that the DW m^{-3} is all zooplankton, which is known to be untrue for the 73-150 μm fraction based on the stoichiometry in

, and for which the calculated grazing rate is therefore ~2-fold high. Note also that the >150μm calculation includes zooplankton >350 μm, i.e. the 150-350 μm grazing rate is 552 mg C m^{-2} d^{-1}. The corrected grazing rates are then 202, 552 and 185 mg C m^{-2} d^{-1} for the 73-150 μm, 150-350 μm and >350 μm fractions, summing to 939 mg C m^{-2} d^{-1} overall, which is in the same order as the average primary production rate (1 g C m^{-2} d^{-1}, as above). These numbers are high and subject to further scrutiny. It is possible that food chains are supported by

allochthonous material rather than in situ production, and that the larger two size fractions are primarily carnivorous. In addition, potential confounding factors relate to the presence of phytoplankton in the 73-150 µm fraction, and that most of the >350 µm size fraction are likely to be carnivores.

Correlation analysis of the water quality and zooplankton variables (Figure 6.10) demonstrate that most of the water quality variables (PN through PP) are strongly positively correlated. Zooplankton biomass (as N-content) in all three size fractions clustered with ETS in the >350 µm size range, and NH_4. A possible interpretation of this grouping is that NH_4 is proportional to zooplankton biomass since this is derived from zooplankton excretion, and that the ETS activity in the >350 µm size fraction is a reflection of carnivory by this size class on the smaller size classes. Similarly, the grouping of ETS in the 73-150 µm and >150 µm size fractions with temperature and chlorophyll is a reflection of herbivory by these smaller zooplankton size fractions, together with respiration scaling with temperature. The AARS activities in all 3 size fractions were inter-correlated but were not strongly correlated with any other variables.

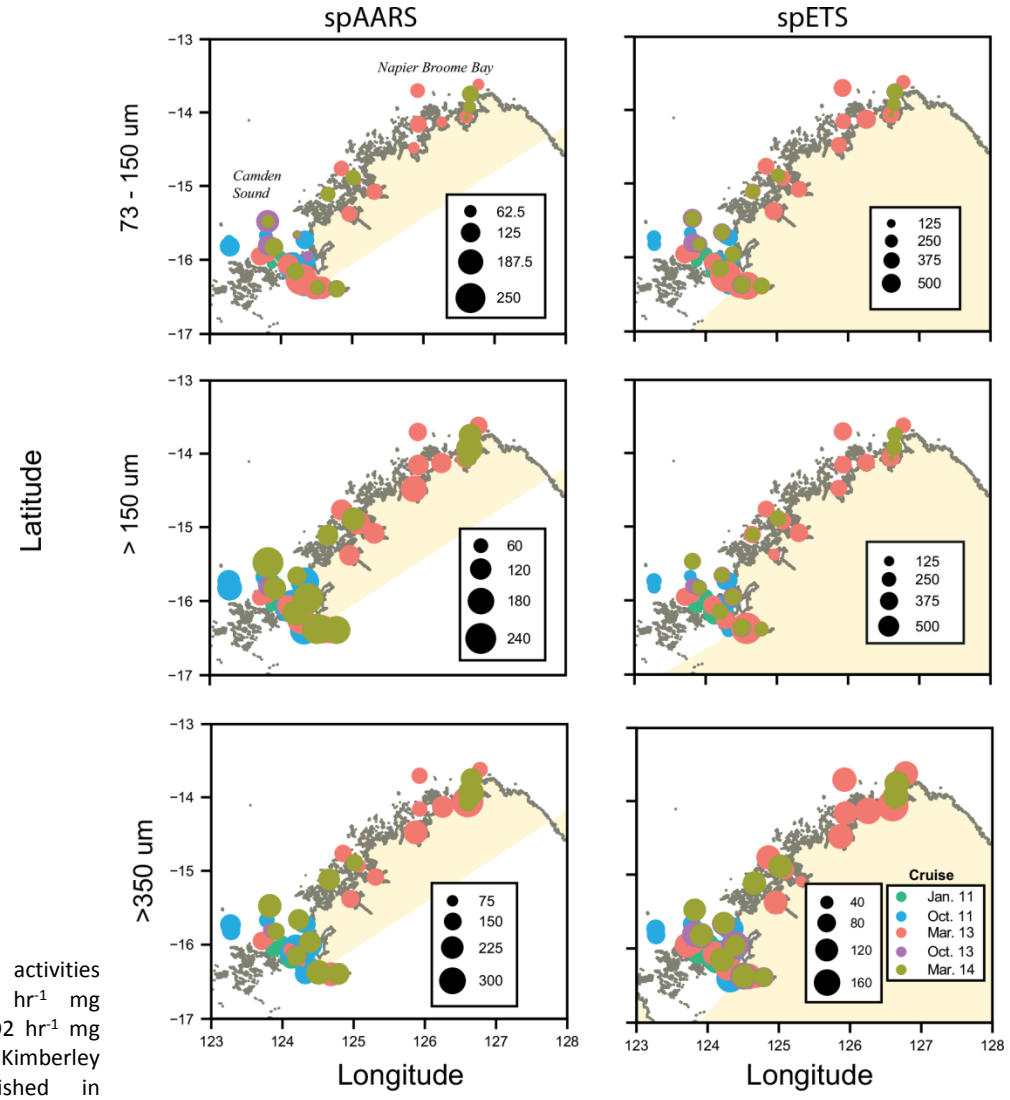

Figure 6.7. Enzyme activities (spAARS: nmol PPi hr^{-1} mg $protein^{-1}$; spETS: µL O2 hr^{-1} mg $protein^{-1}$) in the Kimberley region. First published in McKinnon et al. (2015).

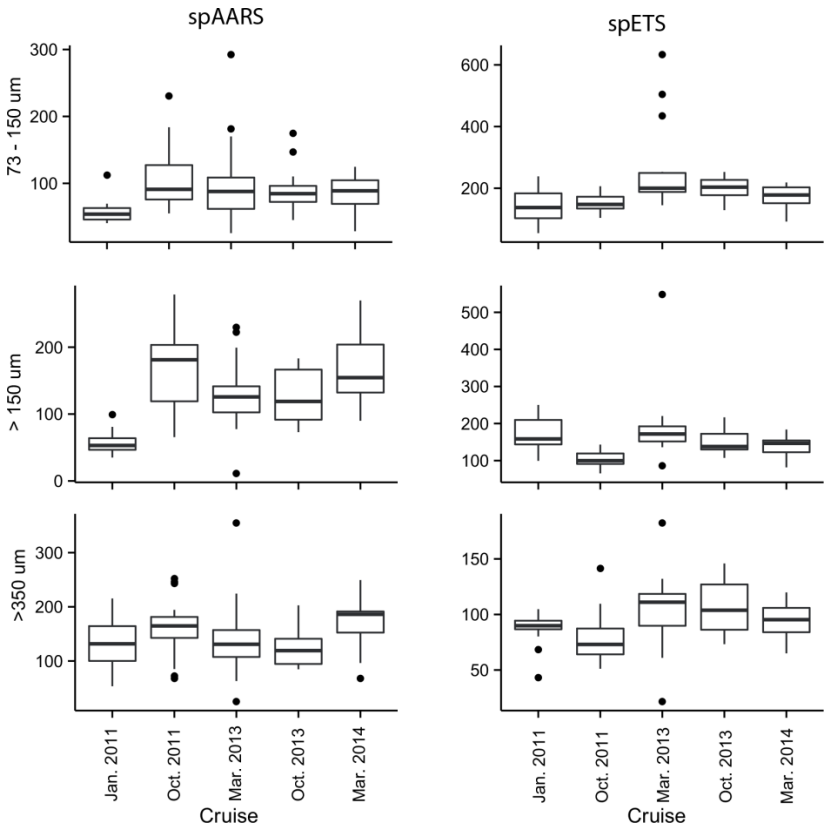

Figure 6.8. AARS activity (nmol PPi mg protein^{-1} hr^{-1}) and ETS activity (µL O_2 µg protein^{-1} hr^{-1}) in three size fractions (73-150 µm, >150 µm and >350 µm) on each cruise.

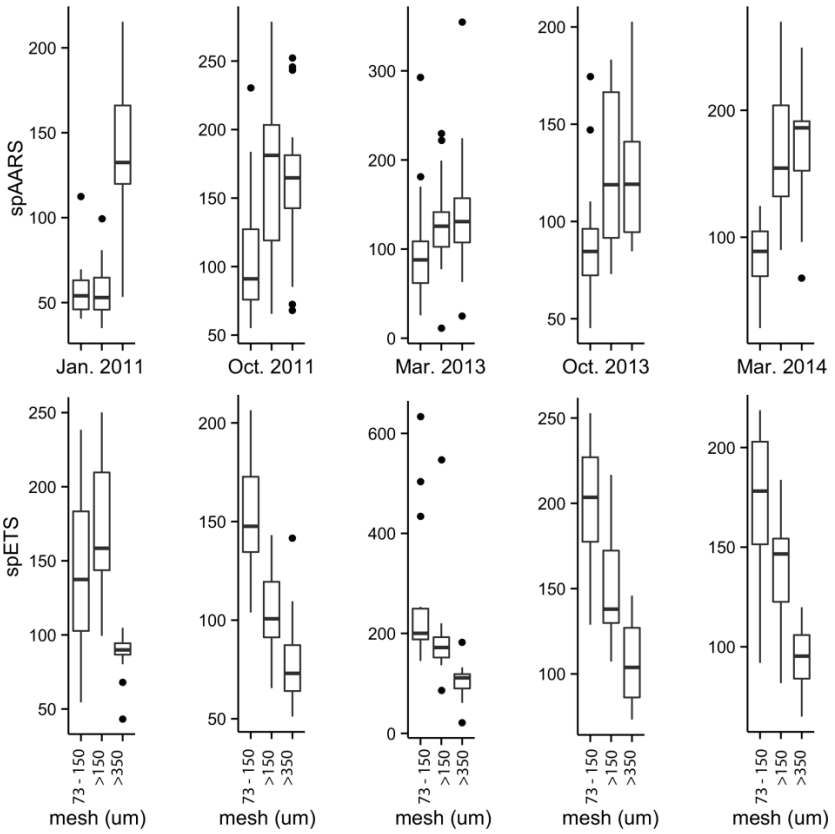

Figure 6.9. AARS activity (nmol PPi mg protein^{-1} hr^{-1}) and ETS activity (µL O_2 µg protein^{-1} hr^{-1}) in three size fractions (73-150 µm, >150 µm and >350 µm) on each cruise.

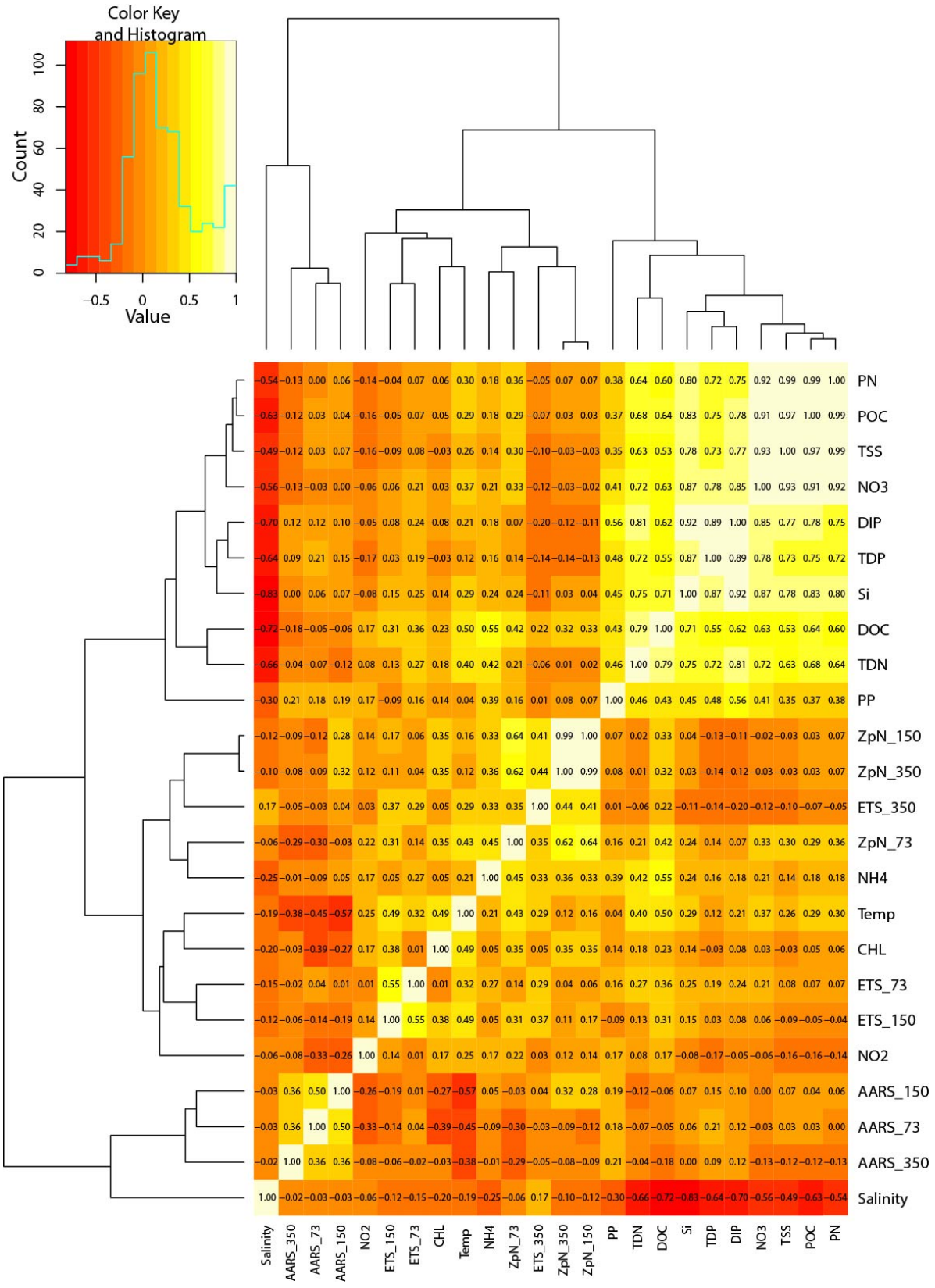

Figure 6.10: Heatmap of correlation coefficients (Pearson's r) for water quality and zooplankton variables. PN, particulate nitrogen; POC, particulate organic carbon; TSS, total suspended solids; NO3, nitrate; DIP, dissolved inorganic phosphate; Si, silicate; DOC, dissolved organic carbon; TDN, total dissolved N; PP, particulate P; ZpN_150, zooplankton N >150 µm; ZpN_350, zooplankton N >35 µm; ETS_350, ETS activity in >350 µm zooplankton; ZpN_73, zooplankton N >73 <150 µm; NH4, ammonium; Temp, temperature; CHL, chlorophyll a; ETS_73, ETS activity in >73 <150 µm zooplankton; ETS_150, ETS activity in >150 µm zooplankton; NO2, nitrite; AARS_150, AARS activity in >150 µm zooplankton; AARS_73, AARS activity in >73 <150 µm zooplankton; AARS_350, AARS activity in >350 µm zooplankton.

6.4 Discussion

Volume-specific CR appears to be lower in the dry season than in the wet season, and the data from the three wet seasons sampled appear comparable even though they cover a range of inflow magnitudes. Unfortunately, no data are available for the October 2013 field trip to add confidence to the only dry season data available – from Camden Sound in October 2011. The rates of CR observed are comparable to those measured in the lagoon of the Great Barrier Reef (McKinnon et al. 2013) and the Gulf of Papua (McKinnon et al. 2007), though high measurements are more comparable to rates measured in turbid tropical harbours such as Darwin and Gove (Burford et al. 2008; Alongi and McKinnon 2011).

Calculation of area-specific net community production rates (NCP) in the waters of the Kimberley coast is at best approximate because of the very shallow euphotic zone caused by high water column turbidity. For instance, the 1% light level, which is often taken to represent the limit of the euphotic zone, occurs at depths as shallow as 5.6 m (Walcott Inlet, March 2014). It is therefore very difficult to calculate areal production on such a steep light gradient. Surface rates of NCP can be very high, and are sufficient to subsidise respiration throughout the water column below. Nevertheless, there was no convincing evidence of seasonal differences in net production in our data. Though it is reasonable to expect that runoff during the wet season, together with higher water temperature, can result in higher rates of primary production (see Revill et al. 2017), this effect appears to be modulated by the more overcast conditions and lower insolation. Primary production is clearly light-limited in the near-shore regions (Chapter 5), and assuming an overall average primary production of 1 g C m^{-2} d^{-1}, as indicated in Figure 5.3, then the rates of pelagic secondary production are comparable to those observed in the Great Barrier Reef (0.73g C m^{-2} d^{-1}; Furnas et al. 2005; McKinnon et al. 2013), within Exmouth Gulf (0.2-4.6 g C m^{-2} d^{-1}; Furnas 2007), and numerous other sites (Figure 6.11).

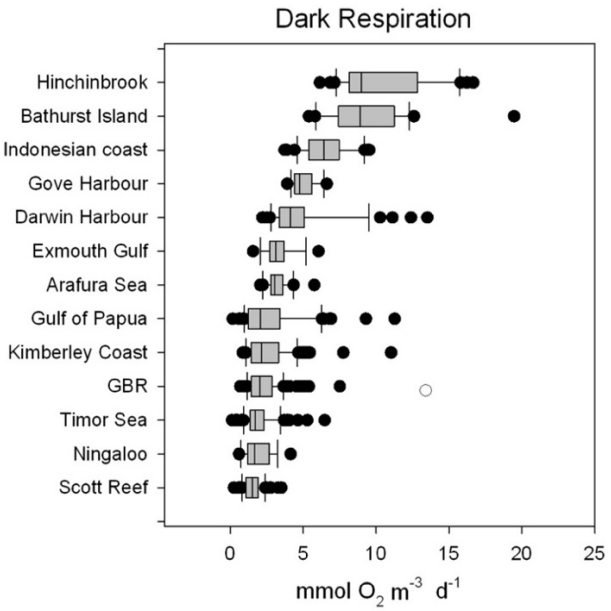

Figure 6.11. Boxplot of (dark) community respiration (CR) measured at locations in tropical Australia and Indonesia, comparing the present estimates from Kimberley waters with other regions.

Relatively high levels of spAARS activity (growth) measurements in the Kimberley were noted, relative to similar studies undertaken in the Great Barrier Reef (McKinnon et al. 2015), and spETS activity (respiration) showed similar differences in scale between the two northern Australian coasts. Based on these measurements, it is estimated that >150 µm zooplankton grazing accounted for ~7% of primary production in the Kimberley. Also, area-specific respiration by >73 µm zooplankton was estimated to be 7-fold higher in the Kimberley than on the Great Barrier Reef, and production by >150 µm zooplankton was of the order of 278 mg C m^{-2} d^{-1} in the Kimberley and 42 mg C m^{-2} d^{-1} on the Great Barrier Reef. We hypothesize that the much stronger physical forcing on the North West shelf is the main driver of higher rates in the west than in the east of the continent.

7 Regional Drivers of Kimberley Productivity

7.1 Introduction

Previous chapters in this report have outlined in detail the spatial distribution of nutrients, phytoplankton and zooplankton, and typical rates of primary and secondary productivity. However, questions remain as to our understanding of the system, for example – is the productivity driven primarily from oceanic upwelling or terrestrial inputs? What is the role of the unique physical conditions in shaping productivity? How does the large gradient in light near the coast impact coastal vs shelf productivity? Some insights into these questions has been covered in previous chapters, however, this Chapter describes simulations conducted with a 3-dimensional regional-scale coupled physical-biological model of the Kimberley coast covering the region between Admiralty Gulf and Roebuck Bay in order to more systematically tackle these questions. The main output of the model experiments was to provide an assessment of oceanic nutrient supply to the Kimberley shelf and nearshore regions compared to that from terrestrial nutrient supply.

7.2 Model description

7.2.1 Physical model

A medium resolution shelf model has been developed using the Regional Ocean Modelling System (ROMS) in collaboration with WAMSI KMRP Project 2.2.7 ("*Climate change: knowledge integration and future projection*"; Feng et al. 2017) to simulate the coastal circulation off the Kimberley for the period 2009-2012. This model is also being employed in the WAMSI KMRP Project 1.1.3 ("*Ecological connectivity*").

The ROMS model is nested within the 10 km resolution Bluelink Ocean Forecasting Australia Model (OFAM3), and setup on a rotated horizontal grid with uniform 0.02° resolution. The x-axis of the grid is roughly 40° from the circles of latitude, so that it aligns with the coastline (Figure 7.1), and the vertical grid is divided into 30 layers on an s-coordinate system with increased resolution at the surface and seabed. Atmospheric fluxes are calculated using the COARE bulk parameterization (Fairall et al. 2003). Horizontal mixing is harmonic. The vertical mixing scheme is essentially the k-w model with the stability functions by Canuto et al. (2001), and reformulated based on the generic length scale model by Umlauf and Burchard (2003).

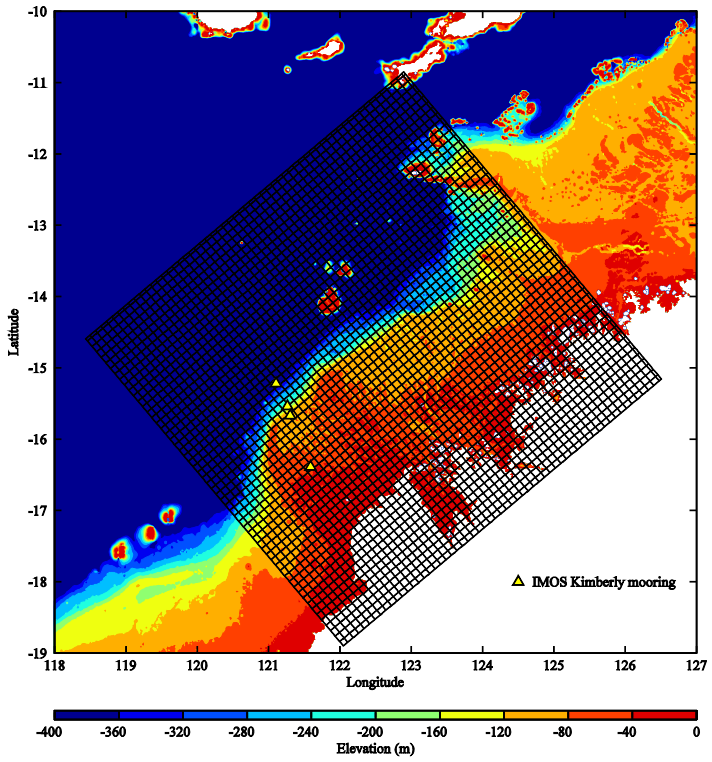

Figure 7.1. Model extent and bathymetry (m) used for the Kimberley regional nutrient assessment simulations. The bathymetric colour scale has been arranged to emphasise the 0-200 m depth range. White dots indicate the position of the nitrate and chlorophyll stations occupied during the 2010 Southern Surveyor cruise, used for comparison with the model. Note the grid indicated is only indicating every 4th grid cell for clarity; see text for specific grid cell resolution.

Bathymetry is taken from STRM30plus (Becker et al. 2009) with a minimum depth of 7 m. The wetting-drying scheme is not implemented (note this is addressed in the model presented in Chapter 8). Initial conditions and horizontal open boundary conditions are taken from daily-mean output of OFAM3 (Zhang et al. 2016; http://www.marine.csiro.au/~oke060/OFAM.htm). Horizontal boundaries are also forced with tides from TPXO7.2 (Egbert and Ray 2003). Atmospheric forcing is given by three hourly winds, air temperature, humidity, and radiative fluxes from the Japanese 55-year reanalysis (JRA) (Kobayashi et al. 2015). For the purpose of validation of the physical model (undertaken in WAMSI KMRP Project 2.2.7), river discharges from the Fitzroy River and Mitchell River are based on the climatology from Dai et al. (2009). A horizontal dispersion coefficient of 5 m^2/s is calculated from the grid resolution and the relationship given in Okubo (1971). Sponge zones are used along the open boundaries.

The performance of the ROMS physical model is assessed in detail in WAMSI KMRP Project 2.2.7 (Feng et al. 2017). Briefly, the output compares well with tidal constituents observed at several IMOS moorings across the shelf (indicated on Figure 7.1), and with the seasonal variation in sea surface temperature and salinity that is observed from satellite. Seasonal variations in the model simulated coastal circulation also agree well with the OFAM3 global simulation.

7.2.2 Biological model

For use in this project, the physical model was coupled with a simple biological model of the pelagic nitrogen cycle. The biological model is described in detail in Fennel et al. (2006). The model includes seven state variables: phytoplankton, zooplankton, nitrate, ammonium, small and large detritus, and phytoplankton chlorophyll. A simple representation of the benthic mineralisation process is also included as a seabed boundary condition. Benthic plants and animals are not included. For the main biological model runs, river discharge and associated river nitrogen inputs into King Sound and Collier Bay, were based on regional estimates of river run-off provided by WAMSI KMRP Project 2.2.6 (Revill et al. 2017). Phytoplankton growth and underwater light parameterisations were arranged to favour open-shelf rather than near coastal conditions based on data presented in Chapter 5. All other parameter values were selected based on commonly used values (Fennel et al. 2006). Several passive tracers were added to the model to aid interpretation, one for each of the rivers, and a third to trace nutrient-rich oceanic water from below 200 m.

7.2.3 Initial and boundary conditions

The oceanic passive tracer was initialised with a value of unity (1 kg m^{-3}) below 200 m water depth and zero everywhere else. The river passive tracers are added to the model according to freshwater input for each river, at a concentration of 1 kg m^{-3}. Initial and boundary conditions for nitrate were provided by the CSIRO Atlas of Regional Seas (CARS) climatology. All other biological variables were set initially to a homogenous small value of 0.01 mmol N m^{-3}. This approach has been shown to work well (Fennel et al. 2006) because the adjustment timescales for these variables are short (days to weeks). Since the biological component of our model is only implemented in the ROMS domain, open boundary conditions for the biological state variables had to be prescribed without reference to an outer model domain. We used the same procedure for prescribing the boundary concentrations as for the initial conditions. Consequently, phytoplankton and zooplankton concentrations entering the domain are unrealistically low resulting in boundary artefacts. However, these only occur in the close vicinity of inflow boundaries, and do not unduly affect the main area of the Kimberley shelf which is the focus of the analysis presented below.

7.3 Results

The ROMS model was initialised with the physical state of the OFAM3 model at January 1 2009, spun up for one year, and then integrated for the following year (2010). The passive tracers were initialised at the completion of the spin-up.

7.3.1 Model-data comparison

Results from the biological model have been compared with observations made during 2010 from the Southern

Surveyor (SS2010; see Chapter 2). Over 100 profiles of nitrate and chlorophyll were collected during SS2010 covering a range of shelf depths from 30 – 2000 m (Figure 2.1). These profiles have been collated into groups representing three different bathymetric domains <50 m, 50-100 m, and >100 m, and compared with comparative annual average profiles of nitrate and chlorophyll simulated by the model (Figure 7.2). The most notable difference between the observations and model is the position of the offshore nitracline (the depth where nitrate starts to increase rapidly with depth). The model underestimates this depth by approximately 20 m in comparison with SS2010 observations (Figure 7.2e). One consequence of this is that the model also underestimates the depth of the sub-surface chlorophyll maximum (Figure 7.2c). The model reflects the observations most closely in the 50-100 m depth range (Figure 7.2b&d), where the vertical distribution of chlorophyll is characterised by a sub-surface maximum of ~0.75 mmol N m^{-3} at 40 m, and nitrate concentrations increase steadily with depth below 40 m reaching a maximum concentration of ~6 mmol N m^{-3}. At depths less than 50 m the observed and modelled nitrate concentrations were similar, both with concentrations below 1 mmol N m^{-3} and little vertical structure (not shown). For this depth range (<50 m) the observed chlorophyll vertical distribution is roughly homogenous at a concentration of ~0.75 mg Chl*a* m^{-3} (Figure 7.2a, lower panel). The model achieves the observed concentrations below ~20 m but underestimates at the surface, leading to the simulation of a 'hook' shaped profile (Figure 7.2a, upper panel).

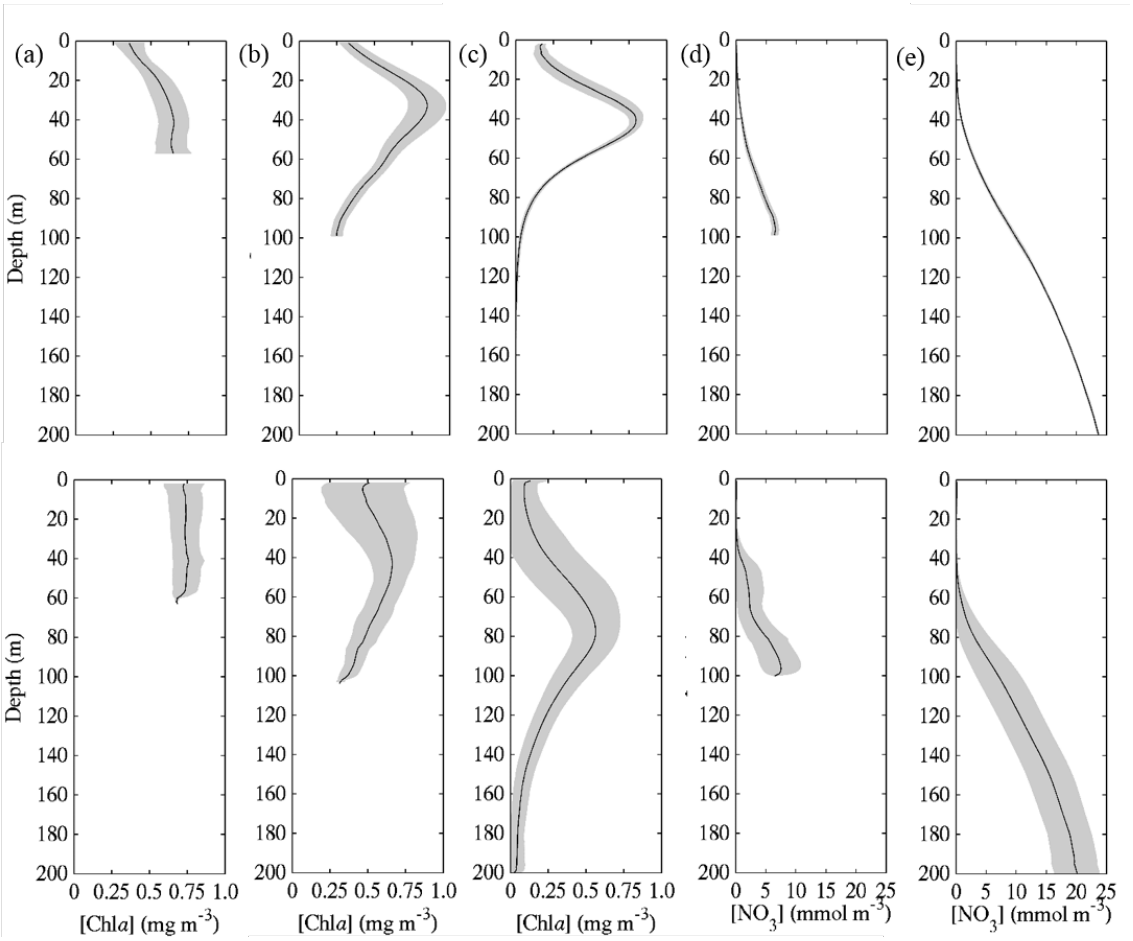

Figure 7.2. Comparison of mean vertical distribution of chlorophyll (mg m^{-3}) (panels (a), (b), and (c)), and nitrate (mmol N m^{-3}) (panels (d) and (e)) simulated by ROMS (upper panels) and observed during the 2010 Southern Surveyor cruise (lower panels). The data is split into three regions: (a) less than 50 m deep, (b and d) between 50 m and 100 m deep, and (c and e) more than 100 m deep. Refer to Figure 2.1 for sampling sites; profiles of nitrate for the region <50 m are not included.

Closer inspection of the observations made during SS2010 reveals a cross shelf trend in depth-integrated (0 m to the depth of the 1% isolume) chlorophyll and nitrate with enhanced concentrations in the vicinity of the

shelf edge (Figure 7.3). Enhancement of chlorophyll and nitrate at the shelf-edge is also a prominent feature of the model simulation (Figure 7.4), although on average the levels of chlorophyll at the 200 m depth position are over-estimated compared to the observations. The model also under-estimates the concentration of chlorophyll in the 50 m depth range compared with the SS2010 observations.

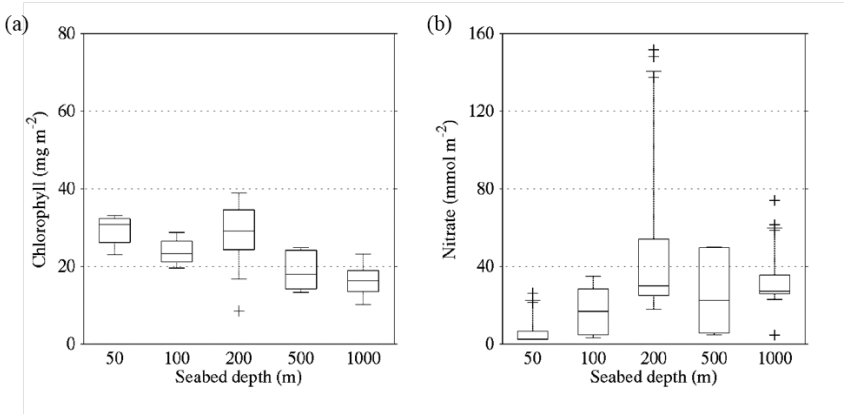

Figure 7.3. Variation in depth-integrated (a) chlorophyll (mg m^{-2}) and (b) nitrate (mmol N m^{-2}) measured during the SS2010 cruise. Quantities are integrated between the surface and the base of the euphotic layer as defined by the 1% isolume. The horizontal line across the centre of each box shows the median value, the limits of the box represents ± one standard deviation, the whiskers show the 10 and 90 % confidence limits and the '+' symbols indicate outliers.

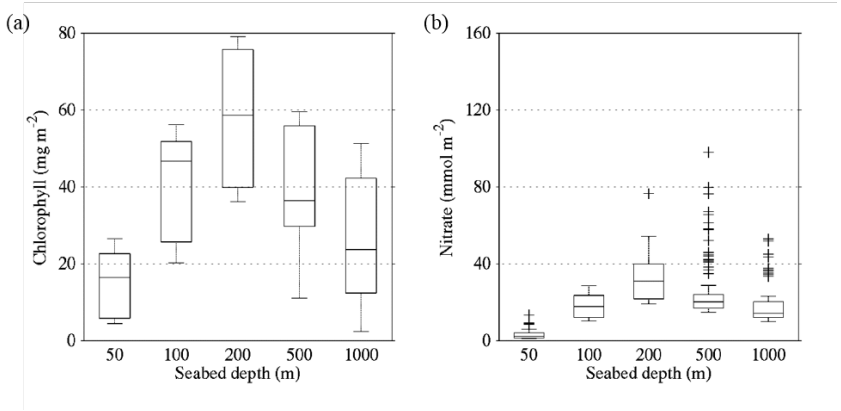

Figure 7.4. Variation in the annual mean depth-integrated (a) chlorophyll (mg m^{-2}) and (b) nitrate (mmol N m^{-2}) simulated by ROMS. Quantities are averaged for the region covered by the SS2010 observations (Figure 2.1), and integrated between the surface and the base of the euphotic layer as defined by the 1% isolume.

Hourly vertical profiles of temperature and chlorophyll *a* measured during SS2010 at a fixed location close to the 200 m isobath (-15.72S, 121.05E) during a 12 hour tidal cycle, revealed vertical displacements of the thermocline and the deep chlorophyll maximum of up to 40 m consistent with the presence of internal tides in this region (Figure 7.5). Matching ROMS model output (location and timing) shows similar temporal features in the vertical structure of temperature, chlorophyll, and nitrate, despite some differences in the temperature stratification and overall depth of the deep chlorophyll maximum (Figure 7.6).

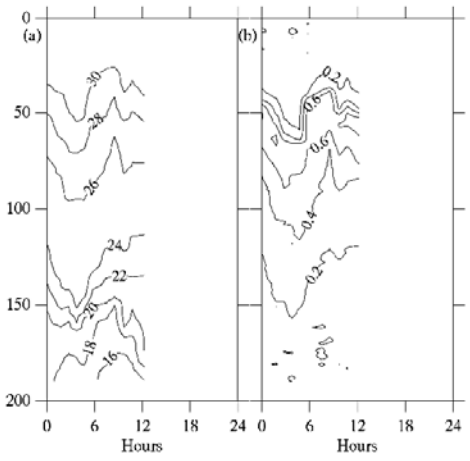

Figure 7.5 Variation in vertical structure of (a) temperature (^{0}C) and (b) chlorophyll *a* (mg Chl*a* m^{-3}) measured at a location near the 200 m isobath (-15.72S, 121.05E) over a 12 hour period during SS2010. Time zero is 16.25 WST on 27th April 2010.

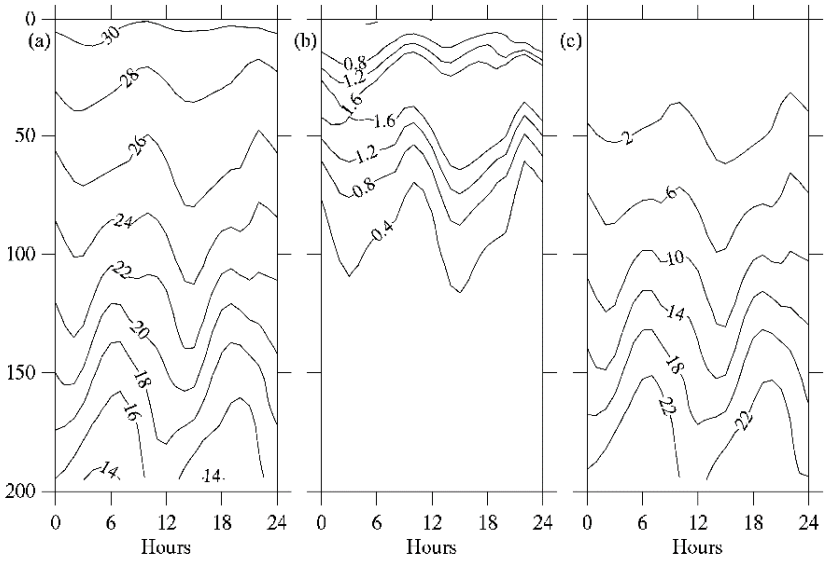

Figure 7.6 Variation in model simulated vertical structure of (a) temperature (^{0}C), (b) chlorophyll *a* (mg Chl*a* m^{-3}) and (c) nitrate (mmol N m^{-3}) at a location and time matching the SS2010 observations shown in Figure 7.5. Contours are constructed from hourly model output.

7.3.2 Oceanic nutrient supply

Additional evidence from the model is presented here in an effort to explain the reason for the enhanced biological response simulated (and observed in the SS2010 data) at the shelf edge. The first piece of evidence comes from analysis of the oceanic passive tracer field. Over time, the oceanic tracer (initially distributed below 200 m only) is transported upward through the water column, and appears at the surface. The resulting tracer distribution is patchy in time and space due to intermittent supply of tracer from below and subsequent mixing and advection, but on average shows maximum accumulation between the 100 and 200 m depth contours, and in the central region of the domain where the shelf edge bathymetry is the steepest (Figure 7.7). There is also some surface accumulation of tracer in the vicinity of Scott Reef.

Elevated concentrations of nitrate and chlorophyll also often occur in the model simulation between the 100 m and 200 m depth contours (Figure 7.8). This is consistent with the accumulation of passive oceanic tracer (Figure 7.7), suggesting that vertical supply of nitrate from below the nitracline is fuelling phytoplankton production at the shelf edge. In addition, to the biological response observed at the shelf edge, the model also predicts enhanced nitrate and chlorophyll in the vicinity of the 50 m isobath (Figure 7.8).

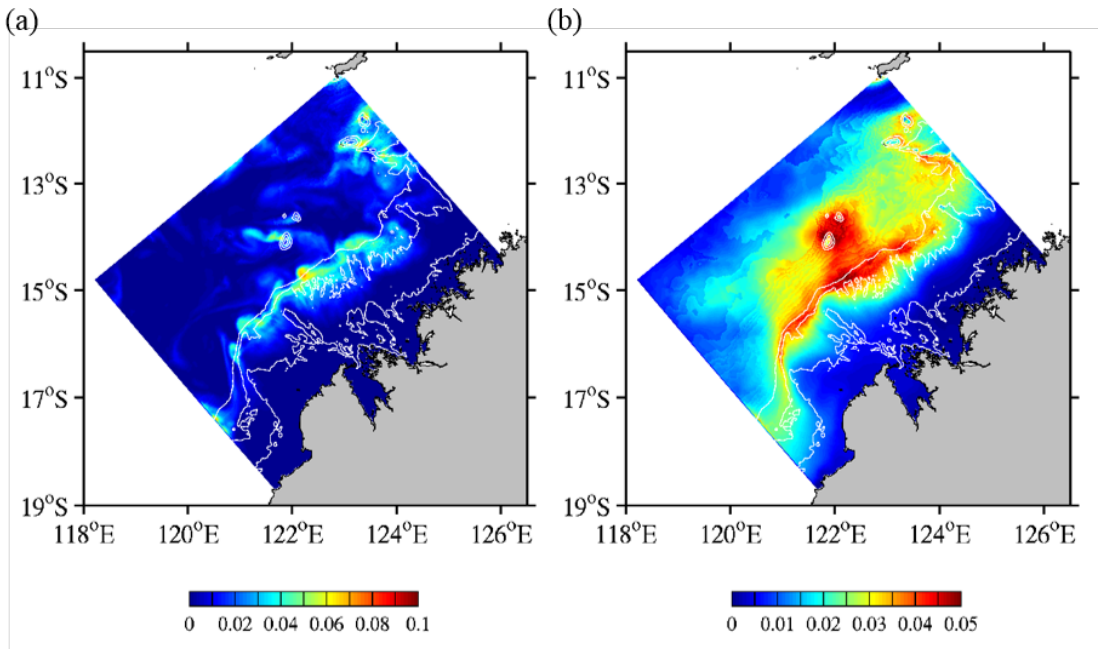

Figure 7.7 Mean concentration of oceanic passive tracer (kg m^{-3}) in the upper 100 m. Panel (a) shows a typical example of the daily average distribution, and (b) shows the annual mean. White lines depict the 50, 100 and 200 m isobaths. Note that the colour scale is reduced by a factor of two in panel (b).

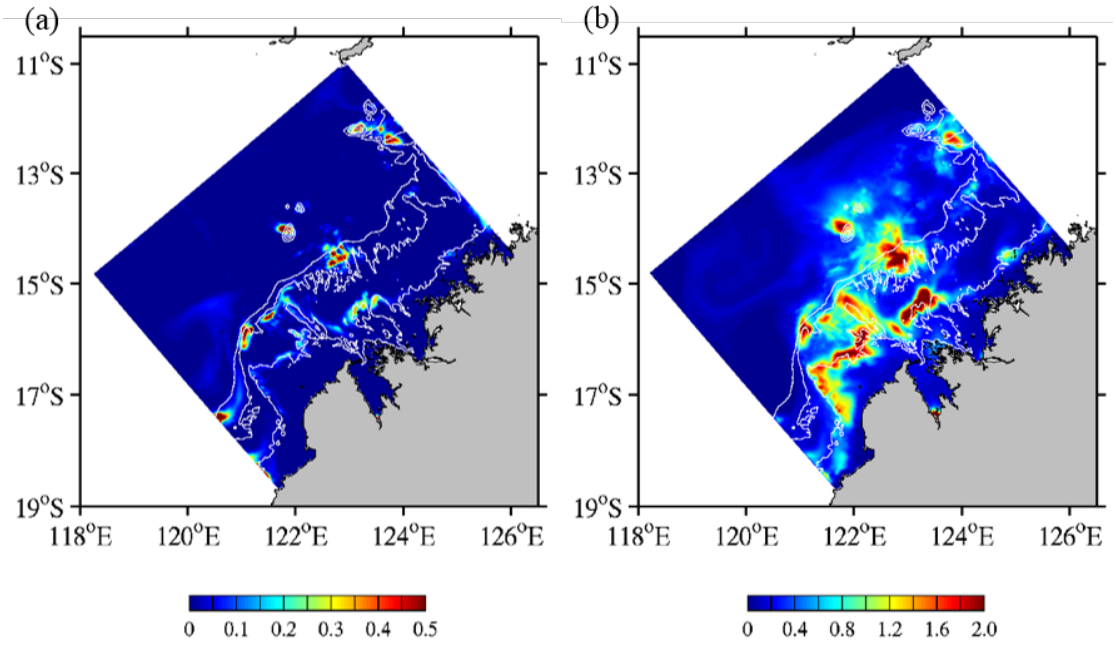

Figure 7.8 Example of daily mean surface (0-10 m) concentration of (a) nitrate (mmol N m^{-3}), and (b) chlorophyll (mg m^{-3}). White lines depict the 50, 100 and 200 m isobaths.

Strong vertical velocities occur in the model along the shelf edge, particularly in the central region where the 100 and 200 m isobaths are closest (Figure 7.9a). We suspect that the upward motions are responsible for the supply of oceanic tracer and nitrate from deeper down in the water column leading to enhanced phytoplankton biomass at the surface. Re-running the model without tides removes the vertical motion otherwise observed at the shelf edge (Figure 7.9b), and any associated biological response (not shown). The enhancement in surface nitrate and chlorophyll further inshore in the vicinity of the 50 m isobath (Figure 7.8a&b) coincides with an increase in vertical mixing that is also absent when tides are removed (Figure 7.10).

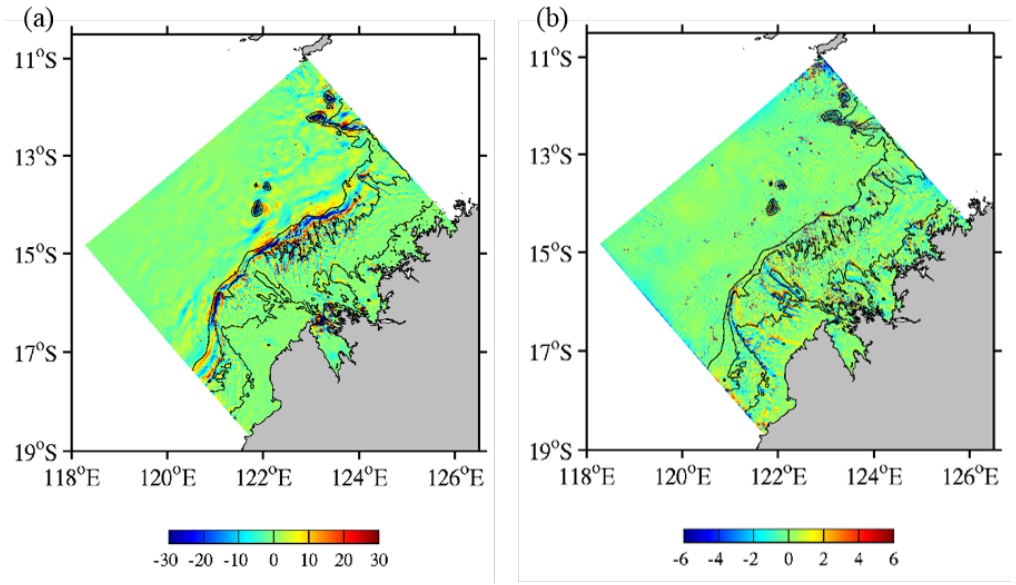

Figure 7.9 Annual mean (depth averaged 0-200 m) vertical velocity (m d^{-1}) (a) with tides showing enhanced vertical motions at the shelf edge, and (b) without tides. Note that the colour scale in panel (b) is reduced by a factor of 5. Black lines depict the 50, 100, and 200 m isobaths.

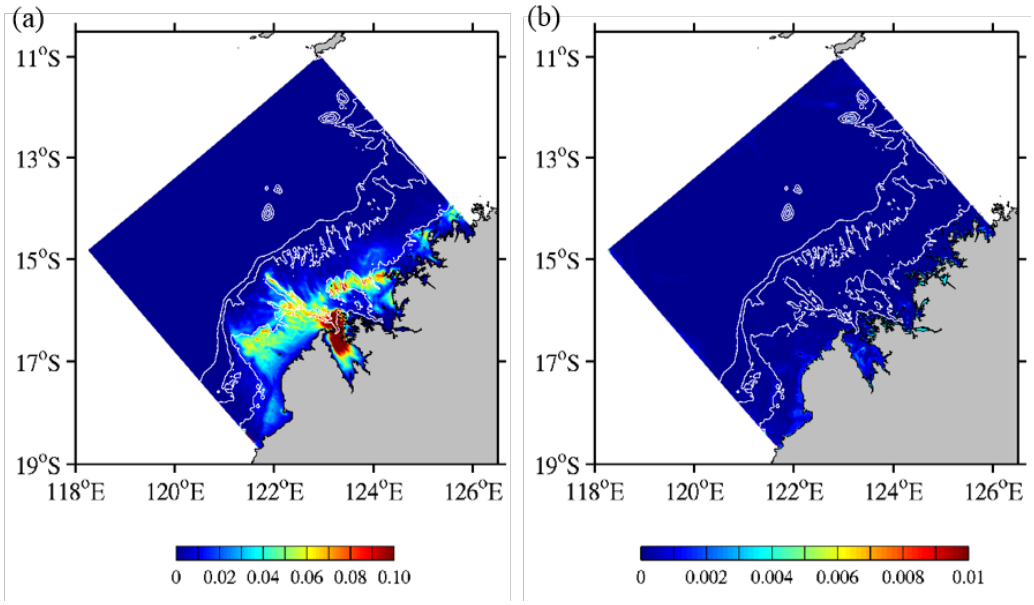

Figure 7.10 Example of daily mean (depth averaged 0-100 m) vertical mixing (m^2 s^{-1}) (a) with tides showing enhancement along the 50 m isobath, and (b) without tides. White lines depict the 50, 100, and 200 m isobaths. Note that the colour scale in (b) has been reduced by a factor of 10.

7.3.3 Regional extent of riverine influence

Riverine discharge in the Kimberley region is highly variable both seasonally, and from year to year. An example of this is provided by stream gauge measurements made in the Fitzroy and Isdell rivers between 2009 and 2012 (Figure 7.11). Major flow is restricted to the months of Jan-Mar, and variations between years can be an order of magnitude or more. The nature of the terrestrial-ocean interaction is further assessed in WAMSI KMRP Project 2.2.6 (Revill et al. 2017) and further in Chapter 8, however, is explored here at the shelf-scale to ascertain the relative significance of river nutrient supply relative to oceanic upwelling.

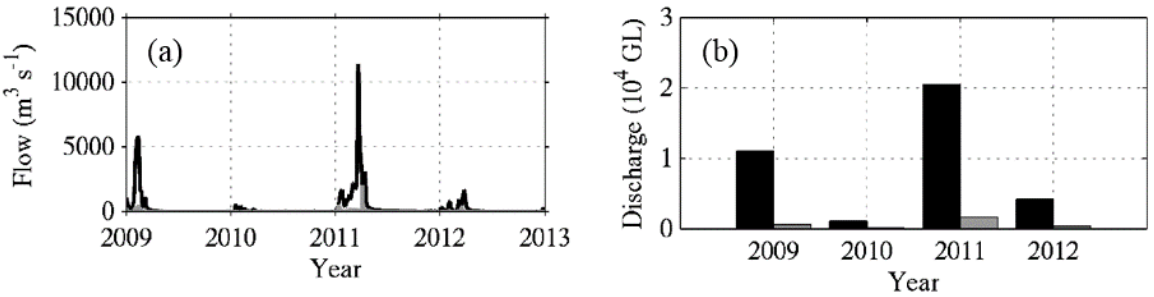

Figure 7.11. (a) Daily flow (m^3s^{-1}), and (b) total discharge (GL), measured in the Fitzroy River (black) and Isdell River (grey) between 2009 and 2012.

River tracers were added to the model for the Fitzroy River (discharge into King Sound) and Walcott Inlet (discharge into Collier Bay) at flow rates based on either stream gauge measurements (Fitzroy) or estimates made in WAMSI KMRP Project 2.2.6 (Walcott Inlet) at a concentration of 1kg m^{-3} to help determine the region influenced by terrestrial nutrient input under varying river flow conditions. River concentrations of total nitrogen in the Fitzroy River are estimated to be ~17 mmol N m^{-3}, and the same nitrogen content was used for inputs into Walcott Inlet. At present, all nitrogen inputs are assigned to nitrate. We define the geographical region of influence as 1% of the source concentration. Two tracer simulations were conducted, one with 2010 flow conditions (simulation A), and a second with the flow conditions multiplied by a factor of 10 (simulation B). The total area of influence (to the nearest 100 km^2) of the Fitzroy River tracer is estimated to be 1600 km^2 for simulation A, and 15,300 km^2 for simulation B. During high-flow years (e.g. simulation B) the region of influence of the Fitzroy may well extend beyond the entrance to King Sound, into Collier Bay to the north and Roebuck Bay to the south. For the Walcott Inlet tracer the area of influence is much reduced largely due to the lower flow volumes, covering just 500 km^2 for simulation A, and 1,800 km^2 for simulation B (Figure 7.12). In addition, any impact of nutrient input from Walcott Inlet appears to be mainly restricted to the eastern side of the Bay.

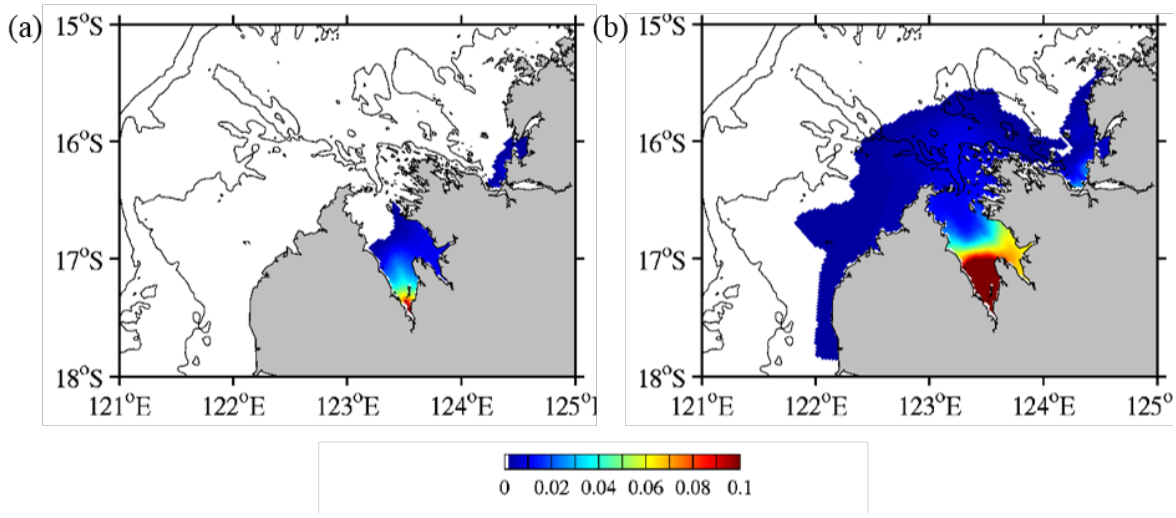

Figure 7.12. Annual mean concentration of river tracers (kg m^{-3}) (a) for 2010 flow conditions, and (b) for 10 times the 2010 flow conditions. Concentrations less than 0.01 kg m^{-3} have been omitted to define the outer edge of river tracer plume at 1% of the source concentration.

7.4 Discussion

The application of a regional-scale biological model has brought attention to the role of tides in stimulating phytoplankton production on the continental shelf. Although, shelf-edge phytoplankton production appears to be exaggerated in the present model due to an unrealistically shallow nitracline, the model response is generally consistent with ship-based observations made during 2010, suggesting that tidal forcing plays an important role in the biological productivity of the outer shelf. An additional effect of tides on the intensity of vertical mixing in the vicinity of the 50 m isobath has also been identified in the model. This elicits a strong biological response in the model, and may explain uniform vertical distributions of nitrate and chlorophyll observed in this depth range near Collier Bay. The exact role of tides in producing these effects requires further work, but overall the model results suggest that oceanic forcing affects biological productivity on the shelf at least as far inshore as the 50 m isobath. Although during the model simulated year (2010) the region of riverine influence was restricted to depths shallower than the 50 m isobath, wetter years could extend the region influenced by terrestrial nutrients beyond the 50 m isobath, effectively overlapping with the region influenced by oceanic nutrients.

The present model simulations have been deliberately tailored to the light climate and growth conditions of the outer and mid-shelf regions. Consequently further inshore, where light conditions are known to be strongly influenced by suspended river sediments, the model response is unreliable. Rather surprisingly, despite over-supply of light to inshore waters, the model underestimates total phytoplankton biomass shoreward of the 50 m isobath according to 2010 conditions. In other words, observed pelagic productivity in the sediment laden nearshore waters, is higher than would be predicted otherwise if the waters were sediment free. This unusual result is consistent with the finding elsewhere in this project that coastal phytoplankton in the Kimberley region have specialized to be highly productive despite the turbid water conditions. Since this growth specialization is not included in the ROMS model used in this Chapter, a general underestimation of productivity results even though light is abundant. In reaching this conclusion, it should be acknowledged that riverine inputs of nitrogen may also have been underestimated in the model, accounting for some of the short-fall in simulated chlorophyll biomass. The factors controlling productivity within the coastal embayments are explored in more detail in Chapter 8.

8 Controls on Coastal Productivity

8.1 Introduction

In addition to the ROMS simulation covering the Kimberley shelf described in Chapter 7, a 3-D coupled physical-biological model optimised for capturing bay and estuary scale dynamics of the Kimberley coast was developed for Collier Bay and Walcott Inlet. The main aim of the model experiments in this Chapter were to provide an assessment of physical and biogeochemical controls on productivity, to better quantify the conceptual pathways described in Figure 8.1. The analysis looks closer at issues raised in Chapter 7 related to the contribution of oceanic vs terrestrial nutrient supply, how different phytoplankton groups deal with the sharp gradient in light, and the complex circulation and turbidity dynamics that are created by wetting and drying as a result of the large tidal excursion. In conjunction with Chapter 7, this work therefore contributes to Research Objective 3, to develop a coupled hydrodynamic-biogeochemical model able to integrate data collected throughout the project. Note that this analysis and model development exercise has been undertaken in conjunction with the WAMSI KMRP Project 2.2.6 (Revill et al. 2017), which focuses on the hydrodynamic and material transport aspects of Collier Bay and Walcott Inlet dynamics.

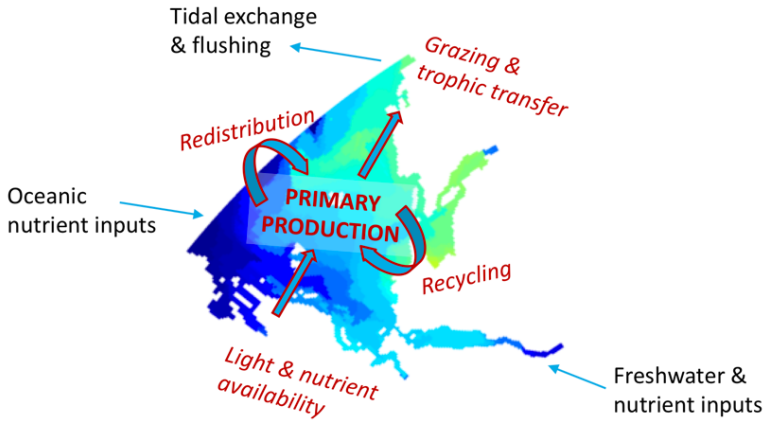

Figure 8.1. Overview of external (black) and internal (red) drivers of primary productivity in large Kimberley embayments. The purpose of the coastal model developed in this chapter is to resolve these nutrient pathways.

8.2 Model description

8.2.1 Physical model

The hydrodynamic model adopted for this analysis was the TUFLOW-FV finite volume platform (BMT WBM, 2013), which employs a flexible mesh (in plan view), consisting of triangular and quadrilateral elements of different size (Figure 8.2). The extent of the domain was defined to be similar as in the WAMSI KMRP Project 2.2.1 (Ivey et al. 2017), extending to the 100m isobath. The finite-volume nature of the model allowed the model to capture the inter-tidal zone and associated wetting-drying dynamics, and the mesh was configured to have finer resolution along the complex coastal boundary, and the numerous islands within the archipelago. The mesh resolution was reduced after the 50m isobaths as our focus in these simulations was to capture dynamics within Collier Bay itself.

The model was configured to be 3-D by adopting a vertical mesh discretization with z-coordinates below the tidal range and sigma-coordinates within the tidal (25 vertical layers in total); see Bruce et al. (2014) and Jovanovic et al. (2015) for recent descriptions of the TUFLOW FV hydrodynamic and turbulence modelling approach. Evaluation of the hydrodynamic model for this environment is summarized in the WAMSI KMRP Project 2.2.6 report (Revill et al., 2017), to which the reader is also referred.

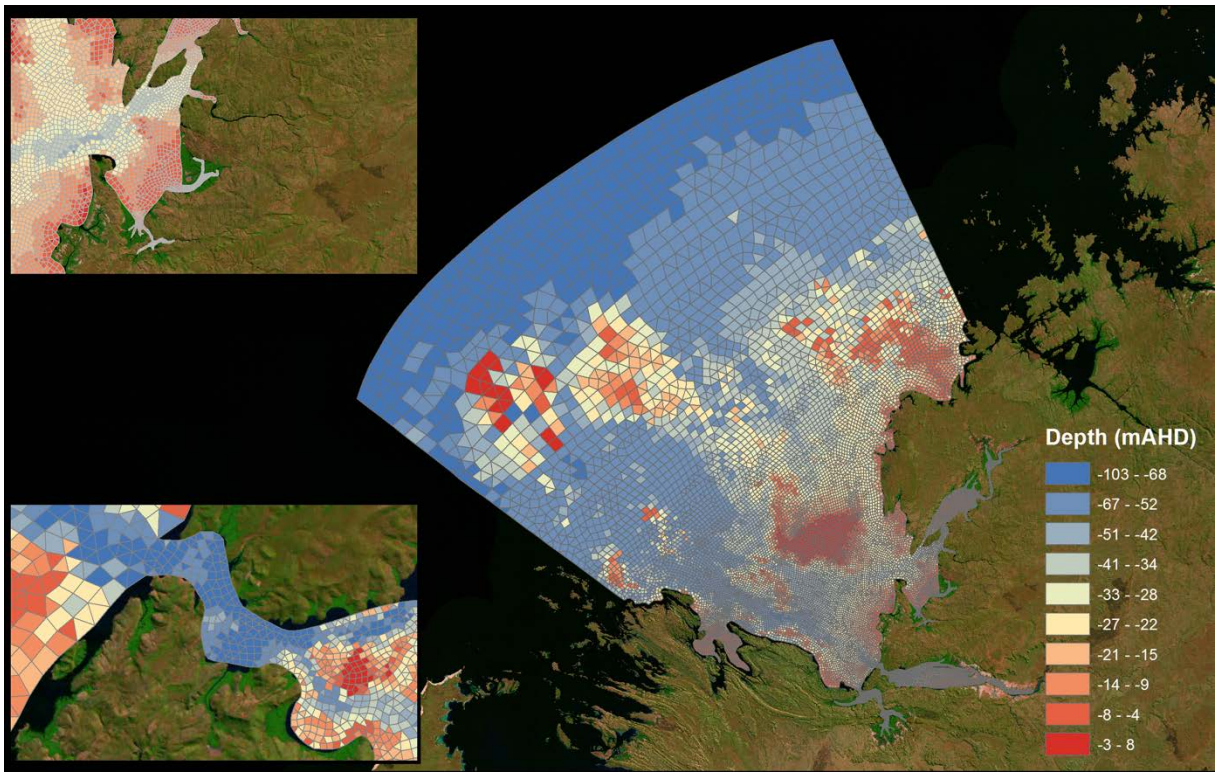

Figure 8.2. Finite volume mesh used for the hydrodynamic-biogeochemical model of Walcott Inlet and Collier Bay.

8.2.2 Biogeochemical model

The TUFLOW-FV hydrodynamic model was dynamically coupled to the Aquatic Ecosystem Dynamics (AED2) biogeochemical model library (Hipsey et al., 2013) for simulation of sediment, biogeochemistry and algal productivity. The AED2 Model was configured to simulate a range of physical, chemical and biological processes relevant to computing biogeochemical dynamics for the region, including:

- water column kinetic (time-varying) chemical / biological transformations (e.g., denitrification or algal growth)
- water column equilibrium (instantaneous) chemical transformations (e.g., PO_4 adsorption)
- vertical sedimentation of particulates
- biogeochemical transformations in the sediment or biological changes in the benthos
- fluxes across the air-water interface
- fluxes across the sediment-water interface
- feedback of chemical or biological attributes to physical properties of water (e.g light extinction)

The model is organised as a series of interconnected "modules" each with a set of state variables, kinetic equations and associated parameters. State variables used in the Walcott Inlet/Collier Bay TUFLOW-FV AED2 model are summarized in Table 8.1, along with a brief summary of processes being considered. The configuration was chosen in light of the conceptual model developed in Chapter 4, based on review of the available data collected for the region, and bearing in mind the need for a computationally tractable simulation.

8.2.3 Simulation setup and parameterisation

The main simulation period was configured to run over a 6 month simulation period, spanning the two field campaigns described in Chapter 2, from 1 Oct 2013 – 31 Mar 2014, and providing a suitable spin-up time. The model was forced on the land-side of the domain by three river inflows, based on predictions from the hydrology model described in Revill et al. (2017), and values for flow, salinity, turbidity and nutrients were

prescribed for each. At the ocean boundary, and the surface meteorological boundary, data was prescribed based on parallel physical modelling studies outlined also in Revill et al. (2017). Nutrient and turbidity values at the ocean boundary were specified based on data summarized in Section 3.4.

Table 8.1. State variables used in the Walcott Inlet / Collier Bay model configuration

Variable	Units *	Common Name	Process Description
Physical variables			
V	m/s	Velocity	Velocity modelled by TUFLOW-FV, subject to inflows, tide and wind forcing
T	°C	Temperature	Temperature modelled by TUFLOW-FV, subject to surface heating and cooling processes
S	psu	Salinity	Salinity simulated by TUFLOW-FV, impacting density. Subject to inputs and evapo-concentration
EC	uS cm^{-1}	Electrica l conductivity	Derived from salinity variable
I_{PAR}	mE m^{-2} s^{-1}	Shortwave light intensity	Incident light, I_0, is attenuated as a function of depth
I_{UV}	mE m^{-2} s^{-1}	Shortwave light intensity	Incident light, I_0, is attenuated as a function of depth
η_{PAR}	m^{-1}	PAR extinction coefficient	Extinction coefficient is computed based on organic matter and suspended solids
η_{UV}	m^{-1}	UV extinction coefficient	Extinction coefficient is computed based on organic matter and suspended solids
Core biogeochemical variables			
DO	mmol O_2 m^{-3}	Dissolved oxygen	Impacted by photosynthesis, organic decomposition, nitrification, surface exchange, and sediment oxygen demand
FRP	mmol P m^{-3}	Filterable reactive phosphorus	Algal uptake, organic mineralization, sediment flux
PIP	mmol P m^{-3}	Particulate inorganic phosphorus	Adsoprtion/desorption of/to free FRP
NH_4^+	mmol N m^{-3}	Ammonium	Algal uptake, nitrification, organic mineralization, sediment flux
NO_3^-	mmol N m^{-3}	Nitrate	Algal uptake, nitrification, denitrification, sediment flux
DOC	mmol C m^{-3}	Dissolved organic carbon	Mineralization, algal mortality/excretion
DON	mmol N m^{-3}	Dissolved organic nitrogen	Mineralization , algal mortality/excretion
DOP	mmol P m^{-3}	Dissolved organic phosphorus	Mineralization, algal mortality/excretion
POC	mmol C m^{-3}	Particulate organic carbon	Breakdown, settling, algal mortality/excretion
PON	mmol N m^{-3}	Particulate organic nitrogen	Breakdown, settling, algal mortality/excretion
POP	mmol P m^{-3}	Particulate organic phosphorus	Breakdown, settling, algal mortality/excretion
TP	mmol P m^{-3}	Total Phosphorus	Sum of all P state variables
TN	mmol N m^{-3}	Total Nitrogen	Sum of all N state variables
TKN	mmol N m^{-3}	Total Kjedahl Nitrogen	Sum of all N state variables
Plankton groups			
BAC	mmol C m^{-3}	Heterotrophic bacteria (*)	
PIPICO	mmol C m^{-3}	Photo inhibited picoplankton (<2µm)	Chlorophytes including Prasinophytes and
PICO	mmol C m^{-3}	Non photo inhibited picoplankton	Cyanobacteria including Synechoccus
MICRO	mmol C m^{-3}	Marine diatom and flagellates	Pseudo-nitzschia spp., Chaetoceros spp and Haptophytes (incl. coccolithophorids)
TCHLA	ug L^{-1}	Total Chlorophyll-a	Sum of relevant phytoplankton groups
ZOO_z	mmol C m^{-3}	Zooplankton groups (*)	Grazing, excretion, respiration and mortality
Sediment and related properties			
SS	g SS m^{-3}	Suspended soilds (inorganic)	Resuspension and sedimentation
Turbidity	NTU	Turbidity	Computed based on SS, POC and TCHLA concentrations

(*) – indicates a variable defined in the 2.2.2 project conceptual model but not simulated here.
BOLD – indicates a simulated state variable, other variables are derived

The AED2 biogeochemical model was parameterized based on algorithms and parameter values adopted from literature or based on studies undertaken during this project, as indicated next.

Light and turbidity : The light climate in the model domain varies considerably from the semi-enclosed Walcott Inlet, the near shore region and open ocean zones as well as between the west and dry seasons, as indicated in Chapter 3 and 5. The model was therefore configured for light to be attenuated in the water column according

to the Beer-Lambert Law, where K_d is a site specific parameter governing the attenuation:

$$I_i = f_i \, I_0 \exp(-K_{d_i} \, z)$$

where i refers to the specific bandwidth range (e.g., PAR, UV etc) and f_i is the fraction of light intensity within that range at the water surface. Within the domain, various cruises have measured K_d to range from 0.13 m^{-1} in the oligotrophic Camden Sound to a maximum of 8 5m^{-1} at the Walcott Inlet congruence (Chapter 3). Strong variability is associated with changes in tide as well as extreme wet season pulses of highly turbid inflow water. The light extinction coefficient is broken down to account for variability in the concentrations of state variables of phytoplankton (PHY), inorganic (TSS) and detrital particulates (POC) based on specific attenuation coefficients, (K_e):

$$K_d = K_w + K_{e_s} \, SS \; + K_{e_d} \, (DOC + DOCR) + K_{e_p} \, (POC + CPOM) + \sum_{a}^{N_{PHY}} K_{e_a} \, \boldsymbol{PHY_{C_a}}$$

where K_e (m^{-1} (g m^{-3})$^{-1}$) assigned based on both literature values and the correlation model fit from Chapter 3 for King Sound:

$$K_d = 0.04 + 1.22 \, TSS \; + 0.025 \, Chl$$

Turbidity is calculated from the concentration of particulates and compared to turbidity data measured during the cruises as part of the model validation exercise. The turbidity relation is expressed as:

$$Turbidity = f_{t_s} \, SS \; + f_{t_p} \, (POC + CPOM) + \sum_{a}^{N_{PHY}} f_{t_a} \, \boldsymbol{PHY_{C_a}}$$

where the f_{t_s} parameters are empirical coefficients, determined through site specific correlations (Table 8.2).

Table 8.2. Light model related parameters.

Symbol	Description	Units	Value	*Comment*
Light and turbidity				
K_w	Background light extinction coefficient	m^{-1}	0.04	*WAMSI (2015)*
K_{e_s}	Specific light attenuation due to non-volatile SS	m^{-1} (g m^{-3})$^{-1}$	1.22	*WAMSI (2015)*
K_{e_p}	Specific light attenuation due to POM	mmol O_2/m^3		
K_{e_a}	Specific light attenuation due to algae groups	m/s	0.025	*Refer to table 6*
f_{t_s}	Coefficient between turbidity and SS	NTU (g m^{-3})$^{-1}$	0.3	
f_{t_p}	Coefficient between turbidity and POM	NTU (g m^{-3})$^{-1}$	0.2	
f_{t_a}	Coefficient between turbidity and algae	NTU (g m^{-3})$^{-1}$	0.2	

Oxygen, nutrients and organic matter: Dissolved Oxygen (DO) dynamics were set to respond to processes of atmospheric exchange, sediment oxygen demand, microbial use during organic matter mineralisation and nitrification, photosynthetic oxygen production and respiratory oxygen consumption. Dissolved inorganic nutrients were included, and subject to dissolved sediment flux, uptake, mineralization and nitrification. Organic matter was set to be made up of dissolved and particulate pools of carbon and nitrogen, assuming parameters as indicated in Table 8.3 and Table 8.4.

Table 8.3. Summary of water column biogeochemical parameter descriptions, units and typical values.

Symbol	Description	Units	Value	*Comment*
		Atmospheric exchange		
$k_{atm}^{O_2}$	oxygen transfer coefficient	m/s	calculated	*Wanninkhof (1992)*
$[O_2]_{atm}$	atmospheric oxygen concentration	mmol O_2/m^3	calculated	*Riley and Skirrow (1975)*
$dz_{s_{min}}$	Minimum depth of a surface cell for flux computation	m	0.2	*Chosen to prevent large concentrations*
		Chemical oxidation		
$\chi_{N:O_2}^{nitrif}$	stoichiometry of O_2 consumed during nitrification	g N/ g O_2		*14/32*
R_{nitrif}	maximum rate of nitrification	/d	0.5	*Estuary*: 0.5 [B]
K_{nitrif}	half saturation constant for oxygen dependence of nitrification rate	mmol O_2/m^3	78.1	*Estuary*: 78.1 [B]
θ_{nitrif}	temperature multiplier for nitrification	-	1.08	*Estuary*: 1.08 [B]
		Dissolved organic matter transformations		
$\chi_{C:O_2}^{miner}$, $\chi_{C:O_2}^{PHY}$	stoichiometry of O_2 consumed during aerobic mineralization and photosynthesis	g C/ g O_2		*12/32*
R_{miner}^{DOC}, R_{miner}^{DON}, R_{miner}^{DOP}	maximum rate of aerobic mineralisation of labile dissolved organic matter @ 20C	/d	0.5	*Estuary*: 0.001 – 0.006 [D] 0.01 – 0.05 [A] *Estuary*: 0.001 – 0.028 [D]
K_{miner}^{DOC}, K_{miner}^{PON}, K_{miner}^{DOP}	half saturation constant for oxygen dependence on aerobic mineralisation rate	mmol O_2/m^3	31.25	47 – 78 [A]
θ_{miner}^{DOC}, θ_{miner}^{DON}, θ_{miner}^{DOP}	temperature multiplier for aerobic mineralisation		1.08	
R_{denit}	maximum rate of denitrification	/d	0.5	*Estuary*: 0.5 [B]
K_{denit}	half saturation constant for oxygen dependence of denitrification	mmol O_2/m^3	21.8	*Estuary*: 21.8 [B]
θ_{denit}	temperature multiplier for temperature dependence of denitrification	-	1.08	*Estuary*: 1.08 [B]
		Particulate organic matter transformations		
R_{decom}^{POC}, R_{decom}^{PON}, R_{decom}^{POP}	maximum rate of decomposition of particulate organic material @ 20C	/d	0.5	0.01 – 0.07 [A]; 0.008 [C]
K_{decom}^{DOC}, K_{decom}^{PON}, K_{decom}^{DOP}	half saturation constant for oxygen dependence on particulate decomposition (hydrolysis) rate	mmol O_2/m^3	31.25	47 – 78 [A]
θ_{decom}^{POC}, θ_{decom}^{PON}, θ_{decom}^{POP}	temperature multiplier for temperature dependence of mineralisation rate	-	1.08	*Estuary*: 1.08 [B]
ω_{POC}, ω_{PON}, ω_{POP}	settling rate of particulate organic material	m/day	-0.05	-1.0 [B]

[B] Based on Bruce et al. (*2011*) FABM-AED application on the Yarra Estuary (Victoria); estimated from data from Roberts *et al*. (2013).

[C] Based on Hamilton and Schladow (1997) for Prospect Reservoir

[D] Based on incubations by Petrone *et al*. (2009) for Swan Estuary (Western Australia)

[E] Based on regression of data from Salmon *et al*. (2014) based on data review from 6 papers therein

Phytoplankton: Three main groups of phytoplankton were represented in the model: Photo-inhibited picoplankton (<2um PIPICO), non photo-inhibited picoplankton (PICO) and micro plankton (MICRO), mainly comprised of marine diatoms.

PIPICO: *Photo-inhibited picoplankton including chlorophytes, prasinophytes and cyanobacteria Prochlorococcus*

PICO: *Non photo inhibited picoplankton, primarily Synechococcus*

MICRO: *Marine diatoms, including Pseudo-nitzschia spp, Chaetoceros spp, Cylindrotheca (=Nitzschia) closterium, etc and Haptophytes (incl. coccolithophorids*

While community composition was not analysed for samples taken during the KIM5887 and KIM5887 cruises the available chlorophyll-a data have been disaggregated into the three functional groups based on HPLC data (Chapter 5), as well as past cruises in the region where community composition analysis was made differentiating between near shore, off shore, deep chlorophyll maxima and riverine input (Volkman et al. 2007; Thompson and Bonham 2011) (Table 8.5).

Table 8.4. Summary of sediment parameter values for each of two major sediment zones.

Symbol	Description	Units	Intertidal	Sand Delta
$F_{max}^{O_2}$	maximum flux of oxygen across the sediment water interface into the sediment	mmol $O_2/m^2/d$	100[a]	50.0 [a]
$K_{sed}^{O_2}$	half saturation constant for oxygen dependence of sediment oxygen flux	mmol O_2/m^3	150[b]	300
$\theta_{sed}^{O_2}$	temperature multiplier for temperature dependence of sediment oxygen flux	-	1.08	1.08
$F_{max}^{PO_4}$	maximum flux of phosphate across the sediment water interface	mmol $P/m^2/d$	0.146[c]	0.072 [c]
$K_{sed}^{PO_4}$	half saturation constant for oxygen dependence of sediment phosphate flux	mmol O_2/m^3	20	200
$\theta_{sed}^{PO_4}$	temperature multiplier for temperature dependence of sediment phosphate flux	-	1.08	1.08
F_{max}^{DOP}	maximum flux of dissolved organic phosphorus across the sediment water interface	mmol $P/m^2/d$	0.05	0.01
K_{sed}^{DOP}	half saturation constant for oxygen dependence of sediment dissolved organic phosphorus flux	mmol O_2/m^3	150	150
θ_{sed}^{DOP}	temperature multiplier for temperature dependence of sediment dissolved organic phosphorus flux	-	1.08	1.08
$F_{max}^{NH_4}$	maximum flux of ammonium across the sediment water interface	mmol $N/m^2/d$	6.4[c]	1.7 [c]
$K_{sed}^{NH_4}$	half saturation constant for oxygen dependence of sediment ammonium flux	mmol N/m^3	31.25[b]	150
$\theta_{sed}^{NH_4}$	temperature multiplier for temperature dependence of sediment ammonium flux	-	1.08	1.08
$F_{max}^{NO_3}$	maximum flux of nitrate across the sediment water interface	mmol $N/m^2/d$	-0.2[c]	-0.4[c]
$K_{sed}^{NO_3}$	half saturation constant for oxygen dependence of sediment nitrate flux	mmol O_2/m^3	50	150.0
$\theta_{sed}^{NO_3}$	temperature multiplier for temperature dependence of sediment nitrate flux	-	1.08	1.08
F_{max}^{DON}	maximum flux of dissolved organic nitrogen across the sediment water interface	mmol $N/m^2/d$	3.0	1.0
K_{sed}^{DON}	half saturation constant for oxygen dependence of sediment dissolved organic nitrogen flux	mmol N/m^3	50	150.0
θ_{sed}^{DON}	temperature multiplier for temperature dependence of sediment dissolved organic nitrogen flux	-	1.08	1.08

[a] Boynton and Kemp (1985)

[b] Bruce et al. (2014)

[c] Reay et al. (1995)

Table 8.5: Assumptions used to disaggregate phytoplankton into three functional groups. These are qualitatively based on various cruise data from the region.

Group	Ocean BC %	River BC %	Walcott Inlet IC %	Inner Collier Bay IC %	Middle Collier Bay IC %	Outer Collier Bay IC %	DCM Outer Collier Bay %
	% of Obs. DCM at 200m offshore[a]	% of Counts of phyto. sp. excl. diatoms[b]	% of Obs. Chla at 50m offshore[a]	% of Obs. Chla at 50m offshore[a]	% of Obs. Chla at 50m offshore[a]	% of Obs. Chla at 200m offshore[a]	% of Obs. DCM at 200m offshore[a]
PIPICO	34%	73%	15%	15%	15%	21%	34%
PICO	33%	27%	40%	40%	40%	53%	33%
MICRO	33%	0%	45%	45%	45%	26%	33%

[a] Thompson and Bonham (2011)

[b] Volkman et al. (2007)

Parameters describing the physiological properties of each functional group have been based on mean values of representative species taken from laboratory experiments of phytoplankton species taken from the Kimberley (Furnas et al. 2015; McKinnon et al. 2015) or comparable regions (Sarthou et al. 2005; Timmermans et al. 2005; Furnas 2007) (Table 8.6).

Table 8.6: Walcott Inlet and Collier Bay phytoplankton parameters.

parameter	description	units	value		
			PIPICO	PICO	MICRO
R_{growth}^{PHY}	phytoplankton growth rate at 20˚C	/d	1.10[a]	1.6[a]	2.47[a]
I_K	light ½ saturation constant for algal limitation	µE m^{-2} s^{-1}	384[a]	169[a]	392.25[a]
K_e^{PHY}	specific attenuation coefficient	mmol C m^{-3} m^{-1}	0.0060[b]	0.0075[b]	0.0060[b]
ϑ_{growth}^{PHY}	Arrhenius temperature scaling for growth	-	1.08	1.08	1.08
T_{std}	standard temperature	C	24	24	24
T_{opt}	optimum temperature	C	26	26	26
T_{max}	maximum temperature	C	30	30	30
R_{resp}^{PHY}	phytoplankton respiration rate at 20C	/d	0.0792[b]	0.1152[b]	0.174[c]
k_{fres}^{PHY}	fraction of metabolic loss that is respiration	-	0.7	0.7	0.6
k_{fdom}^{PHY}	fraction of metabolic loss that is DOM	-	0.3	0.3	0.4
ϑ_{resp}^{PHY}	Arrhenius temperature scaling for respiration	-	1.05	1.08	1.08
χ_{NCON}^{PHY}	average internal N concentration	mmol N / mmol C	0.0485[d]	0.304	0.137[c]
K_N	half-saturation concentration of nitrogen	mmol N /m^3	1.036[d]	2.63	1.6[c]
χ_{PCON}^{PHY}	average internal P concentration	mmol N / mmol C	0.0029[d]	0.010	0.014[c]
K_P	half-saturation concentration of phosphorus	mmol P /m^3	0.094[d]	0.014	0.34[c]
ω_{PHY}	phytoplankton sedimentation rate	m/d	-0.01[d]	-0.01	-0.8[c]

[a] Furnas (2007)
[b] Furnas et al. (2015)
[c] Sarthou et al. (2005)
[d] Timmermans et al. (2005)

Zooplankton: It is known that both large and small zooplankton populations can play an important role in shaping estuary and coastal productivity and nutrient budgets, and this is considerable in the Kimberley (Chapter 6). Due to the nature of patchy data for parameterisation and calibration, zooplankton are not modelled directly in the model but are set as an upper trophic boundary condition, and accounted for as an additional factor in the mortality term of the phytoplankton model.

Parameterisation of the grazing rates of zooplankton in the model are derived from the results in Chapter 6, as 7% of gross primary productivity. With an assumed GPP efficiency of 30%, the following formula was used to determine the respiration rate, R of each phytoplankton group (day^{-1}).

$$R = R_{phy} + 0.07 * 0.3 * \mu_{max} \quad (8.5)$$

8.3 Results

Validation of the nutrients, turbidity and chlorophyll-a concentration are in Revill et al. (2017) and they indicated the model performs reasonably well in capturing the nutrient, suspended sediment and chlorophyll-a concentrations across the system from Walcott inlet through to the outer station. Cross sections of the model outputs through Walcott Inlet and Collier Bay demonstrate the horizontal and vertical variability in salinity, temperature, nutrients, turbidity and phytoplankton (Figure 8.3 – 8.6). The animations of these may be viewed at: http://www.wamsi.org.au/news/kimberley-coastal-system-links-land-deep-sea

In the dry season the salinity and temperature was relatively well-mixed, however horizontal gradients in nutrients and chlorophyll-a were evident. The drivers of primary production showed that nutrient limitation f(N) varies horizontally, with distance off-shore, whereas the light limitation varies sharply in the vertical, creating a niche area near the coast with high productivity.

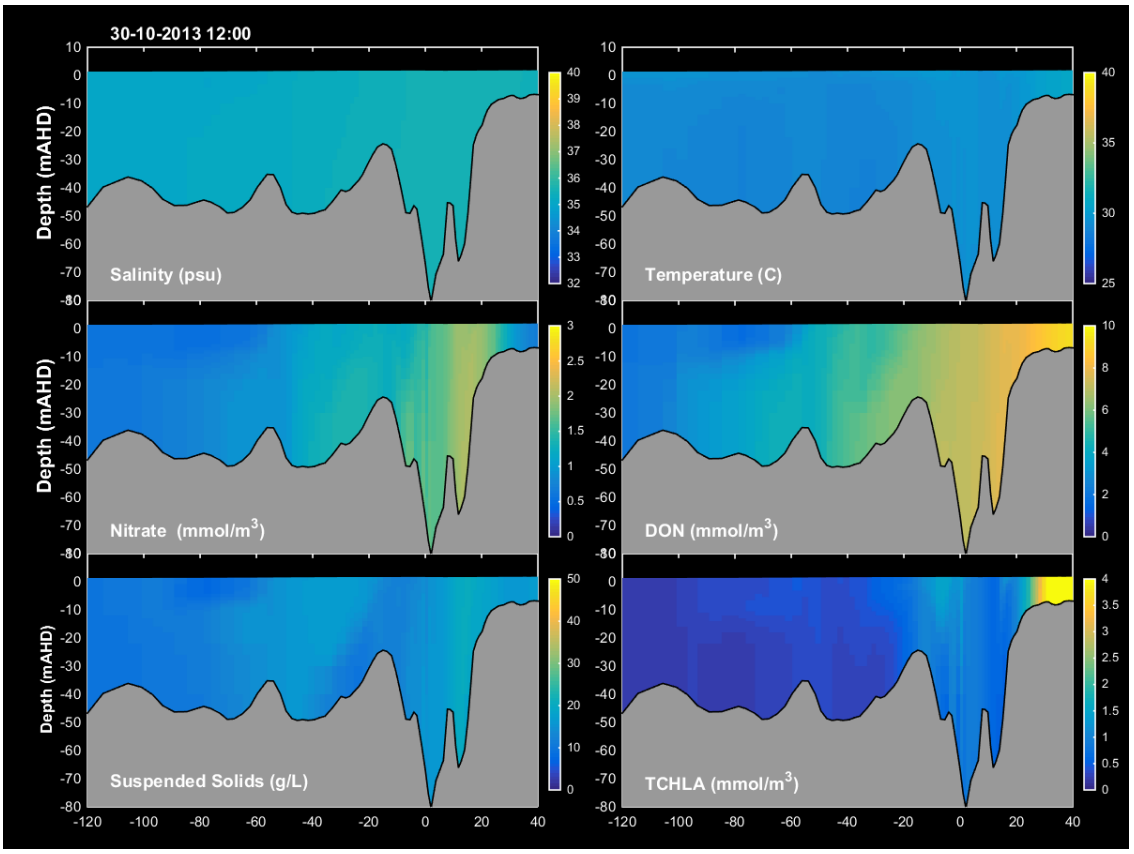

Figure 8.3. Snapshot of model predictions of salinity, temperature, turbidity and nutrient pools during the dry-season, along a transect from Walcott Inlet (right) through Collier Bay.

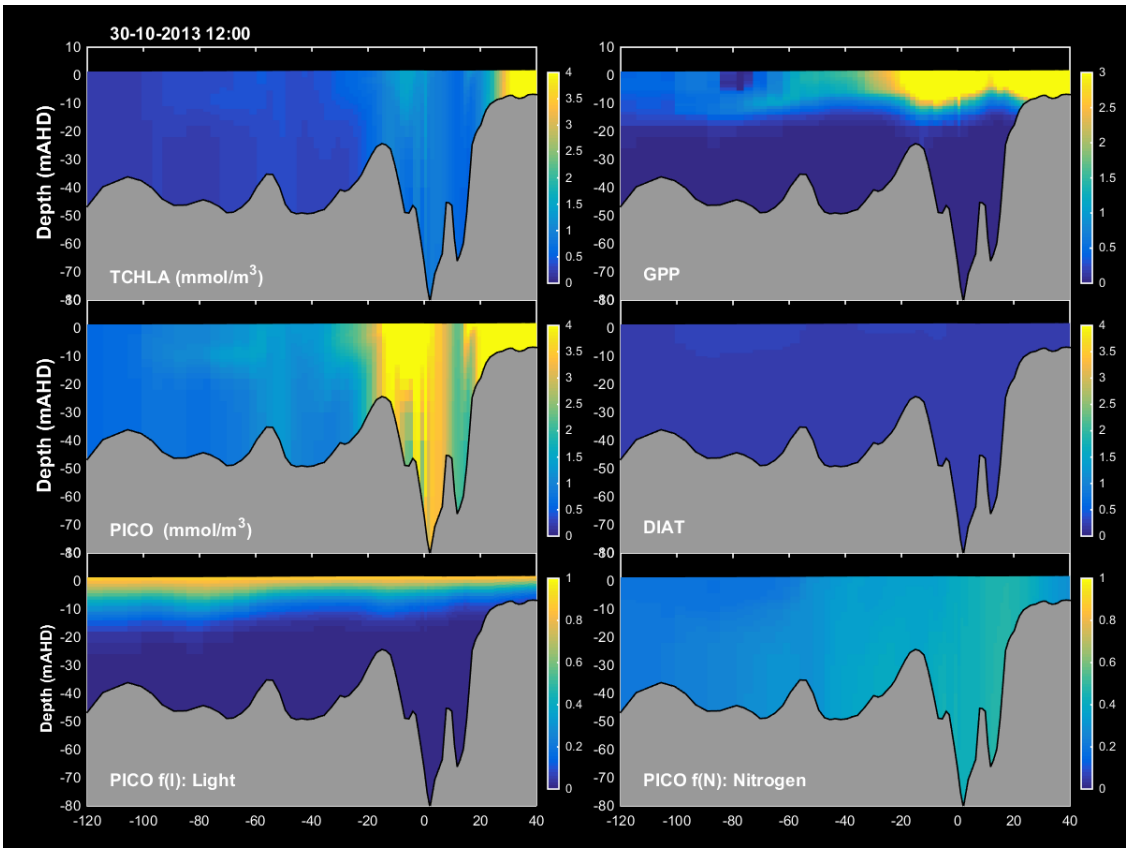

Figure 8.4. Snapshot of model predictions of phytoplankton groups and limitation factors during the dry-season, along a transect from Walcott Inlet (right) through Collier Bay.

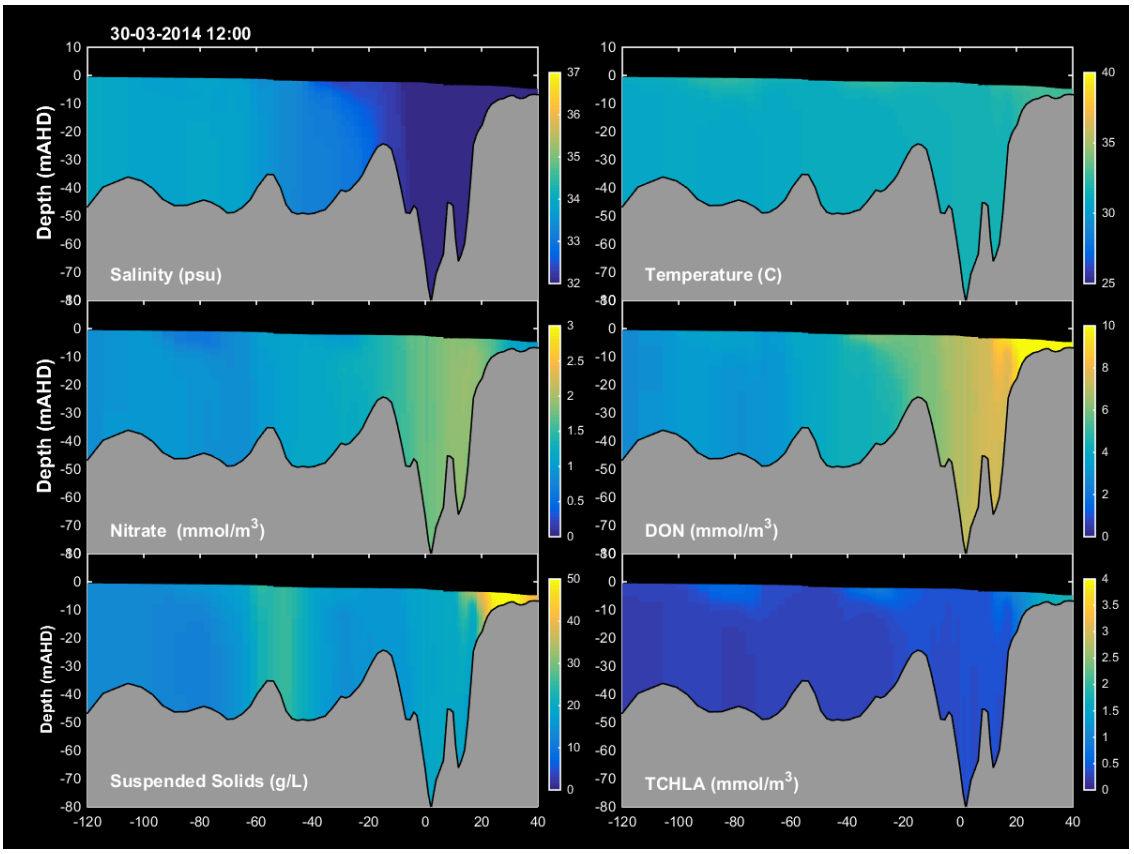

Figure 8.5. Snapshot of model predictions of salinity, temperature, turbidity and nutrient pools during the wet-season, along a transect from Walcott Inlet (right) through Collier Bay.

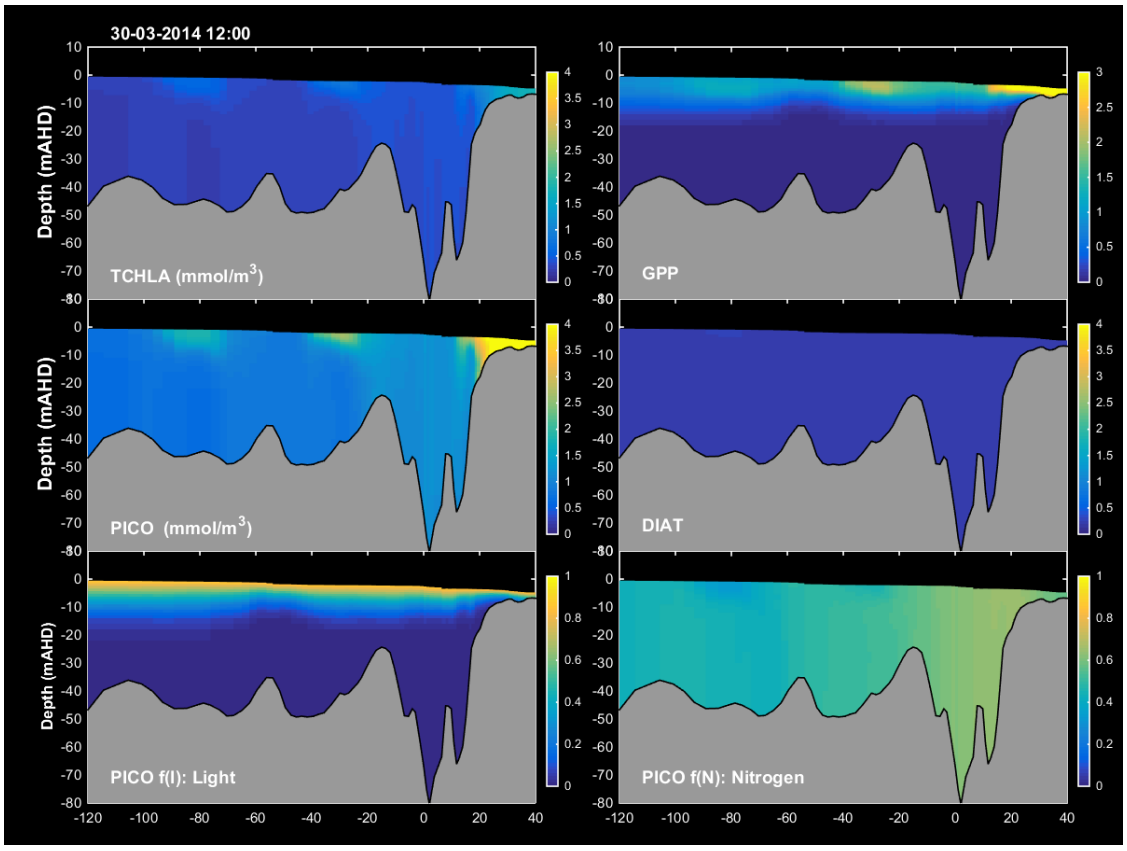

Figure 8.6. Snapshot of model predictions of phytoplankton groups and limitation factors during the wet-season, along a transect from Walcott Inlet (right) through Collier Bay.

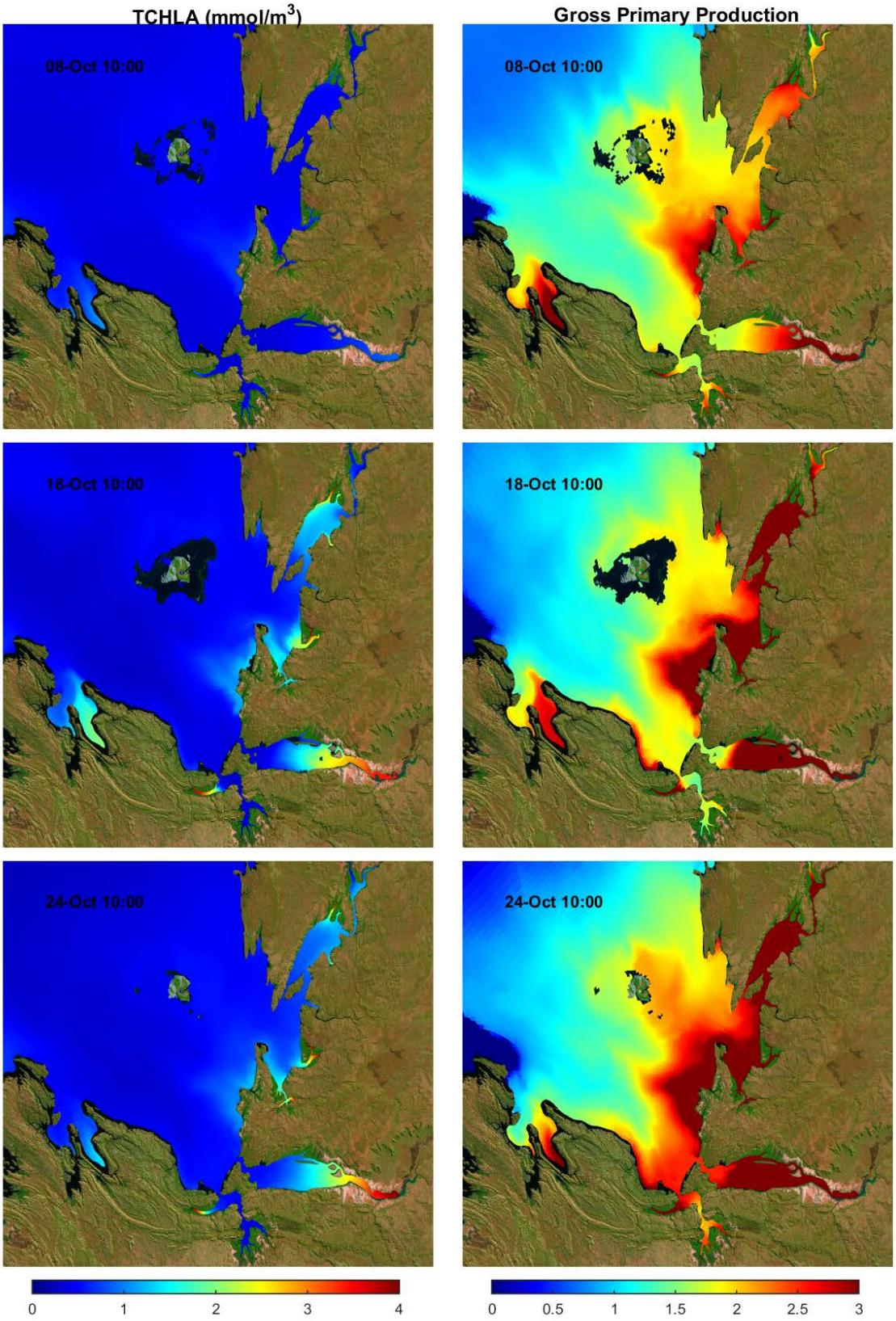

Figure 8.7. Three snapshots of model predictions of total chlorophyll-a and the predicted gross primary productivity (GPP) during the dry-season, indicating the predicted spatial heterogeneity in primary production.

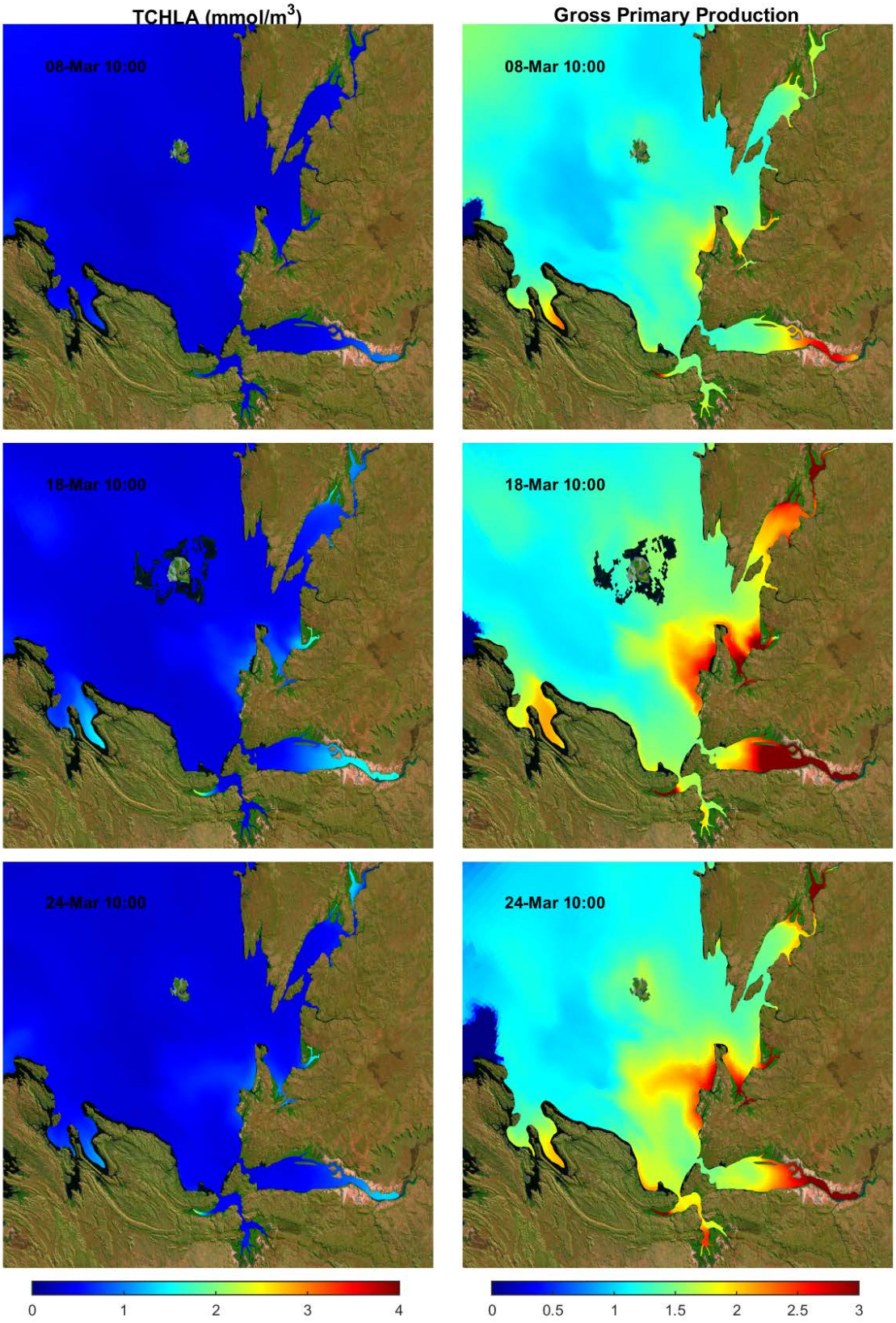

Figure 8.8. Three snapshots of model predictions of total chlorophyll-a and the predicted gross primary productivity (GPP) during the wet-season, indicating the predicted spatial heterogeneity in primary production.

In the wet season, the effect of the freshwater is clearly seen in the bay, however, the magnitude of changes to GPP were relatively minor, with evidence of more light limitation in the vicinity of the flow. The model appears to under-predict the total diatom biomass, potentially suggesting the growth rate was too low or the sedimentation rate was too high, or it is also plausible that resuspension of diatoms from surficial sediment could also be important (but not included in the model). Overall, the results highlight the strong gradients that emerge as with increasing distance from the coast, and the importance of the high vertical mixing rates in recirculating plankton up into the photic zone.

This trend however is further complicated when we take a plan view of the region, and bring into focus the complex circulation patterns that occur in Collier Bay brought about by the interaction of the large tides with the complex bathymetry (Figure 8.7 – 8.8). The results demonstrate the tendency for accumulation of more biomass within the small estuaries and embayments around the Bay, with significant gradients in GPP away from the coast and around the edge of the Bay. These results emerge as a product of the interaction between vertical mixing rate, horizontal dispersion, changes in depth (which effects the time plankton are in the photic zone), light attenuation (based on turbidity), and nutrient availability.

8.4 Discussion

The model presented herein has attempted to integrate our estimates of in situ productivity rates, light sensitivity, nutrient loading and hydrodynamics to compute how productivity varies over space and time within a complex Kimberley coastal embayment. The results show that the gradient in light availability dominates the trends in productivity, and the phytoplankton have adapted to this environment by having short-lived bursts of photosynthesis in the top several metres of water in between times of mixing over the depth of the water column. This is different from the low-light adapted community that exist deeper off the coast and from above the nutricline. The region of the outer bay and inner shelf is therefore a transition region where these two populations can mix.

Whilst validation of the model was undertaken by comparing several model state variables against field observations, uncertainty remains around the accuracy of some aspects of the nutrient flux pathways. Specifically, the model computed distribution of phytoplankton was not as intended based on the size-fractionated data reported in Chapter 5, with a notable under-prediction in the diatom biomass. The increase in productivity predicted by the model near the coast is consistent with data presented in Chapter 5, however, the under-prediction of the diatom group means that we must therefore be over-predicting the rate of picoplankton turnover in this environment. Further work is also required to understand if the bay-scale average rates of phytoplankton grazing predicted were comparable to the values estimated by the enzyme assay data presented in Chapter 6. Therefore, it is recommended that further refinement of the manually set parameters is undertaken to improve predictions of the community composition.

Other extensions are also recommended to continue the development of this model beyond what is presented in this report. These include:

- Incorporation of benthic substrate mapping data into the model, including substrate type and improved estimates of benthic nutrient fluxes.
- Incorporation of three zooplankton size classes and a heterotopic bacteria group, corresponding to the measurements in Chapter 4, to better resolve the microbial loop, and trophic upscaling of the detrital carbon.
- Extension of the model to include the stable isotope concentrations of C and N, in order to improve the validation of the carbon and nutrient trophic transformations.

9 Discussion and Conclusions

9.1 Summary and Highlights of the Dataset

This project has aimed to elucidate the processes controlling carbon and nutrient flows through pelagic ecosystems in the Kimberley region. Specifically, we have sought to link physical processes and riverine inputs to food web structure and function, improving process understanding of pathways and material flows that connect habitats, populations and bioregions in the Kimberley. We have identified sources of nutrients and productivity for consumers, and have developed an improved understanding of how these processes vary across the vast and complex Kimberley region. The project has led to the collection of new data, and analysis of historical and new data, including:

- Characterisation of shelf-scale salinity, light and nutrient variability;
- Characterisation of bay-scale salinity, light and nutrient variability, including across both wet and dry seasons;
- The collection of new data on phytoplankton abundance, size fractionation, rates of productivity, plus a detailed assessment of photosynthesis sensitivity to light intensity across the region;
- Characterisation of zooplankton biomass along the Kimberley coast relative to the shelf, and a novel biochemical dataset on zooplankton growth and respiration used to infer rates of secondary productivity;
- Flow cytometry data of the often ignored picoplankton community, providing a first look at how populations of bacteria, viruses and picophytoplankton vary within a Kimberley embayment;
- An extensive stable isotope dataset spanning from the coast to the shelf-edge, separated both based on size fractioned samples, and organism specific samples.

These data have allowed the development of an improved conceptual model of carbon and nutrient flow both from the coast to off-shore, and also through the planktonic food web. This conceptual model was used as the basis for a two coupled hydrodynamic-biogeochemical models of the region, one at the shelf-scale and one at the bay-scale. Both models have allowed us to refine our understanding of the drivers of primary and secondary productivity, and to answer questions associated with the role of oceanic vs terrestrial nutrient supply.

9.2 Cross-Shelf Variability in Light and Primary Productivity

The overall strong dependence of light attenuation on suspended solids highlights the importance of carefully capturing TSS in any modelling effort. Model simulation of suspended solid concentration was undertaken in the bay-scale model (Chapter 8) and whilst much uncertainty remains, this was the most significant determinant of the overall productivity rate. The relative success in estimating changes in euphotic depth based on Eq. 3.6 both in Collier Bay and the outer King Sound area was an important result, as it provided a simple approach to model the submarine PAR field. The finding that very little light appears to reach the seabed in Collier Bay is also significant as it suggests unfavourable conditions for benthic plants. The extremely high attenuation rates in the vicinity of Walcott Inlet suggests euphotic depths may be restricted at times to < 10cm. Restrictions to vertical model resolution mean that water conditions with euphotic depths < 1 m (light attenuation rates > 5 m^{-1}) would be challenging to simulate.

Some striking cross-shelf trends in the response of phytoplankton to irradiance were seen in the results. Phytoplankton in King Sound and Collier Bay have relatively low initial (α) and high maximum (P_{max}) photosynthetic rates compared with those further offshore. They also show little, if any, sign of photo-inhibition. These characteristics determine a quite distinct predicted irradiance response in comparison to phytoplankton collected further off-shore that form a more traditional deep chlorophyll maximum.

The comparatively small values of α in King Sound and Collier Bay, suggest that phytoplankton in these areas are not particularly well adapted to low light conditions. Compared with the phytoplankton sampled further

offshore (that had much higher α values throughout the water-column), they seem to be relatively inefficient at utilizing low light intensities. This is somewhat counter-intuitive given the relatively high turbidity in these coastal waters. Rather than adapting to high-turbidity / low-light conditions, it seems, from the high P_{max} values and general absence of photo-inhibition, that the coastal phytoplankton have specialized in being able to maximize growth under high intensity light conditions near the surface at the expense of growth further down the water column. This growth strategy only seems viable in well-mixed water-column conditions where excursions to the surface are frequent. This raises questions concerning the daily light history of phytoplankton and variability in vertical mixing. Absence of any noticeable trend in irradiance response with depth either in the King Sound data or in Collier Bay, further suggests that the phytoplankton population is vertically homogenous, consistent with relatively strong mixing. Phytoplankton therefore survive in this region based on short "bursts" of intense photosynthesis, interspersed with periods of no photosynthesis as they are mixed over the water depth.

9.3 Secondary Production and Pelagic Metabolism

Within the Kimberley a range of zooplankton have been identified, but they were similar across the coastal margin and within individual bays. Community respiration, an indicator of secondary metabolism, was estimated to be lower in the dry season than in the wet season. Relatively high levels of spAARS activity (zooplankton growth) in the Kimberley were noted, relative to similar studies undertaken in the Great Barrier Reef, and spETS activity (respiration) showed similar differences in scale between the two northern Australian coasts. Based on these measurements, it has been estimated that >150 µm zooplankton grazing accounted for ~7% of primary production in the Kimberley. Also, area-specific respiration by >73 µm zooplankton was estimated to be 7-fold higher in the Kimberley than on the Great Barrier Reef.

9.4 Model Assessment of Controls on Production

The shelf-scale modelling clearly highlighted the importance of tidally-driven nutrient upwelling at the shelf-edge, providing the most significant source of nutrients for productivity for waters off-shore of the 100m contour. Upwelling hotspots also occurred around islands and more complex bathymetric features. Terrestrial nutrients were identified to play a role in fuelling productivity, but this was in the coastal regions and embayments, and was more sporadic and linked to the size of seasonal river inputs. Under the conditions assessed, the terrestrial nutrients mainly contributed to productivity to within the 50m contour (see also Revill et al. 2017). Inputs of external sediment from river inflows, and resuspension of bottom sediment due to the high water velocities in the inter-tidal zone, contributed to a highly turbid water with the possibility of photosynthesis only in the top several metres of the water column in conjunction with high rates of vertical mixing. Between these two regions, a transition occurs whereby the low-light adapted and high-light adapted communities interact.

9.5 Implications for Management

As one of the few remaining pristine coastal environments in sub-tropical areas of the world, the Kimberley is highly valued for its biodiversity, cultural values, tourism and fisheries, and increasingly in the spotlight for interests focussed on supporting conservation, or encouraging economic development. Ensuring sustainable local management plans and regional policy decisions are made must be founded on evidence about the biophysical character of the systems and robust predictions of how future changes will alter the system. This research has demonstrated the extent to which the Kimberley coast is fuelled by oceanic and terrestrially derived nutrient resources, how nutrients vary seasonally and spatially, and how they are recycled across the region and manifest in areas of high productivity. Changes in productivity may occur in the future due to changes in ocean conditions brought about by climate change, and also due to changes in land-use that would subsequently increase loads of nutrients and sediment to coastal embayments, or from further development of aquaculture. Given the high turbidity levels that are already experienced, it could be argued that strong light limitation would override further anthropogenic increases in nutrients, however, we have demonstrated the

phytoplankton productivity in this region is already highly tuned to the turbid conditions and can rapidly photosynthesise in the top several metres of the water column despite the rapid rates of vertical mixing and high light attenuation. It is therefore possible that productivity could be impacted by increased nutrient inputs, despite the high rates of tidal flushing, however, it remains unclear what magnitude of extra nutrients would be required to create problematic conditions such as algal blooms or low oxygen. Furthermore, this research has not investigated the extent to which land management practices and current development proposals in the Kimberley would increase nutrient export to the coast, however, prior data collection has indicated that hotspots of nutrient input can be significant (Gunaratne et al. 2017), and further research on this at a larger scale across the Kimberley is therefore recommended.

The light data, in particular, may also be used to assist guiding conservation decisions and areas that are set for protection, since in areas where the amount of light reaching the benthos is <1% of the surface light there is limited potential for benthic vegetation and more diverse communities. In addition, this data may also be used to help calibrate algorithms for interpretation of satellite imagery that is available to be used for tracking water colour; this opportunity was not undertaken in this project, but is recommended to be undertaken in the future to allow cost-effective monitoring of the seasonal and long-term water quality changes in the region.

The foundational biophysical datasets on pelagic primary productivity, community metabolism, community and food web structure can provide baseline support development, design and delivery of a more comprehensive program to monitor the long-term health of this ecosystem. Additionally, the raw data in conjunction with the productivity rate estimates, have been used to develop a new conceptual model of how the Kimberley coastal and shelf waters cycle nitrogen and support primary and secondary productivity. The improved conceptual basis can be considered and referred to when forming management plans, making local management decisions, and when communicating science to stakeholders including traditional owners. Furthermore, the conceptual model, alongside the detailed understanding of ecosystem processes developed here, has served as the basis for the development of the coupled hydrodynamic-biogeochemical models. The validated models, and the approaches and parameters which they are based upon, can now be used going forward to assess specific scenarios that can inform an adaptive management processes designed to minimize negative impacts from climate change, tourism, recreational and commercial fisheries, pearling and aquaculture, and other developments associated with port and mining infrastructure.

10 References

Alongi DM, McKinnon AD (2011) Impact of hydrotalcite deposition on biogeochemical processes in a shallow tropical bay. Mar Environ Res 71:111–121.

Armitage AR, Fourqurean JW (2009) Stable isotopes reveal complex changes in trophic relationships following nutrient addition in a coastal marine ecosystem. Estuar Coast 32:1152–1164.

Barnes RSK (1991) Reproduction, life histories and dispersal. In: Barnes RSK, Mann KH (eds) Fundamentals of aquatic ecology. Blackwell Science, Oxford, p 145–171

Becker JJ, Sandwell DT, Smith WHF, Braud J, Binder B, Depner J, Fabre D, Factor J, Ingalls S, Kim S-H, Ladner R, Marks K, Nelson S, Pharaoh A, Sharman G, Trimmer R, von Rosenburg J, Wallace G, Weatherall P (2009) Global bathymetry and elevation data at 30 arc seconds resolution: SRTM30_PLUS. Mar Geod 32:355–371.

Bender M, Orchardo J, Dickson M, Barber R, Lindley S (1999) In vitro O_2 fluxes compared with ^{14}C production and other rate terms during the JGOFS Equatorial Pacific experiment. Deep Sea Res Part A Oceanogr Res Pap 46:637–654.

Bruce LC, Cook PLM, Teakle I, Hipsey MR (2014) Hydrodynamic controls on oxygen dynamics in a riverine salt-wedge estuary, the Yarra River estuary, Australia. Hydrol Earth Sys Sci 18:1397–1411.

Boynton WR, Kemp WM (1985) Nutrient regeneration and oxygen consumption by sediments along an estuarine salinity gradient. Mar Ecol Prog Ser 23: 45–55.

Burford MA, Alongi DM, McKinnon AD, Trott LA (2008) Primary production and nutrients in a tropical macrotidal estuary, Darwin Harbour, Australia. Estuar Coast Shelf Sci 79:440–448.

Canuto VM, Howard A, Cheng Y, Dubovikov MS (2001) Ocean turbulence I: one-point closure model. Momentum and heat vertical diffusivities. J Phys Oceanogr 31:1413–1426.

Dai A, Qian T, Trenberth KE, Milliman JD (2009) Changes in continental freshwater discharge from 1948 to 2004. J Clim 22:2773–2792.

Davies CH, Coughlan A, Hallegraeff G, Ajani P, Armbrecht L, Atkins N, Clementson L et al. (2016) A database of marine phytoplankton abundance, biomass and species composition in Australian waters. Scientific Data *3*: 160043

Dee DP, Uppala SM, Simmons AJ, Berrisford P, Poli P, Kobayashi S, Andrae U, Balmaseda MA, Balsamo G, Bauer P, Bechtold P, Beljaars ACM, van de Berg L, Bidlot J, Bormann N, Delsol C, Dragani R, Fuentes M, Geer AJ, Haimberger L, Healy SB, Hersbach H, Hólm EV, Isaksen L, Kållberg P, Köhler M, Matricardi M, McNally AP, Monge-Sanz BP, Morcrette JJ, Park BK, Peubey C, de Rosnay P, Tavolato C, Thépaut J-N, Vitart F (2011) The ERA-Interim reanalysis: configuration and performance of the data assimilation system. Q J R Meteorol Soc 137:553–597.

Egbert GD, Ray RD (2003) Semi-diurnal and diurnal tidal dissipation from TOPEX/Poseidon altimetry. Geophys Res Lett 30: doi:10.1029/2003GL017676.

Espinasse B, Harmelin-Vivien M, Tiano M, Guilloux L, Carlotti F (2014) Patterns of variations in C and N stable isotope ratios in size-fractionated zooplankton in the Gulf of Lion, NW Mediterranean Sea. J Plankton Res *36*(5):1204–1215.

Eve TM (2001) Chemistry and chemical ecology of Indo-Pacific gorgonians. PhD dissertation, University of California, San Diego, CA.

Fairall CW, Bradley EF, Hare JE, Grachev AA, Edson JB, (2003) Bulk parameterization of air–sea fluxes: updates and verification for the COARE algorithm. J Climate 16:571–591.

Fawcett SE, Lomas MW, Casey JR, Ward BB, Sigman DM (2011) Assimilation of upwelled nitrate by small eukaryotes in the Sargasso Sea. Nature Geoscience *4*:717–722.

Feng M, Slawinski D, Shimuzu K (2017) Knowledge integration and predicting climate change response to climate change. Report of Project 2.2.7 prepared for the Kimberley Marine Research Program, Western Australian Marine Science Institution, Perth, Western Australia.

Fennel K, Wilkin J, Levin J, Moisan J, O'Reilly J, Haidvogel D (2006) Nitrogen cycling in the Middle Atlantic Bight: Results from a three-dimensional model and implications for the North Atlantic nitrogen budget. Global Biogeochemical Cycles *20*: doi:10.1029/2005GB002456.

Froese F, Pauly D (2009) FishBase. www.fishbase.org (accessed 13 Jan 2012).

Furnas M, (2007) Intra-seasonal and inter-annual variations in phytoplankton biomass, primary production and bacterial production at North West Cape, Western Australia: Links to the 1997–1998 El Niño event. Cont Shelf Res 27:958–980.

Furnas M, Carpenter EJ, (2016) Primary production in the tropical continental shelf seas bordering northern Australia. Cont Shelf Res 129:33–48.

Furnas M, Mitchell A, Skuza M, Brodie J (2005) The other 90 %: phytoplankton responses to enhanced nutrient availability in the Great Barrier Reef lagoon. Mar Pollut Bull 51:253–265.

Gehringer JW, Aron W (1974) Field techniques. Chapter 6 in Zooplankton Sampling, Part 1 Reviews on zooplankton sampling methods (D.J. Tranter ed), The Unesco Press, Paris, p87-104.

Gómez M, Torres S, Hernández-León S, (1996) Modification of the electron transport system (ETS) method for routine measurements of respiratory rates of zooplankton. Sth African J Mar Sci 17: 15–20.

Greenwood J, Craig P (2014) A simple numerical model for predicting vertical distribution of phytoplankton on the continental shelf. Ecol Model 273:165–172.

Guerra C (2006) Growth rate determination in larval krill (Euphausia superba Dana) during Antarctic autumn in the Lazarev Sea. A methodology comparison. Master's thesis, University of Bremen.

Gunaratne GL, Vogwill RI, Hipsey MR (2017) Effect of seasonal flushing on nutrient export characteristics of an urbanizing, remote, ungauged coastal catchment. Hydrol Sci J 62:800–817.

Hanski I (2005) The shrinking world: ecological consequences of habitat loss. In: Kinne O (ed) Excellence in ecology, Book 14. International Ecology Institute, Oldendorf/Luhe.

Harris et al., (2000) ICES zooplankton methodology manual. p. 455–532. London: Academic Press

Hernández-León S, Gómez M (1996) Factors affecting the Respiration/ETS ratio in marine zooplankton. J Plankton Res 18:239–255.

Herrera I, Yebra L, Hernández-Léon S, (2012) Effect of temperature and food concentration on the relationship between growth and AARS activity in *Paracartia grani* nauplii. J Exp Mar Bio Ecol 416-417:101–109.

Hipsey MR, Bruce LC, Hamilton DP (2013) Aquatic Ecodynamics (AED) Model Library Science Manual. The University of Western Australia, Perth, Australia. 34p

Holmes RM, Aminot A, Kérouel R, Hooker BA, Peterson BJ (1999) A simple and precise method for measuring ammonium in marine and freshwater ecosystems. Canadian J Fisher Aquat Sci *56*: 1801–1808.

Ikeda T, Torres JJ, Hernandez-Leon S, Geiger SP (2000) Metabolism. In R.P. Harris et al. (eds.): ICES zooplankton methodology manual. p.455–532. London: Academic Press.

Ikeda T, Motoda S (1978) Estimated zooplankton production and their ammonia excretion in the Kuroshio and adjacent seas. Fisheries Bull 76:357–367.

Espinosa-Gayosso A, Lowe R, Jones N, Ivey G (2017). Physical oceanographic dynamics in the Kimberley. Report of Project 2.2.1 prepared for the Kimberley Marine Research Program, Western Australian Marine Science Institution, Perth, Western Australia.

Jovanovic D, Barnes MP, Teakle, IAP, Bruce LC, McCarthy DT (2015) 3D Hydrodynamics and Vertical Mixing in a Stratified Estuary. Proceedigns of the 21st International Congress on Modelling and Simulation, Gold Coast, Australia.

Kobayashi S, Ota Y, Harada Y, Ebita A, Moriya M, Onoda H, Onogi K, Kamahori H, Kobayashi C, Endo H, Miyaoka K, Takahashi K (2015) The JRA-55 Reanalysis: General specifications and basic characteristics. J Meteor Soc Japan 93:5–48.

McKinnon AD, Carleton JH, Duggan S (2007) Pelagic production and respiration in the Gulf of Papua during May 2004. Cont Shelf Res 27:1643–1655.

McKinnon AD, Duggan S, Death G (2005) Mesozooplankton dynamics in nearshore waters of the Great Barrier Reef. Estuar Coast Shelf Sci 63: 497–511.

McKinnon AD, Logan M, Castine S, Duggan S (2013) Pelagic metabolism in the waters of the Great Barrier Reef. Limnol Oceangr 58:1227–1242.

McKinnon AD, Duggan S, Holliday D, Brinkman R (2015) Plankton community structure and connectivity in the Kimberley-Browse region of NW Australia. Estuar Coast Shelf Sci 153:156–167.

McKinnon AD, Doyle J, Duggan S, Logan M, Lønborg C, Brinkman R (2015) Zooplankton growth, respiration and grazing on the Australian margins of the tropical Indian and Pacific Oceans. PLoS ONE 10: e0140012.

Middelburg JJ (2014) Stable isotopes dissect aquatic food webs from the top to the bottom. Biogeosci *11*: 2357–2371.

Okubo A (1971). Oceanic diffusion diagrams, Deep-Sea Res 18: 789–802.

Omori M, Ikeda T (1984) Methods in marine zooplankton ecology. John Wiley and Sons, New York, 332 pp.

Packard TT (1971) The measurement of respiratory electron transport activity in marine phytoplankton. J Mar Res 29:235–244.

Packard TT, Devol AH, King FD (1975) The effect of temperature on the respiratory electron transport system in marine plankton. Deep Sea Res Oceanogr Abs 22:237–249.

Penston MJ, Millar CP, Davies IM (2008) Reduced *Lepeophtheirus salmonis* larval abundance in a sea loch on the west coast of Scotland between 2002 and 2006. Dis Aquat Org 81:109-117.

Platt T, Gallegos CL, Harrison WG (1980) Photoinhibition and photosynthesis in natural assemblages of marine phytoplankton. J Mar Res 38:687–701.

Reay WG, Gallagher DL, Simmons Jr GM, (1995) Sediment-water column oxygen and nutrient fluxes in nearshore environments of the lower Delmarva Peninsula, USA. Mar Ecol Prog Ser 118:215–227.

Revill AT, Jones N, Silberstein R, Furnas M, Donn M, Hipsey MR, Bruce LC (2017). Terrestrial-Ocean linkages: the role of rivers and estuaries in sustaining marine productivity in the Kimberley. Report of Project 2.2.6 prepared for the Kimberley

Marine Research Program, Western Australian Marine Science Institution, Perth, Western Australia.

Riley JP, Skirrow G (1975) Chemical Oceanography. Academic Press, London.

Sarthou G, Timmermans KR, Blain S, Tréguer P (2005) Growth physiology and fate of diatoms in the ocean: a review. J Sea Res 53:25–42.

Soetaert K, Middelburg JJ, Herman PM, Buis K (2000) On the coupling of benthic and pelagic biogeochemical models. Earth Sci Rev *51*:173–201.

Thompson PA, Bonham P (2011) New insights into the Kimberley phytoplankton and their ecology. J Roy Soc West Aust 94:161–170.

Timmermans KR, Van der Wagt B, Veldhuis MJW, Maatman A, De Baar HJW (2005) Physiological responses of three species of marine pico-phytoplankton to ammonium, phosphate, iron and light limitation. J Sea Res 53:109–120.

Umlauf L, Burchard H (2003) A generic length-scale equation for geophysical turbulence models. J Mar Res 61:235–265.

Van der Schalie H (1973) Effects of temperature on growth and reproduction of aquatic snails. University of Michigan Library, Ann Arbor, MI

Van Heukelem L, Thomas CS (2001) Computer-assisted high-performance liquid chromatography method development with applications to the isolation and analysis of phytoplankton pigments. J Chromatography 910:31–49.

Volkman JK, Revill AT, Bonham PI, Clementson LA (2007) Sources of organic matter in sediments from the Ord River in tropical northern Australia. Org Geochemistry 38:1039–1060.

Wanninkhof R (1992) Relationship between wind speed and gas exchange over the ocean. J Geophys Res: Oceans 97(C5):7373–7382.

West TL, Amrose WG (1992) Abiotic and biotic effects on population dynamics of oligohaline benthic invertebrates. In: Colombo G, Ferrari I, Ceccherelli VU, Rossi R (eds) Marine eutrophication and population dynamics. Proc 25th Eur Mar Biol Symp. Olsen & Olsen, Fredensborg, p 189–194

Yang G, Li C, Guilini K, Wang X, Wang Y (2017) Regional patterns of δ13C and δ15N stable isotopes of size-fractionated zooplankton in the western tropical North Pacific Ocean. Deep Sea Res Part I: Oceanogr Res Papers 120:39–47.

Yebra L, Hernández-Léon S (2004) Aminoacyl-tRNA synthetases activity as a growth index in zooplankton. J Plankton Res 26:351–356.

Zhang X, Oke PR, Feng M, Chamberlain M, Church JA, Monselesan D, Sun C, Matear R, Schiller A, Fiedler R (2016) A near-global eddy-resolving OGCM for climate studies. Geosci Model Dev Discuss, doi:10.5194/gmd-2016-17.

11 Abbreviations

1D / 3D	- One dimensional / Three dimensional
AARS	- Aminoacyl-tRNA Synthetases
AED2	- Aquatic EcoDynamics biogeochemical model library
AIMS	- Australian Institute for Marine Science
BGC	- Biogeochemistry
CR	- Community Respiration
CTD	- Conductivity, Temperature, Depth
ETS	- Electron Transport System
HPLC	- High Performance Liquid Chromotography
IMOS	- Integrated Marine Observing System
KMRP	- Kimberley Marine Research Program
mAHD	- metres above the Australian Height Datum
NCP	- Net Community Production
NPZD	- Nutrient-Phytoplankton-Zooplankton-Detritus
OFAM	- Ocean Forecasting Australia Model
P-I	- Photosynthesis-Irradiance
P:R	- Photosynthesis:Respiration ratio
PAR	- Photosynthetically Active Radiation
GPP	- Gross Primary Production
POM	- Particulate Organic Matter
ROMS	- hydrodynamic model termed the Regional Ocean Modelling System
RV	- Research Voyage
TUFLOW-FV	- Finite Volume hydrodynamic model system

12 Communication

12.1 Students supported

Thomas Ngyuen – BSc (Hons)

12.2 Journal publications

Jones NJ, Patten N, Krikke D, Lowe R, Waite A, Ivey G (2014) Biophysical characteristics of a morphologically-complex macrotidal tropical coastal system during a dry season. Estuar Coast Shelf Sci 149: 96–108.

McKinnon AD, Doyle J, Duggan S, Logan M, Lønborg C, Brinkman R (2015) Zooplankton Growth, Respiration and Grazing on the Australian Margins of the Tropical Indian and Pacific Oceans. PLoS ONE 10(10): e0140012.

12.3 Planned manuscripts

McInnes et al – Analysis of marine plankton isotope data paper

McInnes et al – Analysis of cytometry data of picoplankton

Furnas et al – Productivity-Light relationships off the Kimberley coast

Greenwood et al – Nutrient upwelling vs terrestrial nutrient supply to support production in the Kimberely

Zhou et al – Controls on productivity in Collier Bay

12.4 Presentations

Furnas M (2014) High phytoplankton productivity in hyper-physical tropical shelf and coastal system: the Kimberley shelf, NW Australia, ASLO 2014 Marine Science Meeting, Honolulu (Poster presentation).

Hipsey MR, Furnas M, Jones N, Bruce LC, Nguyen T, Greenwood J et al. (2015) Pathways to production - Biogeochemical processes supporting productivity of the Kimberley coast. *Presentation at the Western Australian Marine Science Institute (WAMSI) 2015 Symposium,* Perth, Australia

Hipsey MR, Furnas M, Jones N, Bruce LC, Nguyen T, Greenwood J et al. (2016) Hydrodynamic and Biogeochemical Controls on Productivity in the Kimberley Coast. *Presentation to the Department of Parks and Wildlife lunch and learn session*, October 2016, Perth, Australia.

12.5 Other communications

Brinkman R, Furnas M (2014): Interview on WAMSI activities by ABC TV (Broome) in Broome prior to departure of the October 2013 Solander voyage. Portions of the interview were broadcast locally and nationally on the ABC24 New channel.

Hipsey MR, Ivey G, Greenwood J (2016): Kimberley coastal system: links from the land to the deep sea. Website article: http://www.wamsi.org.au/news/kimberley-coastal-system-links-land-deep-sea

13 Appendices

Appendix 1. This project directly addresses the following questions outlined in the Kimberley Marine Research Program Science Plan.

Key Question	Informed Response
1. What are the rates of pelagic primary productivity and how do these mechanisms and drivers compare with other areas of Australia?	The research project has identified the rates of primary productivity and placed them in comparison with other coastal environments in Australia. The average rates of productivity were comparable to those seen in other Northern waters of Australia including the Great Barrier Reef.
2. Are there large spatial (e.g. inshore-offshore gradients) and temporal (e.g. seasonal, inter-annual) variations in nutrients and pelagic primary productivity in this region?	Changes in productivity were apparent with distance offshore, and also mild differences between wet and dry seasons were noticeable. The areal average (/m2) productivity in the coastal embayments was significantly higher relative to the shelf and shelf-margin.
3. What processes are 'driving' this variation?	Through multiple approaches, the research has identified that productivity is controlled by the shifting balance between light and nutrient availability that occurs with increasing distance off-shore. The light climate is highly turbid in the embayments, however plankton in these regions have adapted to the coincident high vertical mixing rates. Further out along the shelf, the water clarity is much higher and deep chlorophyll maxima form due to lower surface nutrient availability, and higher nutrients at depth. Nutrients are provided to the embayments from the terrestrial catchments, however recycling and cross-shelf transport of nutrients sourced from deep waters following upwelling at the shelf-edge were also demonstrated to be important for supporting pelagic productivity on the shelf itself.
4. How significant is pelagic primary productivity to the maintenance of Kimberley coastal/pelagic ecosystems?	The research computed the rates of secondary production and found high zooplankton abundance and efficient rates of phytoplankton consumption. These were up to 4x higher than in the Great Barrier Reef, and so is thought to be an important local driver of Kimberley ecosystems.
5. How do large-scale oceanic processes influence local physical and biological oceanography? (possible to link to Pilbara from NCB)	The productivity across the region is thought to be controlled by a combination of nutrient delivery from deep-ocean upwelling and from periodic coastal inputs. The macro-tidal nature of the region and the complex coastal archipelagos creates a dynamic mixing environment across the shelf which sets up a gradient of conditions that lead to a transition in the plankton community, most notable around the 50m contour.
6. How might we best monitor changes in physical and biological oceanography, particularly in relation to climate change? Are there key variable that we can monitor (and how) to assist in understanding the system in the future.	Setting up baseline monitoring stations in coastal areas such as King Sound and/or Collier Bay, and on the shelf would allow long-term changes to be assessed and provide guidance for Marine Park management. Ideally, monitoring could include fixed stations, but potentially also could take advantage of Ships of Opportunity. Additionally, the importance of light in shaping productivity lends itself to further investment in remote sensing products capturing turbidity and chlorophyll-a.
NEW QUESTIONS POSED BY MANAGERS	
What impact do localised anthropogenic inputs (cattle in creeks quality and nutrient impacts) have on the system?	These were not quantified in this research project, however the loads are likely to be low compared to the rate of flushing and magnitude of rivers entering the region.
What is the likely impact of silage from boats? (e.g. Hori Falls)	This was not quantified in this research project, however the loads are likely to be low compared to the rate of flushing.
Can you articulate the threatening processes to primary productivity (within the water column) and the risk around them?	Primary productivity is likely to increase through large scale developments changing land-use in the catchment that will inevitably lead to an increase in nutrient loading. However, increased land-clearing and pastoral activities may increase soil erosion and increase suspended sediment in the rivers, leading to further light limitation.
Can we identify a link between primary productivity and some of the key species (values of the park)? e.g.- is barramundi habitat in the Kimberley richer than in other areas of Australia? Are there links to humpback whale preferred habitat in the Kimberley?	This is not clear from the present analysis, however synthesis activities using data collected herein may be able to provide further insights on the links between fisheries, whales and water quality. Evidence from this project suggests the transfer of material up the planktonic food web is active and would contribute to the high fishery productivity in the region.

Is there any information to highlight the value of islands to nutrient inputs into the Kimberley (sediments, guano)?	This research project is unable to answer this question
Do mining companies have useful data for us to use - evidence of elevated levels given development activity? reference sites, etc?	This research project is unable to answer this question
Do the offshore rigs collect water quality data on productivity? (can we access this)	This research project is unable to answer this question